Linköpings universitet
TEKNISKA HÖGSKOLAN

Alternative Cooling and Mounting Concepts for Transition Duct in Industrial Gas Turbines at Siemens Industrial Turbomachinery AB

Johan Östberg
Tomas Öfverstedt

Machine Design

Master Thesis
Department of Management and Engineering
LIU-IEI-TEK-A--11/01049--SE

Abstract

Gas turbine development is constantly moving forward and for higher efficiency hotter turbine inlet temperature is required. Because of that, one of the largest design problems is to find efficient ways to cool the hot parts in the gas turbine. This master thesis at Linköping University has been written at Siemens Industrial Turbomachinery AB in Finspång. The task was to develop and evaluate new alternative cooling and mounting concepts for a transition duct in Siemens latest gas turbine, SGT-750. Transition duct is a hot part and have the task to guide the hot gas from the combustion chamber to the turbine inlet in a gas turbine.

The transition duct of today is cooled by a relative large amount of compressor air which needs to be reduced in case of a power upgrade. The current mounting solution requires three combustion chambers to be removed for one transition duct maintenance, which is time consuming.

A literature study and a market research including patent searches was made to get an overview of solutions used today. Concept was then generated from function/means tree together with morphology matrixes. This was divided in two branches, one for cooling and one for mounting and sealing. The concepts were evaluated with Go-/no go screening, datum method and weighted objectives method. Further development and combination of the concepts led to different concept suggestions which will ease and shorten the maintenance and reduce the cooling air consumption with kept material temperature.

Sammanfattning

Gasturbinutvecklingen går hela tiden framåt och för högre effektivitet krävs hetare turbininloppstemperatur. Ett av de stora konstruktionsproblemen som detta medför är att på ett effektivt sätt kyla de heta delarna i gasturbinen. Detta examensarbete vid Linköpings Universitet har skrivits på Siemens Industrial Turbomachinery AB i Finspång. Uppgiften var att ta fram och utvärdera nya alternativa kyl- och monteringskoncept för en transition duct i Siemens senaste gasturbin SGT-750. Transition duct är en het del som har till uppgift att leda hetgasen från brännkammaren till turbindelens inlopp.

Dagens transition duct kyls av en relativt stor del kompressorluft vilket skulle behöva reduceras vid en eventuell effektuppgradering. Dagens monteringslösning kräver att tre brännare tas bort för att service på en transistion duct ska kunna genomföras, vilket är tidskrävande.

En litteraturstudie och en marknadsundersökning med bland annat patentsökningar har gjorts för att få en överblick av vilka lösningar som används idag. Koncept genererades sedan utifrån funktions/medel träd tillsammans med morfologiska matriser. Detta skedde uppdelat i två grenar, en för kylning och en för montering och tätning. Koncepten utvärderades med elimineringsmatris, datum metoden samt kriterieviktsmetoden. Vidareutveckling och kombinering av koncepten ledde sedan fram till olika konceptförslag vilka skulle underlätta vid servicearbeten samt sänka kylluftsåtgången med bibehållen materialtemperatur.

Preface

There has been an honor for us to write our master thesis here at Siemens Industrial Turbomachinery in Finspång during the spring of 2011. For us it has been a good opportunity to extend and summarize our knowledge of what we learned in our education, Master of Science in Mechanical Engineering at Linköping University.

In the autumn of 2010 we sent an application to David Andersson about writing our master thesis in his group, Research and development Core engine Combustor Design. He responded with the idea of performing a conceptual study regarding alternative cooling and mounting methods on the transition duct located in the new SGT-750 combustion system.

We would like to thank this people who have been of great importance during the project and writing of this master thesis.

Emma Nordin	Design Responsible Combustor SGT-750, RCCD Siemens Industrial Turbomachinery
Olle Lindman	Specialist Combustor Design, RCC Siemens Industrial Turbomachinery
David Andersson	Manager Combustor Design RCCD, RCC Siemens Industrial Turbomachinery
Hampus Gavel	Post-Doctoral Fellow, Department of Management and Engineering Linköping University
Johan Ölvander	Professor, Department of Management and Engineering Linköping University

We also like to thank all employees at SIT AB that have helped us during the work with this master thesis.

Finspång, May 2011

Johan Östberg

Tomas Öfverstedt

Table of Contents

Table of Figures

Table of Tables

Words and Abbreviations

Aft end	-	See Figure a.
Blowing ratio	-	Ratio between the effusion air velocity and density and the hot gas velocity and density.
Central housing	-	The outer shell that encloses the combustor system.
Fore end	-	See Figure a.
HCF	-	High cycle fatigue
Inboard side	-	See Figure a.
LCF	-	Low cycle fatigue
Outboard side	-	See Figure a.
Port hole	-	The hole in the central housing from were the combustor comes out from.
SCC	-	Stress Corrosion Cracking
TBC	-	Thermal Barrier Coating
SIT AB	-	Siemens Industrial Turbomachinery AB
SGT	-	Siemens Gas Turbine
SGT-750	-	Siemens latest gas turbine, 37MW output

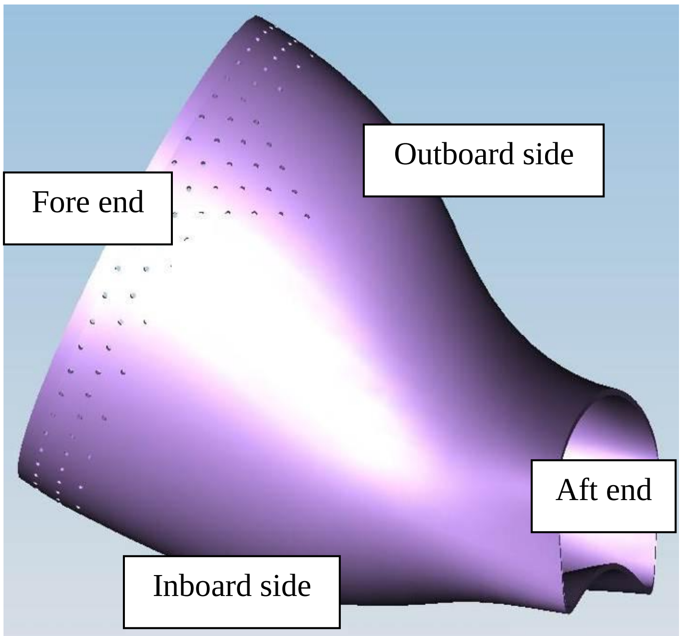

Figure a. Transition duct and its named parts.

1 Introduction

This chapter presents introducing information about this master thesis, a brief background, the aim, problem description and limitations of the thesis. Company presentation and descriptions of gas turbines, combustion chambers and transition duct are presented as well.

1.1 Background

The efficiency of gas turbines becomes more and more important simultaneously as the pollution demands gets harder. Therefore it is important to keep the flame temperature in the region of effective combustion to avoid pollutions. To keep the overall efficiency high, the turbine inlet temperature should be as high as possible. Due to this, cooling of the hot parts must be more efficient and cooling air leakage to the combustion chamber must be reduced.

Today the transition duct in SGT-750, which is a hot combustion component, is cooled with impingement cooling, a proven method for cooling of hot parts. Today this cooling method is allowed to consume a generous amount of compressor air to keep the transition duct material in a good temperature. Due to the interest of continued improvements other cooling methods are of interest to lower the consumption of air and still maintain a good temperature in the transition duct material.

Due to this continued work with improvements, mounting of the transition duct also are of interest. It should be investigated in order to find even more robust mounting methods with lower vibrations and slighter risk for low cycle fatigue.

Today the transition duct mounting consists of many parts that have to be held in place while fitting and tighten the bolts. To reach all bolts to remove or mount a transition duct, three of the combustion casings has to be removed, the one where the actual duct is located and also the adjacent casings. In order to lower the maintenance time for service it is of interest to change this design.

1.2 Aim

The objective of this master thesis is to present alternative cooling and mounting concepts of the transition duct on the SGT-750.

Different cooling methods will be investigated in order to reduce the air consumption used for the transition duct cooling.

Concepts for new ways to mount the transition duct with fewer parts and with just one combustor casing removed will also be investigated. Seals that are suitable for the mounting concepts will also be chosen.

1.3 Problem Description

The task is divided in these five steps.

- Find alternative methods for cooling the transition duct and also concepts for mounting the transition duct with suitable sealing.
- Calculate cooling efficiency for each method.
- General design of the mounting concepts.
- Evaluate the cooling methods and the mounting concepts.
- Combine the strongest cooling methods together with the best mounting concepts to final concepts.

1.4 Limitations

Simulation models of concepts are not used and no Computational Fluid Dynamics, CFD are used in the calculations regarding cooling efficiency. Instead one dimensional heat transfer calculations together with flow calculations are used. The calculations are made on a flat surface with the same area as the mantle area of the transition duct. For the first concept evaluations flow velocities, heat transfer coefficient and other hot gas parameters are calculated at a circular tube with the same diameter as the mean diameter of the real transition duct.

No calculations are made on the mounting concepts. Instead the evaluation is made using comparative methods and in-house knowledge.

This thesis will not result in a final design, instead a few concept suggestions will be presented.

1.5 Company Presentation

Siemens Industrial Turbomachinery AB, SIT AB is a part of Siemens AG, Europe largest company group. SIT AB constructs Siemens mid-rage gas turbines, 15-50 MW and steam turbines, 50-250 MW. It is located in Finspång, Sweden, where turbines have been built since 1913. There are 2 700 employees and SIT AB stands for the whole lifespan of the products, from development and manufacturing to installation and service. SIT AB has an ability to deliver a whole package of combined cycle plants, with gas turbines and steam turbine for heat recovery.

The latest creation from SIT AB is the versatile and robust SGT-750. Introduced in the late fall 2010 at Siemens, Finspång. (SIT internal material, 2011)

1.6 Description of Gas Turbines

A gas turbine is a rotating combustion engine, a machine that transfers energy between a rotor and a fluid. The gas turbine consists of three main parts, compressor, combustor chamber and turbine, see Figure 1. The compressor feed the combustor chamber with high pressurized air. The temperature of the air increases with the pressure in the compressor stage. The hot, pressurized air mixes with fuel in the combustion chamber. When the mixture ignites the temperature rise will result in expansion of the gas during the combustion, which leads to higher speed of the combustion gas. The flow of the combustion gas makes the turbine spin. Energy extracts from the gas at the same time as the temperature and pressure decreases. A part of the extracted energy is required to power the compressor and the rest of the energy is the machines output energy. (Cohen, Rogers & Saravanamuttoo, 1996)

Gas turbines are used in many different applications. Large gas turbines are used in industrial applications, such as offshore oil pumping, gas compressions in pipelines and electricity generation. Smaller gas turbines are used in helicopters, airplanes, tanks et cetera. Jet engines are based on the same principle as the gas turbine, only with a change of turbine stage setup. The turbine stage in a jet engine just powers the compressor and the remaining hot gas will form a jet stream during expansion over the exhaust nozzle, which creates a force vector. (Cohen et.al., 1996)

Advantages of gas turbines are the power to weight ratio and short start stop time. The efficiency is often little lower than other engines, around 40%. In a combined cycle with a heat recovery steam turbine the efficiency for electric generation can be as high as 60%.(Cohen et.al., 1996)

The SGT-750, see Figure 1 is intended to be used for both power generation and mechanical drive with a high efficiency. The main feature of this turbine is the short maintenance time and low emissions. The power output in power generation setup is 36 MW with an electric efficiency of 39%. With the mechanical setup the output are 37 MW, 50’000 bhp with 40% efficiency. To boost the efficiency even more at power generation the SGT-750 can be used in a combined cycle due to the high exhaust temperature. (SGT - 750 - Siemens)

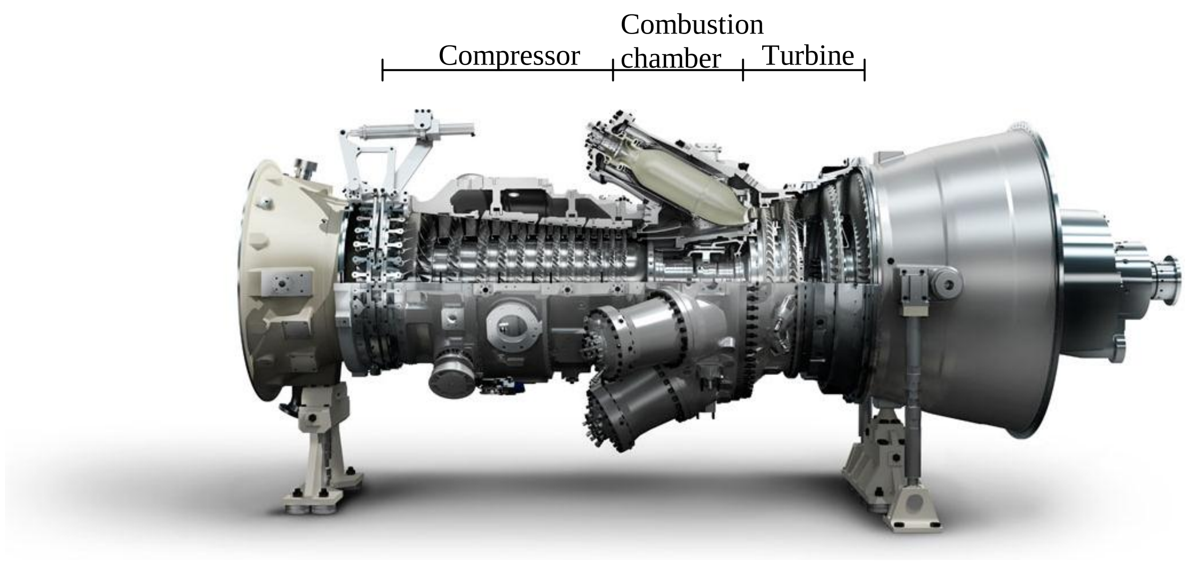

Figure 1. Siemens SGT-750 a gas turbine with combustion chambers of can type.

1.7 Description of Combustion Chambers

The area where the fuel mixes with air and ignites is called combustion chamber. Pressurized air enters the combustor together with the fuel and mixes together. The air/fuel mixture ignites and makes the air expand and therefore accelerate to the turbine, see Figure 2. There are three major types of combustion chambers, annular, can and cannular type. The annular type consists of a single combustion chamber, formed as a ring with the turbine axle in center. The burners are evenly spread around the ring. This enables a radial compact design, but the axle length becomes longer and the combustion system harder to provide a good maintainability. The can combustion chambers consist of multiple cans, evenly spread around the turbine axis with separate transition ducts, see Figure 1 and Figure 2. They serve as separate parts and the compressor air is distributed to each can. This type makes the maintenance easier and can also make the turbine shaft shorter, because the cans don't need to be in line with the gas turbine axle. Because each can is separate the development of new combustion systems is easier to test and evaluate. The last type, cannular is a combination of the other two, where the cans are ending up in an annular gas collector instead of a transition duct. (Cohen et.al., 1996)

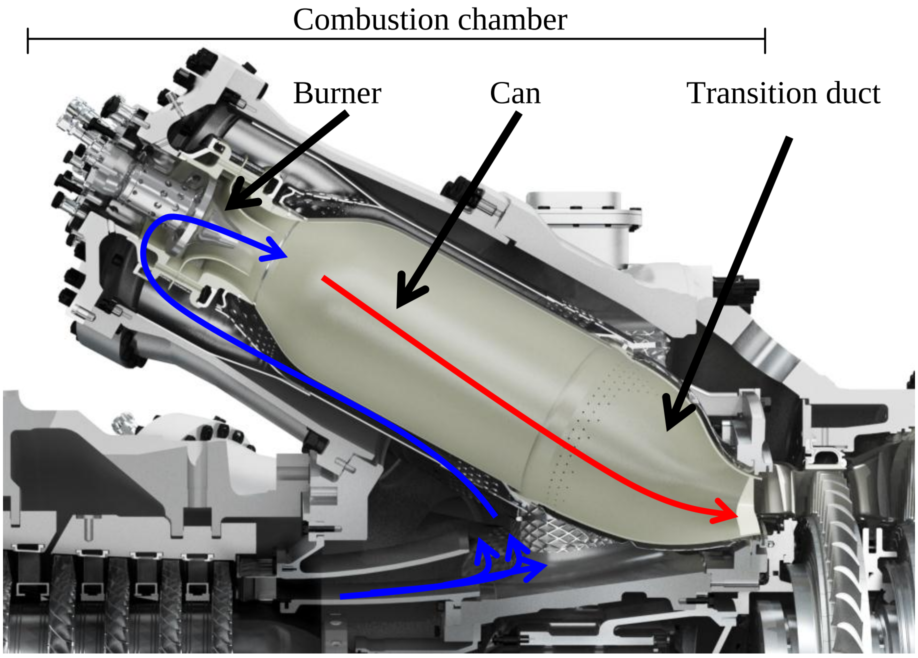

Figure 2. A can type combustion chamber from SGT-750. Compressor air is showed as blue arrows and hot combustion gas are showed as red arrows.

1.8 Description of Transition Ducts

With the annular combustor type the combustor gases has an even spread profile to the turbine. That is not the case with cannular and can type combustors. They need a gas collector or a transition duct to guide the gas from the combustion chamber and at the same time form a nice profile to the turbine inlet. The transition duct, see Figure 2 transforms the gas from circular cross section of the combustion chamber to the kidney formed cross section of the turbine inlet. The transition duct is placed in the central house along with the rest of the combustion parts. In the central housing all of the compressor air enters, although the transition duct is placed in this air stream cooling of the duct is absolutely necessary due to the hot gas inside it. This placement with pressurized air surrounding it and with a lower pressure inside it, different smart cooling techniques can be used to lower the material temperature in the transition duct.

2 Theory

In this chapter the basic theory of heat transfer, fluid dynamics and the mechanics of material are presented in a brief manner. This is theory on which some of the later decisions regarding concept evaluation are to be based on.

2.1 Heat Transfer

At reasonable low moderate temperatures, conduction and convention play the major role in heat transfer. Media in very high temperatures also emits and reflects significant energy through radiation, electro magnetic waves. In temperature range for the transition duct, radiation is significant due to the hot combustion gases and the temperature of the flame. In this part the basics of these things are emphasized to provide a better understanding of the heat transfer.

2.1.1 Conduction

Conduction refers to when heat flows from one high temperature stage in one part of a medium to another part in a lower temperature stage until equilibrium is reached. The rate of heat transfer can be written as Equation 1 referring to Fourier conduction law.

$$\dot{Q} = -kA\frac{dT}{dx} \tag{1}$$

$\dot{Q}$ is the rate of heat transfer through a specific length, dT/dx is the temperature gradient. Each material has a specific thermal conductivity, k and can be defined as the amount of heat conducted per unit time. The heat transfer area, A is always normal to the direction of the heat transfer. Figure 3 shows the principle of the equation. (Storck, Karlsson, Andersson, Loyd, 2003)

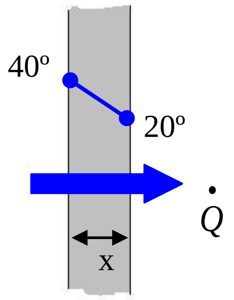

Figure 3. Principle of conduction through a media.

2.1.2 Convection

When heat transferring occurs in fluids instead of solids, it is not just a matter of conduction. It's also heat transfer as a result of macroscopic movements in the fluid, which are called convection. Convection is usually known in two kinds of setups, natural and forced convection. (Storck et.al., 2003)

The dominant driving force in the natural convection is the buoyancy, which depends on temperature difference in the fluid. Forced convection occurs when a velocity field is created by external influence like a fan, compressor or just wind. It is typical used for accelerate the rate of heat exchange. See Figure 4 for the principle of forced convection. (Lakshminarayana, 1996)

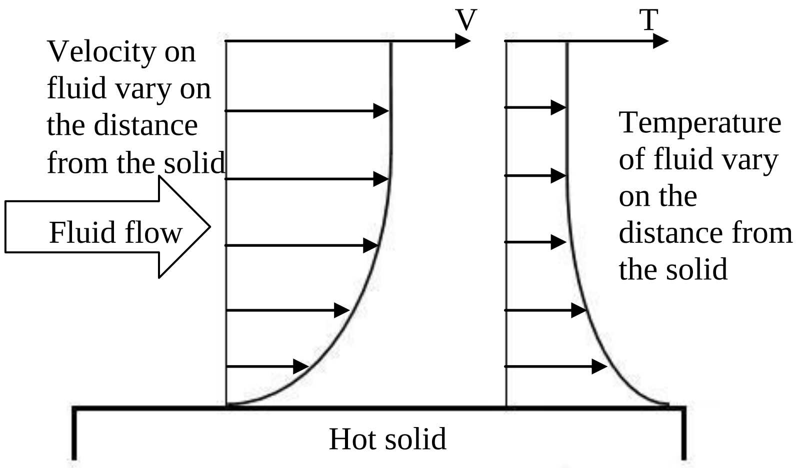

Figure 4. Principle of forced convection. A velocity profile for the fluid to the left and temperature to the right.

Heat from a solid body is transferred to the flowing media if the body has higher temperature than the media. Heat transfer occurs in the viscous layer between the solid and the fluid through both conduction and convection. Energy transport occurs when heat has penetrated into the flowing fluid. (Lakshminarayana, 1996)

The heat transfer is described by Newton's law of cooling, Equation 2. The heat transfer coefficient, α is written as Equation 3 and dependent of the fluids conductivity, *k*, Nusselt number, *Nu* and a characteristic length, *L*. Both the Nusselt number and the characteristic length are dependent of the applied situation. (Storck et.al., 2003)

$$\dot{Q}_{conv} = \alpha_{conv} A \left(T_w - T_{fluid}\right) \tag{2}$$

$$\alpha_{conv} = \frac{kNu}{L} \tag{3}$$

2.1.3 Radiation

All media emits thermal radiation to each other. Radiation is different compared to other heat transfer mechanisms. Heat transfer from radiation is dependent of the temperature to the power of four and no other media is required as a carrier for the energy. The phenomenon behind thermal radiation is electromagnetic waves in the wavelength of 0.1 to 100 μm. The heat transfer, $\dot{Q}$ from a body can be described as Equation 4. The equation consists of two constants, σ is Stefan-Boltzmanns constant and ε is the emissivity of the material. A body both emits and absorbs thermal radiation and the net heat flux between to bodies is described in Equation 5. The resulting emissivity of the two bodies is dependent of the geometries and the emissivity of the material. If the bodies have similar faces faced each other the resulting emissivity is calculated according to Equation 6. Sometimes it is useful to use radiation together with convection and then a heat transfer coefficient is needed. Heat transfer coefficient from thermal radiation is described in Equation 7. The heat transfer coefficient from both convection and radiation can be combined to a total heat transfer coefficient, described in Equation 8. Then the total heat transfer is described in Equation 9. (Storck et.al., 2003)

$$\dot{Q}_{rad} = \sigma \varepsilon A T^4 \tag{4}$$

$$\dot{Q}_{rad} = \sigma \varepsilon_{12} A \left(T_1^4 - T_2^4\right) \tag{5}$$

$$\varepsilon_{12} = \frac{1}{\frac{1}{\varepsilon_1} + \frac{1}{\varepsilon_2} - 1} \tag{6}$$

$$\alpha_{rad} = \sigma \varepsilon_{12} \frac{T_1^4 - T_2^4}{T_1 - T_2} \tag{7}$$

$$\alpha = \alpha_{conv} + \alpha_{rad} \tag{8}$$

$$\dot{Q} = \alpha A \left(T_w - T_{fluid}\right) \tag{9}$$

2.1.4 Thermal Resistance

Heat transfer from a fluid through a wall and to another fluid can be described with thermal resistance. On both sides of the wall both convection and radiation occurs. The heat transfer coefficient can be described as a resistance according to Equation 10. Conduction occurs inside the wall and the resistance through one layer of a wall is described in Equation 11. If the wall consists of multiple layers of material, each material has their own resistance. (Çengel & Turner, 2005)

The total resistance is calculated as if the resistances are connected in series with each other according to Equation 12. Heat transfer calculations with thermal resistance are calculated according to Equation 13. From Equation 13 is it possible to calculate a specific surface temperature of the wall according to Equation 14, where all resistances between the known fluid temperature and the specific surface are subtracted. (Çengel & Turner, 2005)

$$R_{HTC} = \frac{1}{\alpha A} \tag{10}$$

$$R_{wall} = \frac{x}{kA} \tag{11}$$

$$R_{tot} = R_{HTC1} + \sum_{i} R_{walli} + R_{HTC2} \tag{12}$$

$$\dot{Q} = \frac{\left(T_{fluid1} - T_{fluid2}\right)}{R_{tot}} \tag{13}$$

$$T_j = T_{fluid1} - \dot{Q}\left(R_{HTC1} + \sum_{i=0}^{j} R_{wall\,i}\right) \tag{14}$$

2.1.5 Temperature Rise in Channel

When air flows through a channel with hot walls the temperature of the air rises. If the temperature difference is high enough and the channel are long enough the temperature of the cooling air raises so much that the properties of the air changes. The fact that the total heat transfer is dependent of the air temperature, see Equation 13 makes the temperature raise an important factor to take in consideration. To calculate the heat transfer from a channel the mean temperature is used as air temperature along the whole channel to get the best result. The air and flow properties are also considered at the mean temperature. The mean temperature of the air is calculated with Equation 15 where ΔT refers to the temperature difference between the wall and the air at a specific point, see Figure 5. The exit temperature is calculated with Equation 16, where A_w is the hot channel wall surface area. The wall temperature is considered to be constant along the channel. (Bejan, 2004)

$$\Delta T_{mean} = \frac{\Delta T_{in} - \Delta T_{out}}{\ln\left(\Delta T_{in} / \Delta T_{out}\right)} \tag{15}$$

$$\ln \frac{\Delta T_{in}}{\Delta T_{out}} = \frac{\alpha A_w}{\dot{m} c_p} \tag{16}$$

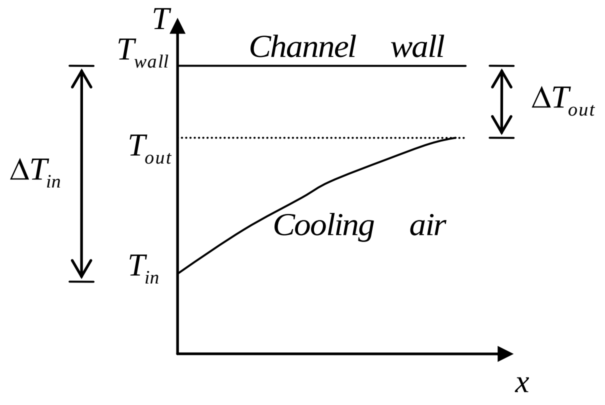

Figure 5. Temperature of flowing cooling air inside a channel with constant wall temperature.

2.2 Fluid Dynamics

In this part the fundamental equations for fluid dynamics are presented. Fluids in movement will create friction against the channel walls which have to be taken in to consideration when calculating. Fluids are also creating reaction forces when the velocity changes due to area variations.

2.2.1 Fundamental Equations

To determine the turbulence of a flow the Reynolds number is used, see Equation 17, where *L* is a characteristic length. For example in channel flow the characteristic length is the hydraulic diameter. Prandtl number is a dimensionless property of the medium that approximate the ratio of thermal diffusivity and kinematic viscosity. It is calculated according to Equation 18. Ideal gas law is the relation between temperature and density of a gas, Equation 19. Continuity equation, Equation 20 is the relation between mass flow and velocity of a streaming fluid (Storck et.al., 2003)

$$\mathrm{Re} = \frac{uL}{\nu} = \Big/ \ \nu = \frac{\mu}{\rho} \Big/ = \frac{uL\rho}{\mu} \tag{17}$$

$$\mathrm{Pr} = \frac{\mu c_p}{\lambda} \tag{18}$$

$$pV = mRT \tag{19}$$

$$\dot{m} = A\rho u \tag{20}$$

2.2.2 Pipe/Channel Flow

In order to calculate heat transfer, fluid mechanics regarding gas flow through pipes or channels is commonly used. In that kind of applications the fluid usually are forced to flow by a fan or compressor. Friction in pipes has a direct relation to the pressure drop through the pipes. By using the pressure drop, the rate of mass flow through the pipe can be determined. To do this calculation the extended Bernoulli's equation is used. (Çengel & Turner, 2005)

Extended Bernoulli, Equation 21 has proven to be a powerful tool which approximates relations between pressure, velocity, elevation and losses in pipes, given that the flow is reasonable incompressible. Losses can be friction in channels, and/or minor losses due to valves, inlets, elbows and so on. (Çengel & Turner, 2005)

$$p_1 + \frac{1}{2}\rho u_1^2 + \rho g z_1 = p_2 + \frac{1}{2}\rho u_2^2 + \rho g z_2 + \Delta p_f + \rho \omega_t \tag{21}$$

In equation 21 $\rho\omega_t$ reflect on the technical work performed from point 1 to point 2. Δp_f are the losses in the pipe. The loss factor ζ in Equation 22 is dependent of the geometric shape and loss type. For minor losses due to elbows, contractions and so on are the loss factor listed in tables found in the literature. The loss factor due to friction is calculated according to Equation 23. The friction coefficient λ depends on the roughness Δ and Reynolds number as long as the Reynolds number are in a certain interval, see Equation 24. (Storck et.al., 2003)

$$\Delta p_f = \zeta \frac{1}{2}\rho u^2 \tag{22}$$

$$\zeta = \lambda \frac{L}{d} \tag{23}$$

$$\lambda = \frac{1}{\left[1{,}8\log\left\{\frac{6{,}9}{\mathrm{Re}_d} + \left(\frac{\Delta}{3{,}71 * d_h}\right)^{1{,}11}\right\}\right]^2} \qquad (2300 \le \mathrm{Re}_d \le 10^5) \tag{24}$$

The amount of air spent on cooling can be calculated with the pressure loss in a pipe, Equation 22 and the continuity equation, Equation 20 according to Equation 25. If the cross section area is described as Equation 26 the mass flow is written as Equation 27. Then it is easy to add different losses in series by Equation 28.

$$\left.\begin{aligned} &\Delta p = \zeta \frac{\rho u^2}{2} \rightarrow u = \sqrt{\frac{2\Delta p}{\rho}}\frac{1}{\sqrt{\zeta}} \\ &\dot{m} = \rho A u \end{aligned}\right\} \rightarrow \dot{m} = \rho A \sqrt{\frac{2\Delta p}{\rho}}\frac{1}{\sqrt{\zeta}} = A\frac{1}{\sqrt{\zeta}}\sqrt{2\Delta p \rho} \tag{25}$$

$$A_{eff} = A\frac{1}{\sqrt{\zeta}} \tag{26}$$

$$\dot{m} = A_{eff}\sqrt{2\Delta P\rho} \tag{27}$$

$$\frac{1}{A_{eff\,tot}{}^{2}} = \frac{1}{A_{eff\,1}{}^{2}} + \frac{1}{A_{eff\,2}{}^{2}} + \ldots + \frac{1}{A_{eff\,n}{}^{2}} \tag{28}$$

2.2.3 Forces due to Fluid Dynamics

All surfaces are exposed for pressure in one or another way, the pressure creates a force according to Equation 29. This can often be neglected because an opposite pressure/force of the same magnitude is acting on the other side of the surface. If this is not the case the resultant force acting on a surface is calculated according to Equation 30. (Storck et.al., 2003)

A flowing fluid raises a force when it changes velocity. The velocity of fluid, Equation 31 can be calculated with the continuity equation, Equation 20 and the ideal gas law, Equation 19. The force is calculated with the momentum, Equation 32 together with Equation 31. (Storck et.al., 2003)

$$F = pA \tag{29}$$

$$F_P = (p_1 - p_2)A \tag{30}$$

$$u = \frac{\dot{m}}{A\rho} = \Big/\ \rho = \frac{m}{V} = \frac{p}{RT}\ \Big/ = \frac{\dot{m}RT}{Ap} \tag{31}$$

$$F_f = \dot{m}(u_2 - u_1) \tag{32}$$

2.3 Mechanics of Material

When designing parts that have to stand forces and temperature variations it is important to understand the fundamentals of mechanics of materials.

2.3.1 Fatigue

Normally a material breaks when the fracture point is reached, but a failure can occur before that. Material that is frequent exposed to plastic deformation will have a short lifetime and will break after a few load cycles, this is called low cycle fatigue, LCF. Also materials that is exposed to lower stress cycles inside the elastic region will break if the loads and number of cycles is high enough, called high cycle fatigue, HCF. (Dahlberg, 2001)

Corrosion caused by high temperature and hostile environment can trigger stress corrosion cracking, SCC, which also cause failure with loads below the yield strength. It is a combined action of stress and corrosion which can lead to crack propagation inside the material. Even if the material shows small signs of attack the cracks can be deep inside the material. A high content of nickel, above 30%, in the alloy is known to prevent SCC. (Flowserve, 2008)

The combination of high temperature and stress in a material can cause creep. Creep is a sort of deformation, a permanent deformation at stresses below the yield strength under presence of high temperatures. When a material creeps it actually flows slowly. Diffusion, dislocation and grain boundary sliding can speed up the process. (Askeland & Phule, 2005)

2.3.2 Thermal Expansion

Almost every material expands with increased temperature. The expansion is not permanent and return when the temperature decreases. The expansion is caused by movement of the atoms. If you imagine the atoms are held together with springs, low temperature means low energy, the atoms vibrate with low amplitude and the springs hold the atoms close together. When the temperature rises, the energy increases and so does the amplitude of the vibrations, which cause the springs to elongate. The volume of the material will therefore increase with temperature. Almost all materials expands in each direction, a few does not, such as wood and single crystal materials. Within a certain range the expansion is often directly proportional to temperature. All dimensions expands according to Equation 33, it can be, thickness, height, length or diameter for example. The volume increase is described in Equation 34. α is the coefficient of linear expansion and β is the coefficient of volume expansion, for solid materials the relation between the coefficients is $\beta=3\alpha$. The coefficients depend on material and the temperature and can be found in material tables. (Young & Freedman, 2003)

$$\Delta L = \alpha L_0 \Delta T \tag{33}$$

$$\Delta V = \beta V_0 \Delta T \tag{34}$$

2.3.3 Thermal Stress

Due to thermal expansion, stresses occur in the material if it is not allowed to move. If the material is clamped in the ends and heated, expansion is not possible. Compressive stresses will occur in the material. If the temperature is decreased instead of increased tensile stress occurs instead. The stress is calculated with Equation 35. Thermal stress will also come up in materials with different temperature inside the body. (Young & Freedman, 2003)

$$\sigma = \frac{F}{A} = -E\alpha\Delta T \tag{35}$$

3 Method

For several thousands of years human have had the urge to develop and improve products and processes of different complexity. In recent years the product development process has been documented in order to try making a general layout for this process, without success. Today there are a number of methods for different approaches in use, depending on which kind of product or process to be developed. There are also various standards at different companies including guidelines for choice of method. Usually the concept development process is divided into following steps.

- Product Specification
- Concept Generation
- Concept Evaluation and Selection

Each step includes a number of useful methods to choose depending on the project structure. Methods used in this project are emphasized in this chapter.

3.1 Product Specification

The goal in this step is to establish a list of design criteria that in engineering terms explaining the customer requirements. To achieve that, good knowledge about the problem has to be established. To reach that state of knowledge the problem first has to be inspected critically to discover what the problem is, who has the problem, what should the product achieve and what are the limitations.

It is also necessary to investigate if similar products or techniques exist. Doing a “state of the art” brings information about other similar products. There can also be other products in other areas that solve similar problems in an interesting way. Patents are a good source to find these interesting solutions as well as study literature within the area.

In the list of design criteria, properties are established which the product has to fulfill to satisfy the problem. The list serves two purposes, the first is to serve as a guide in the design process and the second is to help in the evaluation stage. There are typical two types of criteria in the list, requirements and wishes. The requirement criteria have to be fulfilled and the wish will gain the positive response from the customer if it is accomplished. (Liedhom, 1999)

3.2 Concept Generation

With the list of design criteria as base and with systematical procedures conceptual design solutions are generated in this step. In order to find the best design it is important to generate a great number of concepts in this step. To make the output from this process easy to address, certain methods are used to visualize the design solutions.

3.2.1 Function- Means Tree

Function- means tree, F/M tree is used to find possible solutions for a design problem. A design problem has often one main function that has to be solved. The main function is possible to breakdown into sub functions, which is solved by means. The idea is to list functions that are needed and possible means that realizes the function, see Figure 6. (Liedhom, 1999)

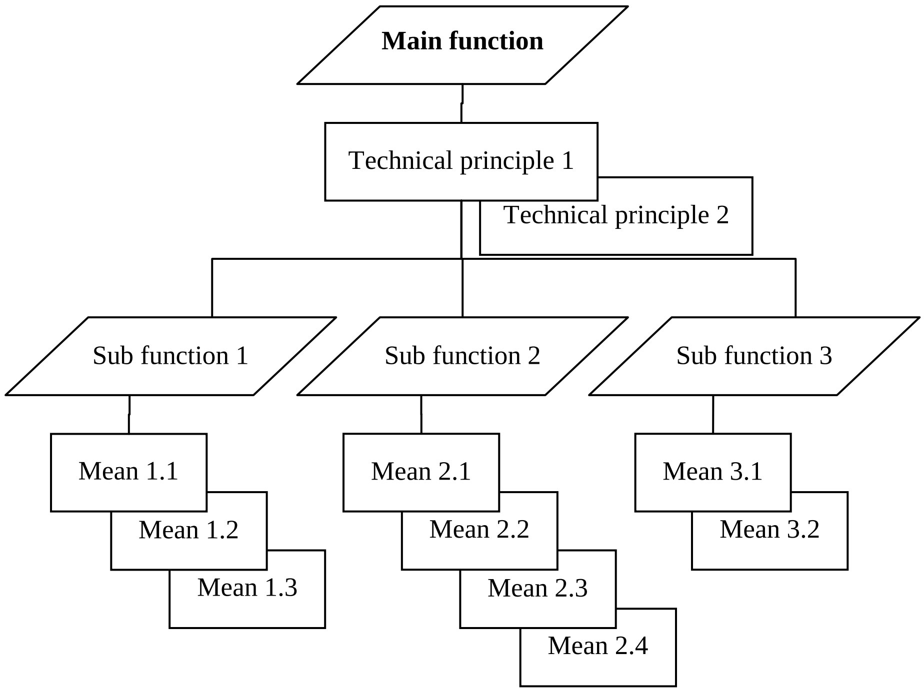

Figure 6. Example of a function- means tree.

3.2.2 Morphology Matrix

The function- means tree easily grows and might be hard to follow. Then a morphology matrix can visualize the solutions for the sub functions. Table 1 is an example of a morphology matrix. The morphology matrix shows the bottom level of the function-means tree. It is easy to combine concepts from the morphology matrix. The theoretical number of concepts generated from the morphological matrix is the numbers of means for each sub function multiply each other. This may results in too many concepts and it is important to only choose feasible combinations. The example in Table 1 can theoretically result in $3 \times 4 \times 2 = 24$ individual concepts. (Ullman, 2010)

Table 1. Example of a morphology matrix.

Functions	**Means**			
Sub function 1	**Mean 1.1**	**Mean 1.2**	**Mean 1.3**	
Sub function 2	**Mean 2.1**	**Mean 2.2**	**Mean 2.3**	**Mean 2.4**
Sub function 3	**Mean 3.1**	**Mean 3.2**		

Concept 1	**Concepts 2**	**Concepts 3**

3.3 Concept Evaluation and Selection

In this step all concepts will be compared against each other with methods emphasized in this chapter. The goal is to sort out the best concept or concepts for further development.

3.3.1 Go-/ No Go Screening

Go-/ no go screening is an easy method used to eliminate concepts in an early stage of the concept evaluation phase. The criteria are based on the set of customer requirements developed during the product specification part, which the concepts have to fulfill. These criteria should be formulated as yes and no questions and then applied at each concept. The answer on those questions decides if the concept is a “Go” or “No Go”. “Yes” and “maybe” answers will send the concept to the next step in the evaluation, while a “No” rejects the concept, unless changes can be made to make it a “Go”. To visualize this method a matrix is used like the one in Table 2. (Derelöv, 2002)

In this method it can also be helpful to consult an expert in the particular area to make the answers more defined. It can be implemented by structured or semi-structured meetings with the expert and weak concept can be eliminated faster to save time later on in the evaluation process. (Derelöv, 2002)

Table 2. Example of a Go-/ no Go screening.

Go-/ no Go screening							
	Elimination Criteria (+) Yes (-) No (?) More information necessary				**Decision** (+) Go (-) No go (?) More information necessary		
	A: Solves the problem						
		B: Meets all requirements					
			C: Realizable				
				D: Within cost limits			
					F: fits the company		
Concept	**A**	**B**	**C**	**D**	**F**	**Comment**	**Decision**
Concept 1	+	+	+	?	+	Uncertain	Ongoing
Concept 2	+	-					No go
Concept 3	+	+	+	+	+	Meets requirements	Go

3.3.2 Pairwise Comparison

All criteria are not equally important all the time. It is therefore a good idea to weight them against each other. Pairwise comparison is a good method for weighting criteria. The idea of this method is to compare pairs of criteria and summarize the result in a table, see Table 3. If a criterion has equal importance to another it gets a value of 1, if it is less important the value is 0 and 2 if it is more important. The sum of a row describes the importance of the criterion. There are different ways of using the result from this method. One way is to use rang between the criteria, but that does not always show the right picture. Then a normalized sum can be an alternative. The normalized sum is the percentage of the total values a specific criterion. It is calculated according to Equation 36 or Equation 37 depending on what scale to use, see Table 3. The disadvantage of a normalized sum is the fact that a criteria with value 0 is left without any sentence. Then a scale from 1-10 or 1-5 can be fairer. It is calculated according to Equation 38 or Equation 39 depending of what scale to use, see Table 3. (Cross, 1994)

Table 3. Example of a pairwise comparison of four criteria.

								Norm Sum		**Scale**	
Criteria	**A**	**B**	**C**	**D**	**Sum, x_i**	**Rang**		**0-100**	**0-1**	**1-10**	**1-5**
A	-	0	2	1	3	3		25	0,25	6	3
B	2	-	2	1	5	1		42	0,42	10	5
C	0	0	-	0	0	4		0	0,00	1	1
D	1	1	2	-	4	2		33	0,33	8	4
	Total Sum				**12**			**100,00**	**1,00**		

$$\lambda_{norm,100} = \frac{x_i}{\sum x_i} \cdot 100 \tag{36}$$

$$\lambda_{norm,1} = \frac{x_i}{\sum x_i} \tag{37}$$

$$\lambda_{scale,10} = 1 + \frac{(x_i - \min(x_0,..,x_n))}{\max(x_0,..,x_n) - \min(x_0,..,x_n)} \cdot (10-1) \tag{38}$$

$$\lambda_{scale,5} = 1 + \frac{(x_i - \min(x_0,..,x_n))}{\max(x_0,..,x_n) - \min(x_0,..,x_n)} \cdot (5-1) \tag{39}$$

3.3.3 Datum Matrix

This method also known as Pugh's method, named after the British engineer Stuart Pugh. It is an easy method that can be used to rank the concept in a relative early state of the project, when the information of the concepts is not complete. The method compares the ability to reach criteria of each concept with a reference, datum. Values can be estimated if it is not known. The method does not consider how good the ability is, just if it is better, worse or equal to the reference. The reference can be an existing product or one of the concepts. It is an iterative process where the datum reference is changed between the iterations to get a better interpretation. To get a better view of the result, the criteria can be weighted. Table 4 is an example of a datum matrix with weighted criteria. One way to weight the criteria is pairwise comparison, see chapter 3.3.2. It is important to analyze the result with an open mind, it is not always the best concept wins or the worst loses. A good idea is to look what makes a good concept bad and see if is possible to make it better. (Ullman, 2010)

Table 4. Example of a datum matrix with weighted criteria.

		Concepts					
Criteria	**W**	I	II	III	IV		
A	3	DATUM	0	+	-		+ Better
B	1		-	0	+		- Worse
C	4		-	0	+		0 Equal
D	2		-	-	+		
Total		0	-3	0	2		
Weighted total		0	-7	1	4		
Rank		3	4	2	1		

3.3.4 Weighted Objectives Method

In this method the concepts are evaluated directly against the criteria, independent of the other concepts. To be able to succeed with this method both the criteria and concepts must be well defined. The criteria must be weighted and this can be done with pairwise comparison, see chapter 3.3.2.

One of the most important steps in this method is to set up the right utility scores. The score scale is individual for each criterion but should be in the same range. Range in the interval of 0-1.0, 0-5 and 0-10 is usual. The score range does not have to be linear, it can be higher resolution for more interesting intervals or described in a graph. The measurable value of each criterion, *m* in Table 5 for each concepts gives a specific score from a utility score table. Table 7 is an example of utility scores for fuel consumption of a car. If it is hard to set a value of the criteria, judgment scales is needed, see Table 6. The score can be set by someone with good understanding of that criterion, for example a serviceman when the criterion is “good serviceability”. A simple example of car engine concept evaluation with weighted objectives method is showed in Table 5.

With the weighting from the pairwise comparison, *W* and the score generated from the criteria values, *V* each concept gets its final total score, *OWV* in Table 5. From this value all the concepts can be arranged in order from the concept that fulfills the criteria best to the one that are fulfilling worst. (Cross, 1994)

Table 5. Example of weighted objectives method applied at car concepts.

			Concepts								
			Ideal solution			I			IV		
Criteria	W	Unit	Magnitude m_{i1}	Score V_{i1}	Weighted score WV_{i1}	Magnitude m_{i2}	Score V_{i2}	Weighted score WV_{i2}	Magnitude m_{i3}	Score V_{i3}	Weighted score WV_{i3}
Low fuel consumption	2	[l/km]	0,03	5	10	0,1	0	0	0,058	3	6
Good serviceability	5	[-]	Perfect	5	25	Weak	1	5	Good	3	15
Low weight	1	[kg]	50	5	5	200	0	0	110	3	3
High power	4	[kW]	150	5	20	10	0	0	100	4	16
Sum W_i	12			OWV_1	60		OWV_2	5		OWV_3	40
				OWV_{1norm}	1		OWV_{2norm}	0,083333		OWV_{3norm}	0,666667

Table 6. Example of utility scores of two judgment scales, 11 point and 6 point scale for unmeasurable values.

Judgment scales			
11 point scale		6 point scale	
Score	Meaning	Score	Meaning
0	totally useless solution	0	inadequate
1	inadequate solution		
2	very poor solution	1	weak
3	poor solution		
4	tolerable solution	2	adequate
5	adequate solution		
6	satisfactory solution	3	satisfactory
7	good solution		
8	very good solution	4	good
9	excellent solution		
10	perfect solution	5	excellent

Table 7. Example of utility scores for cars fuel consumption.

Fuel consumption	
Value [l/km]	Score
> 0,1	0
0,10-0,085	1
0,085-0,07	2
0,07-0,055	3
0,055-0,04	4
< 0,04	5

3.3.5 Design Optimization

Design optimization is a method to speed up and improve the design process. In product development there are several objectives that have to be solved without violating any constrains. This can be seen as an optimization problem, which is normally a mathematical genre. The idea is to explain the design problem in a function that has to be optimized. All design work can not be done with design optimization, there are always parts of the design process that need to be handled by humans. One way of using design optimization is shown in Figure 7, where the optimization is used in the concept evaluation. (Ölvander, 2010)

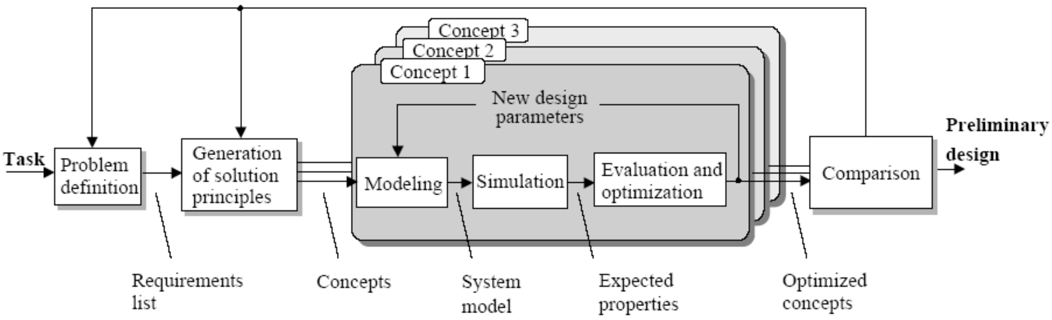

Figure 7. Example of design optimization used in the product development process. (Ölvander, 2010, p 9)

There are many different optimization techniques, one of them are Newton's method. Newton's method is a derivative method, which uses the derivate and the second derivate to get a better solution from the starting one. The method is an iterative process and jumps from point to point to find the optimal solution, see Figure 8. A disadvantage of the method is the fact that it does not separate local and global optima. To obtain good result, the starting point has to be chosen carefully. (Onwubiko, 2000)

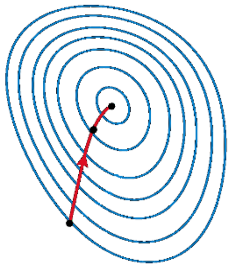

Figure 8. Newton's method used at a optimization problem.

4 State of The Art

In this chapter, techniques of useful cooling, mounting and sealing methods are investigated. This is the fundamental base on which the project starts from, in order to construct new innovative solutions regarding cooling and mounting techniques. The result of the patent search can be found in Appendix 1.

4.1 Current Transition Duct Design

As mentioned in chapter 1.8, the transition duct serves as a guide for the hot gas from the combustion chamber to the first stage in the turbine.

Pressurized air from the compressor flows around the transition duct on its way to the combustion chamber. From this point the pressure is dropping when the air travels through the combustion system, creating a lower pressure inside the combustion chamber and the transition duct. All of the compressor air is not used for the combustion and some part of it, around 17 % is used for cooling. The transition duct is constructed with two skins of high temperature resistant metals. The outer skin contains over 1000 small holes, around 1,5-2 mm in diameter evenly spread over the whole surface. The cooling air flows through the holes and hits the inner skin with high velocity. This is called impingement cooling, see chapter 4.2.1. Most of the impingement air flows between the skins to the upstream part and dumps into the transition duct via holes at the inner skin. The dumped air creates a cooling film near the duct wall. The rest of the impingement air flows downstream and cools the outlet lip.

The transition duct is mounted with a flange to the stator ring. The flange is welded to the transition duct and goes around the whole outlet end. The flange is not completely fixed in the stator ring, which enables thermal expansion. The outboard flange rests at a heel at the stator ring that keeps the transition duct from moving in radial direction. The inboard side is not fixed in radial direction and is therefore thermal flexible. Clamping bars are attached over the flange on each side of the transition duct. The clamping bars are pressed against a heel on the stator ring with bolts. This creates a slot between the stator ring and the clamping bars. In which the flange is mounted with a small clearance, allowing the flange to move because of expansion.

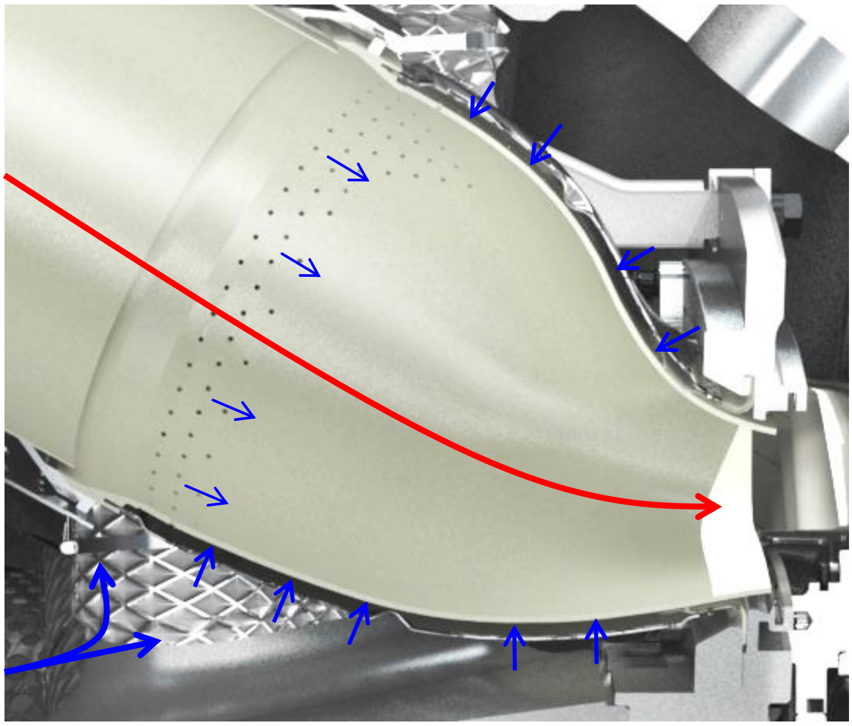

Figure 9. Current transition duct with air flow and hot gas flow marked with blue respective red.

4.2 Cooling Methods

This part presenting the techniques used today in order to cool hot structures in the gas turbine combustion area.

4.2.1 Impingement Cooling

Impingement cooling is of forced convection type where two shells are needed, a jet plate and the target plate, see Figure 12. High velocity jet streams of air are ejected through holes or slots in the jet plate and hit the target surface, see Figure 10. It has one of the greatest potentials to achieve high local heat transfer coefficient, compared to other cooling methods. (Han, Dutta, Ekkad, 2000)

After the jet streams have hit the target plate it flows between the plates and helps to transfer away the heat. The cross flow has also one major drawback, it deflects the jet stream from the target surface which leads to lower heat transfer coefficient. (Han et.al., 2000)

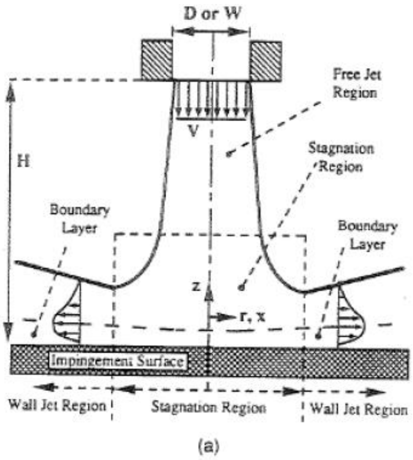

Figure 10. A single jet propagation between two surfaces. (Han et.al., 2000, p 252)

4.2.2 Rib Cooling

Rib cooling is a common cooling type in turbine blade channels. Ribs are placed vertical to the airflow to disturb the flow, see Figure 11. The ribs makes the flow more turbulent and mixes cool and hot air near the wall. Ribs can be angled relative the flow. Both the heat transfer coefficient and pressure drop depends on the rib shape and angle. (Han et.al., 2000)

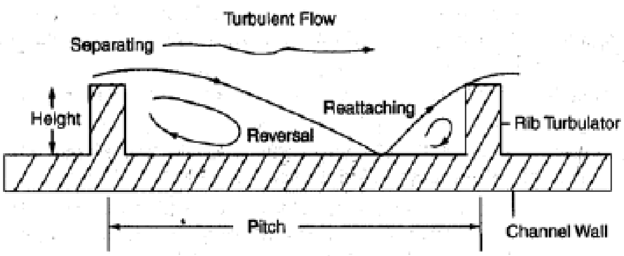

Figure 11. Principle of rib cooling. (Han et.al., 2000, p 288)

4.2.3 Film Cooling

There are different ways of film cooling. All of those inject air to the hot side of the surface to create a thin cool air film near the wall, see Figure 12. The film acts like an insulator for the hot gases. The simplest way to achieve film cooling is with slots that leads the flow near the wall. It is important to get a uniform distribution, otherwise hot spots can appear. The effect of film cooling is highest near the opening and decreases downstream. This works quite well together with other non injecting cooling methods on the cold side between the ejecting slots. (Abdon, 2001)

4.2.4 Transpiration Cooling

Transpiration cooling is another way to create film cooling and this type is very effective, up to tree times more efficient to other cooling techniques. The air injection is made by many small pores in the wall where the air leaks out and creates a homogeny film, see Figure 12. The pores increase the convection inside the wall, before the air exits at the hot side. Due to impurities in the air, the pours can get blocked and the cooling effect decrease. (Abdon, 2001)

4.2.5 Effusion Cooling

Effusion is a cooling method that is quite similar to transpiration cooling. The method uses many small inclined drilled holes instead of pores, see Figure 12. It enhances the convection inside the wall as well and creates a homogenous film. The effectiveness is a little bit less than with pores wall, but better than other film cooling techniques. (Zhang, Lin, Xu, Liu & Song, 2009)

4.2.6 Cooling Channels

Cooling channels may be used to cool large areas. The channels is often produced of bonded sheets of metal, with for example one middle sheet with the channels and an outer and inner sheet with inlet respectively outlet hole. The thermal gradient is lowered by decreasing the distance between the channels and by alternately changing flow direction inside the channel.

4.2.7 Commercial Methods

There are some commercial solutions to reduce the amount of cooling air. They try to imitate the transpiration cooling and have much better thermo-mechanical resistance. Transply® is built up with several laminates with small holes and channels. The holes are not concentric and create a labyrinth thru the laminates where the air flows. Lamilloy® is similar to transply but consist of laminated metal sheets with small distances between. The air travels between the sheets in small holes, see Figure 12. (Cerri, Giovannelli & Fedrizzi, 2007)

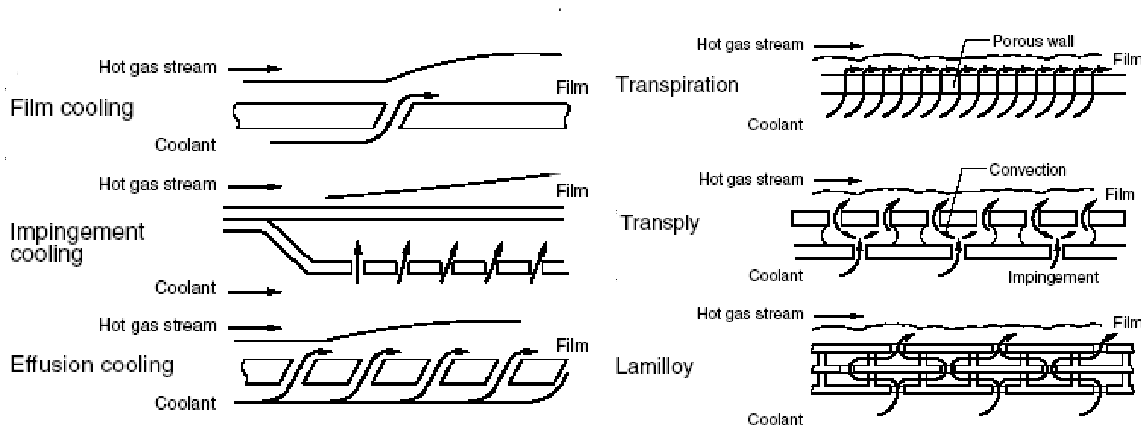

Figure 12. Principle of different cooling methods. (Cerri et.al. 2007, p 693)

4.2.8 Thermal Barrier Coating

Thermal barrier coatings, TBC, consist of an intermetallic oxidation-resistant bond coat overlaid with a ceramic material as top-coat. TBC are used as an insulator on hot parts in the turbine. For example turbine blades, guide vanes and combustors. Due to low thermal conductivity the TBC not just serves as a good insulator, it also makes the temperature distribution more homogenously over the surface. This lowers the thermal stress in the coated material. In order to get a long lifetime of the TBC it is central that the bond coat not get overheated.

The top-coat is either deposit with atmospheric plasma spray, APS, or electron-beam physical vapor deposition, EB-PVD. The APS creates a splat-based layered structure which has the best insulation and this method is most cost effective. EB-PVD creates a coating with superior thermal shock resistance and strain tolerance. (Han et.al., 2000)

4.3 Mounting and sealing methods

When designing hot structures in gas turbines many parameters have to be taken in consideration to avoid failure. This is not made by all of the manufactures but many of them. The transition duct can not be mounted in a way that do not allow the part to move due to temperature expansion or in a way that causes high temperature gradient. Both of these parameters will exhaust the material which may lead to failure.

From the patent search result, which is summarized in Appendix 1 many solutions have been studied in order to gain the knowledge of hot structure design. These solutions are presented here in a brief way.

4.3.1 Bracket Mounting

One commonly used mounting method is a bracket fitted on the outboard side of the transition duct connecting it to the central housing via a more or less strict joint. Figure 13 shows a solution of a bracket seen from the side. This bracket allows the duct to rotate around the bolt in point 36. The ability to move allows the duct to find the best position with the lowest reacting forces during thermal expansion. Bracket mountings are often used as an extra support along with a week mounting in the aft end which not is made to handle large forces.

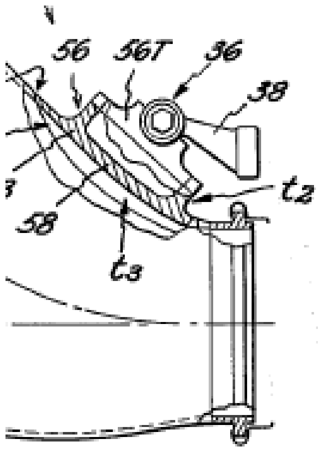

Figure 13. Bracket mounting on the outboard side. (Power Systems Mfg 2002)

4.3.2 Flange Mounting

The patent search has showed that different types of flange arrangements often are used to position the transition duct in the aft end. Flanges have the ability to handle relatively large movement and bending due to the small thickness/length ratio. That makes it possible to attach the flange arrangement both on the transition duct and the connection to the central housing. The flange is often welded to the duct as the connection to the central housing can be either strict bolted or mounted in some sort of groove. These solutions have to have a balance between stiffness and thermal flexibility in order to be secured without exhausting the material. Today the transition duct in the SGT-750 uses the method with a flexible flange mounted in a groove, shown in Figure 14.

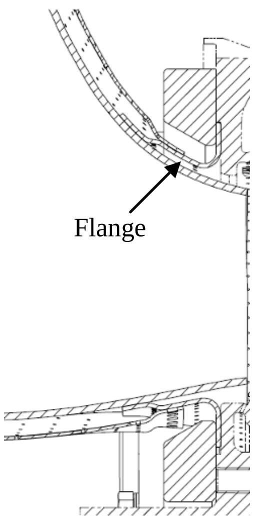

Figure 14. Flange mounting, used today at the SGT-750.

4.3.3 Frame Mounting

Different types of frames are also commonly used to support the duct in the aft end. The basic idea is to fasten the frame in the aft end in some way and then fix the frame strictly in the central housing. The two figures Figure 15 and Figure 16 shows two principles. Figure 15 is the principle that is used most. This frame is either clamped around some sort of flange or in some cases welded directly to the duct. The welded solution is said to be a poor solution in the matter of low cycle fatigue. Even the clamped frame can be a victim of low cycle fatigue depending on how much expansion clearance the flange has in the frame. Figure 16 is a support that not is fasten in the aft end, instead the duct is just pushed inside the frame and then locked with some sort of extra support. The solution has not showed in any commercial turbines but is a patent from Siemens in Orlando. This solution requires a sealing that is able to handle all of the movement due to thermal expansion.

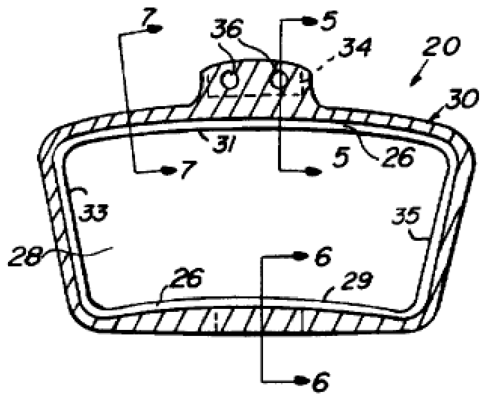

Figure 15. Principle of a frame mounting with a flange. (General Electric Company, 1988, p 3)

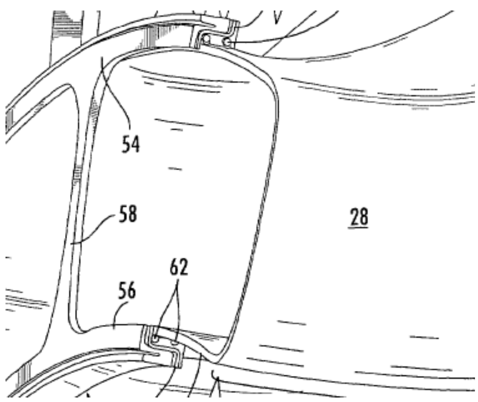

Figure 16. Principle of a frame mounting. (Siemens Energy Inc, 2009, p 5).

5 Concept Development

In this part of the development, concepts are generated and visualized using methods presented before together with the design specifications, see section 5.1.

In order to make the concept generation process more perspicuous the concepts are divided in two divisions. One processing new cooling methods and the other one processing methods to mount and seal the transition duct. This can be done because of the rather stand-alone characteristic in the solutions of cooling and mounting together with sealing. Later the cooling concepts are referred to CX, mounting concepts to MX and sealing solutions to SX, where X is a number.

From the list of design specifications and knowledge gathered in the State of The Art chapter, a function- means tree with all functions of the transition duct is made, the tree can be found in Appendix 2. In this tree the function of cooling, mounting and sealing are selected and branched down in two separate function- means trees.

5.1 Project Specification

At the start of the project a preliminary project specification list was constructed. The list has been developed together with personnel at SIT AB during the whole project as more facts about the problem have been discovered. The final list is presented here on the next page.

5.1.1 Project specification list

Each criterion is marked with either a R for requirement or W for wish.

1. Function

Guide hot gas from the combustion chamber to the turbine.	R

2. Function-controlling properties

Aft end should be dynamic rigid	R
Aft end should allow radial thermal expansion	R
Controllable leakage flow in the aft end	R
Thermal axial expansion should be in line with the combustor can	R
Same internal shape as the present transition duct	R
Temperature of the material should be lower than 1100K	R
Slim design in respect to the total volume	W
Low temperature gradient in the material	W
Spend as little cooling air as possible	W

3. Life cycle characteristics

Mounting the transition duct should be easy	W
Easy to maintain through one ”port hole”	W
Possible to repair	W
Same lifetime as current design	W

4. Manufacturing characteristics

Possible to manufacture with known techniques	R
Possible to manufacture in the present workshop	W
As low cost as possible	W

5.2 Concept Generation Cooling

As described before, mounting and cooling concepts are separated at the first concept phase. This chapter considers generation of cooling concepts. The chapter begins with a function mean tree to illustrate possible solutions and continuing with a morphology matrix to combine different cooling concepts that is later evaluated in chapter 5.3.

5.2.1 Function- means Tree Cooling

The branch regarding cooling of the transition duct material is showed in Figure 17. The “Air cooling” mean contains functions which improves the cooling. In the “Cooling method” branch at least one mean has to be chosen. The other two branches are functions that have potential to gain the cooling efficiency together with some of the cooling methods.

Later in the process some of the means under the cooling function may be combined to shape new concepts to cool the transition duct. For example impingement can be possible to combine with effusion cooling method.

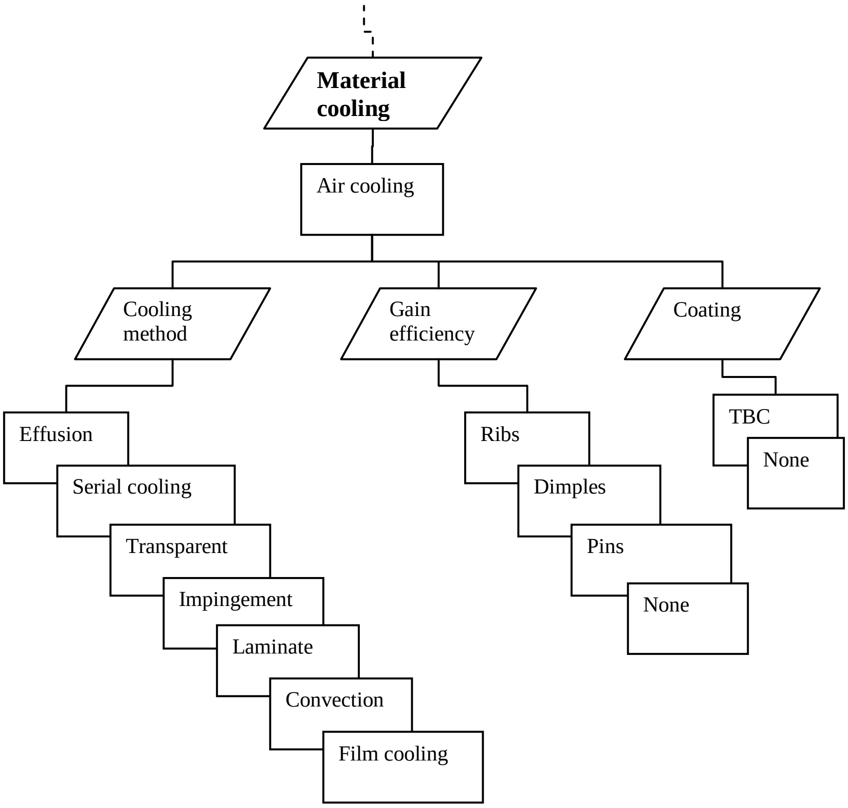

Figure 17. Function- means tree for cooling concepts.

5.2.2 Morphology Cooling

This is the first stage where all basic cooling methods are visualized with no respect taken to the effectiveness of the cooling.

From the branch regarding cooling of the material the first brief morphology is made to give a visualization of possible combinations of the means. The table is created from the lowest function level in the tree, with its associated means. In this matrix, Table 8, possible combinations are shown with different shaped and colored symbols. Each concept refers to a specific symbol with a specific color. There are totally 28 concepts combined and a table of these combined concepts can be found in Appendix 3. Not that no concepts are combined with the mean "Transparent" due to the fact that it is an infeasible solution in this context. The pores in transparent cooling is smaller than the smallest hole diameter that is allowed to use in a gas turbine at SIT AB.

Table 8. Morphology matrix for cooling concepts. Each concept refers to a specific symbol with a specific color.

Functions	Means						
Cooling meth	Effusion	Serial cooling	Transparent	Impingement	Laminate	Convection	Film
Gain efficienc	Ribs	Dimples	Pins	None			
Coating	TBC	None					

5.3 Concept Evaluation Cooling

In order to be able to evaluate the concepts in a more honest way calculations will be performed, but that can not be done at all of the 28 concepts. Instead a first elimination is performed to decrease the number of concepts based on knowledge and limitations of the project.

In this first step of the evaluation, the method of Go/no go-screening is used to eliminate concepts that are not suitable to solve the technical problem in a satisfying way. This screening contains all of the above mentioned concepts and is found in the Appendix 4. The remaining cooling concepts which will be further evaluated are presented here in Table 9, Figure 18 and in the following text.

Table 9. Remaining concepts after the first elimination, Go/noGo screening.

■	C1	Effusion
■	C2	Effusion with TBC
◎	C5	Serial with ribs
◎	C6	Serial with ribs and TBC
◎	C9	Serial
◎	C10	Serial with TBC
◆	C11	Impingement
◆	C12	Impingement with TBC
☾	C19	Laminate
☾	C20	Laminate with TBC
▲	C27	Film
▲	C28	Film with TBC

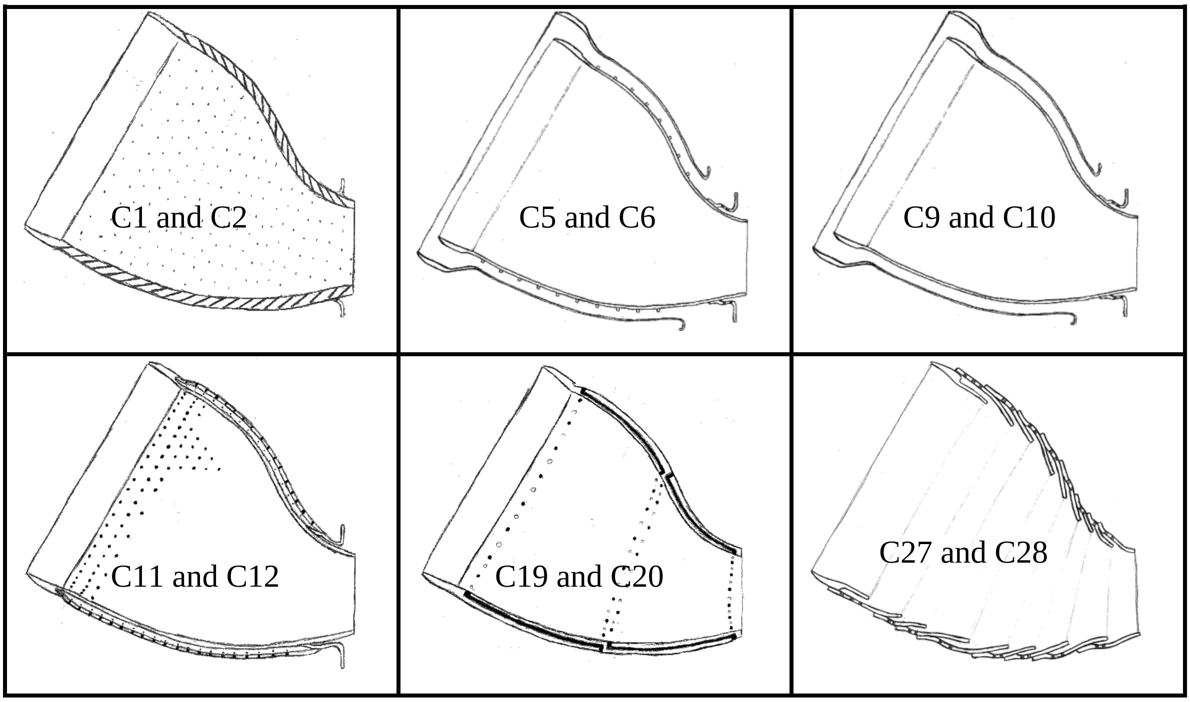

Figure 18. Sketches of remaining concepts. Each sketch contains two concepts, one without and one with thermal barrier coating.

Concept C1 and C2, Effusion cooling without and with TBC

Effusion cooling, also known as film cooling is a well known cooling method, it is especially used at guide vanes and blades in the turbine. These concepts are made of one shell and the idea is to have small angled holes drilled in the shell. Air leaks through the holes and create an insulating film between the wall and the hot gas. The material is also cooled by the air flowing through the holes due to convection. The holes are angled to the surface to get a larger cooling area and to get a smooth transition from hole to film. The difference between concept C1 and C2 is that TBC is applied to concept C2. Thermal barrier coating is a thin layer of insulating material applied at the hot side wall.

Concept C5, C6 Serial cooling with ribs, without and with TBC

These concepts are made of two shells. The idea is to force all or a part of the combustion air to flow between the hot duct wall and an outer shell before it reaches the burner. Due to the high air velocity the heat transfer coefficient will be rather high. To increase the heat transfer coefficient small ribs is used to disturb the flow. Difference between concept C5 and C6 is TBC.

Concept C9 and C10 Serial cooling without ribs, without and with TBC

Just as concept C5 and C6 theses concepts are made of two shells which the air flows between. No ribs are used to disturb the flow and therefore a larger amount of air is forced this way. Serial cooling with thermal barrier coating and without ribs is used today at the combustor can. Difference between concept C9 and C10 is TBC.

Concept C11 and C12 Impingement cooling, without and with TBC

Today the transition duct is cooled by impingement without TBC and ribs. Two shells are used in these concepts. Small holes are drilled in the outer shell and some holes are drilled in the inner skin. Air ejects from the holes in the outer skin and hits the inner skin with high velocity and then the air passes the holes in the inner skin and dumps in the hot gas. The difference between concept C11 and C12 is that TBC is applied to the inner skin.

Concept C19 and C20 Laminated sheets, without and with TBC

Laminated sheets are a relatively new technique based on longitudinal channels inside the material in which cooling air flows. The channels are many in numbers and rather small in diameter. Flow direction in adjacent channels alternates to keep a low temperature gradient. The difference between concept C19 and C20 is TBC.

Concept C27 and C28 Film cooling, without and with TBC

Film cooling is rather similar to effusion cooling but these concepts create the insulating film via slots instead of holes. One shell is needed but the shell is made of rings. Between the rings is an annular slot located. The slot lip is cooled by impingement jets, which are later transformed to an insulating film. The difference between concept C27 and C28 is TBC

5.3.1 Datum Matrix

Due to the time limit of this project the concepts have to be reduced even more and a datum matrix is used. This is done in the beginning of the heat transfer calculations when relative low facts about the concepts are known. The result can be seen in Table 10. The criteria used in this evaluation are ranked based on the importance. The concept based on film cooling, Concept C27 & C28 are eliminated as well as the effusion concept without TBC. The film cooling concepts are eliminated because the manufacturing process will be very hard and expensive. Experience at SIT AB has also shown that it is an air consuming method. Effusion cooling without TBC will be removed due to the fact that the temperature gradient will be too high.

Table 10. Datum matrix for cooling concepts.

Criteria	W	Concepts						
		C1&C2	C5&C6	C9&C10	C11&C12	C19&C20	C27&C28	
Low air consumption	4	0	+	+	DATUM	+	-	+ Better
Low temperature gradient	3	-	0	0		0	-	- Worse
Slim design	2	+	0	0		+	0	0 Equal
Cost	1	0	-	0		-	-	
Total		0	0	1	0	1	-3	
Weighted total		-1	3	4	0	5	-8	
Rank		5	3	2	4	1	6	
Decision		go	go	go	go	go	no go	

5.3.2 One Dimensional Heat Transfer Calculations

In order to be able to compare the remaining concepts in regards of cooling effectiveness calculations are performed on the different methods. These calculations are made using different correlations which are results from years of research and testing. In order to get the best results optimization with Newton's method have been used for all cooling calculations.

Assumptions are made regarding the surface on the transition duct and the heat transfer coefficient at the hot side. All calculations are made at a flat surface with the same area as the transition duct to take our limitations in consideration. The heat transfer coefficient is set to a calculated constant value on the hot gas side of the wall and is equal for the different cooling methods except the case with effusion cooling.

The rates of effectiveness is calculated by setting a maximum allowed temperature of 1100K on the hot side of the wall, and then calculate the least possible consumption of cooling air for each concept. To see the possibilities to improve the cooling with each concept, an overcooling test is performed. The same calculations are made with lower maximum temperature of 1050K and the difference of spent cooling air is referred as a performance. The overcooling test is used to see if the concepts are able to reach lower wall temperatures for safety reasons. Current design gives a wall temperature of 1032K in our calculations. In the calculations regarding the serial cooling method two design cases have been established due to the uncertainty regarding the permitted pressure loss through the duct. One design case is calculated with a permitted pressure loss of 0,25% and the other case is calculated with 0,50%. In the result table, the index 0,25 and 0,50 are added to the concept name to show which design that is used.

These results will be considered in the later concept evaluation process. The calculation steps can be found in Appendix 5 and the result can be found in Table 11.

*Table 11. Results of one dimensional heat transfer calculations. * Serial cooling does not consumes any air. The numbers presented for these concepts are the amount of air that flows over the transition duct. Two cases are calculated, a pressure drop of 0,25% and 0,5%. **Current design gives a wall temperature at 1032K in our calculations.*

		Cooling air					
		1100K wall temp			1050K wall temp		
Concept	**Name**	**[kg/s]**	**of total air [%]**	**% of current design****	**[kg/s]**	**of total air [%]**	**Compared to 1100K wall**
C2	Effusion with TBC	0,49	5%	35%	--	--	--
C5	Serial with ribs 0,25*	1,68	16%	118%	4,44	42%	264%
	Serial with ribs 0,5*	0,78	7%	55%	2,18	21%	279%
C6	Serial with ribs and TBC 0,25*	0,6	6%	42%	2,20	21%	366%
	Serial with ribs and TBC 0,5*	0,48	5%	34%	1,11	11%	231%
C9	Serial 0,25*	9,35	89%	658%	--	--	--
	Serial 0,5*	3,45	33%	243%	--	--	--
C10	Serial with TBC 0,25*	2,58	24%	182%	8,77	83%	340%
	Serial with TBC 0,5*	1,18	11%	83%	3,22	31%	273%
C11	Impingement	0,65	6%	46%	0,95	9%	146%
C12	Impingement with TBC	0,46	4%	32%	0,63	6%	138%
C19	Laminate	0,34	3%	24%	0,59	6%	174%
C20	Laminate with TBC	0,2	2%	14%	0,34	3%	170%

5.3.3 Cost Calculations

In order to calculate the cost of each concept some simplifications are made. The calculations are based on the cost of the transition duct with current design. As some of the concept are quite like current design the cost of some operations and material are scaled down or up. New costs are added with some estimations. The mounting is not considered here and therefore removed in the comparison. Simplifications and estimations can be found for each concept in Appendix 6. The result can be found in Table 12 where it is presented in percent of the current cost.

Table 12. Results of cost calculations in percent of the current design. Note that 100% is the same cost as the current.

Concept	**Name**	**Cost compared to current design**
C2	Effusion with TBC	102%
C5	Serial with ribs	110%
C6	Serial with ribs and TBC	127%
C9	Serial	105%
C10	Serial with TBC	123%
C11	Impingement	101%
C12	Impingement with TBC	118%
C19	Laminate	77%
C20	Laminate with TBC	94%

5.3.4 Weighted Objectives Method

With the intention of making weighted objectives method possible, some substantially criteria regarding the cooling specification are chosen. These criteria are then compared to each other with the method pairwise comparison in order to get the right order of importance. In this case, a criterion of cooling performance mentioned in chapter 5.3.2 has been taken in consideration in the evaluation. This performance factor is determined from how much cooling air relative the results at 1100K that are used to lower the temperature by 50 degrees. The reason of using this extra criterion is to insert a safety factor which should enable decrease of material temperature without major redesign. The other criteria are taken from the design specification. This pairwise comparison with its scoring results is seen in Table 13.

From this score the weight of each criterion is determined by using, in this case a 1-10 relative scale. The scaled weight that later is used in the evaluation are showed in the gray field in Table 13.

With result from the calculations, scores on each criterion is set using Table 14. On the "low temperature gradient" criterion there is no measurable value given from the calculations and a judgment scale is used instead, see chapter 3.3.4.

Table 13. Pairwise comparison for criteria in the cooling concept evaluation. The gray field shows the scale that is used in the evaluation.

Criteria	Low air consumption	Low temperature gradient	Slim design	Performance	Cost	Sum, x_i	Rang	Scale 1-10
Low air consumption	-	2	2	2	2	8	1	10
Low temperature gradient	0	-	1	1	2	4	3	5
Slim design	0	1	-	0	1	2	4	2
Performance	0	1	2	-	2	5	2	6
Cost	0	0	1	0	-	1	5	1
Total Sum						**20**		

Table 14. Utility scores used in weighted objectives method for cooling concepts evaluation.

Air consumption		Cost		Shell thickness		Performance	
Value [kg/s]	Score	Value [%]	Score	Value [mm]	Score	Value [%]	Score
> 1,5	0	> 140	0	> 20	0	>200	0
1,15 - 1,5	1	130 - 140	1	16 - 20	1	185 - 200	1
0,8 - 1,15	2	120 - 130	2	12 - 16	2	170 - 185	2
0,45 - 0,8	3	110 - 120	3	8 - 12	3	155 - 170	3
0,1 - 0,45	4	100 - 110	4	4 - 8	4	140 - 155	4
< 0,1	5	< 100	5	< 4	5	< 140	5

With the scores and weights implemented in the weighted objectives method all concepts are given values of how good they full fill the whishes. In Table 15 a summary of the result are showed and the main matrix is found in Appendix 7. Serial cooled concepts are scored with a 5 on the air consumption and performance because no cooling air is lost. An exception is concept C9, which is not able to lower the material temperature and have therefore a score 0 at performance. All the serial concepts are scored very high except concept C9 with the low pressure drop due to the lack of performance. Concept C2, effusion cooling has the lowest score but has potential in a combination with impingement cooling. The other concepts, impingement and laminated sheets have similar scores. It is thermal barrier coating that makes the difference and is preferred to use.

*Table 15.Result of cooling concept evaluation. Each concept are scored with a normalized score and an ideal solution have the score 1. Two cases for each serial concept are evaluated, one with the pressure drop of 0,25% and the other one 0,5% which have the *.*

Concept	**Type**	**Normalized score**
C2	Effusion	0,41
C5	Serial Ribbs	0,90
C6	Serial Ribbs TBC	0,94
C5*	Serial Ribbs	0,92
C6*	Serial Ribbs TBC	0,94
C9	Serial	0,62
C10	Serial TBC	0,94
C9*	Serial	0,67
C10*	Serial TBC	0,94
C11	Impingement	0,60
C12	Impingement TBC	0,70
C19	Laminated sheets	0,63
C20	Laminated sheets TBC	0,72

5.4 Concept Generation Mounting and Sealing

With respect taken to the slight connection between mounting and sealing concepts both of them are placed in the same chapter. The chapter begins with a function mean tree in order to visualizing how function can be solved with different means for both mounting and sealing. Mounting concepts are combined with a morphologic matrix. All sealing solutions are explained and later combined with mounting concepts.

In order to generate feasible solutions the forces acting on the transition duct have to be known. The mass flow of the combustion gas and pressure difference outside to inside of the transition duct causes forces, forces that the mounting should handle. Calculations show that the large force comes from the pressure difference between the compressor air, outside the transition duct and the combustion gas, inside the transition duct. The total static forces are 3316N in radial direction and -720N in axial direction. The forces are relative small in this context regarding mounting structures. These calculations can be found in Appendix 8.

5.4.1 Function- Means Tree Mounting and Sealing

This function- means tree in Figure 19 is branched down from the main tree in Appendix 2. It consists of functions and means that are helpful in the development of concepts regarding mounting and also sealing of the transition duct. The branch regarding mounting is used to visualize where and how the transition duct can be secured. The same principle regards the sealing concepts. The mean that says “Free” under each mounting function indicates that no mounting on that side is used.

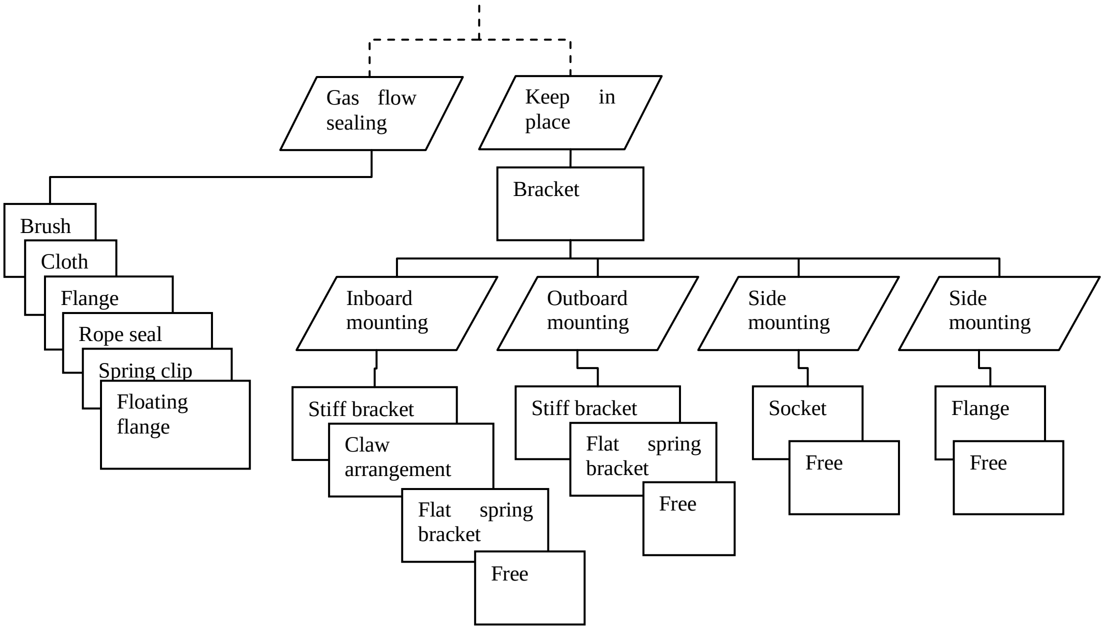

Figure 19. Function mean tree for mounting and sealing concepts.

5.4.2 Morphology Mounting

To be able to combine different mounting concepts a matrix is set up with means from the function mean tree. As the sealing is a rather stand-alone function, it is leaved out in the first step and combinations of different mounting techniques are done alone. Sealing variants is evaluated in a later chapter. In Table 16 possible combinations are shown with different shaped and colored symbols. Each concept refers to a specific symbol with a specific color, which are presented in Table 17.

Table 16. Morphology matrix for mounting concepts.

Functions	**Means**				
Inboard mounting	**Stiff bracket** △	**Claw arrangement** ☆ ☾	**Flat spring bracket** ★ ◎ ■	**Socket** ⭘	**Free** ✭ □
Outboard monting	**Stiff bracket** ■ ✭	**Flat spring bracket** ◎ ☆	**Free** ⭘ ★ △ ☾ □		
Side mounting	**Socket** ⭘ ★ ◎	**Free** △ ■ ☆ ☾ ✭ □			
Other mounting	**Anular flange** ☾ ✭ □	**Free** △ ☆ ★ ◎ ■ ⭘			

Table 17 First set of mounting concepts.

△	M1	**Inboard stiff bracket**
☆	M2	**Inboard claw arrangement with flat spring braket on the outboard**
☾	M3	**Inboard claw arrangement with anular flange in the aft end**
★	M4	**Inboard flat spring bracket with sockets on the sides**
◎	M5	**Inboard flat spring bracket with flat spring bracket on the outboard and side sockets**
■	M6	**Inboard flat spring bracket with stiff bracket on the outboard**
⭘	M7	**Inboard socket with sockets on the sides**
✭	M8	**Outboatd stiff bracket with annular flange in the aft end**
□	M9	**Annular flange on the aft end**

In Figure 20 all of the concepts are showed in order to emphasize the functionally principles. The locations of the mounting parts are chosen with respect to the static forces acting on the transition duct. The idea on most of the concepts is to eliminate the torque with a smart location of the mounting parts, the transition duct is free from torque along a line, see Appendix 8. The calculations of the forces and torque can also be found in Appendix 8.

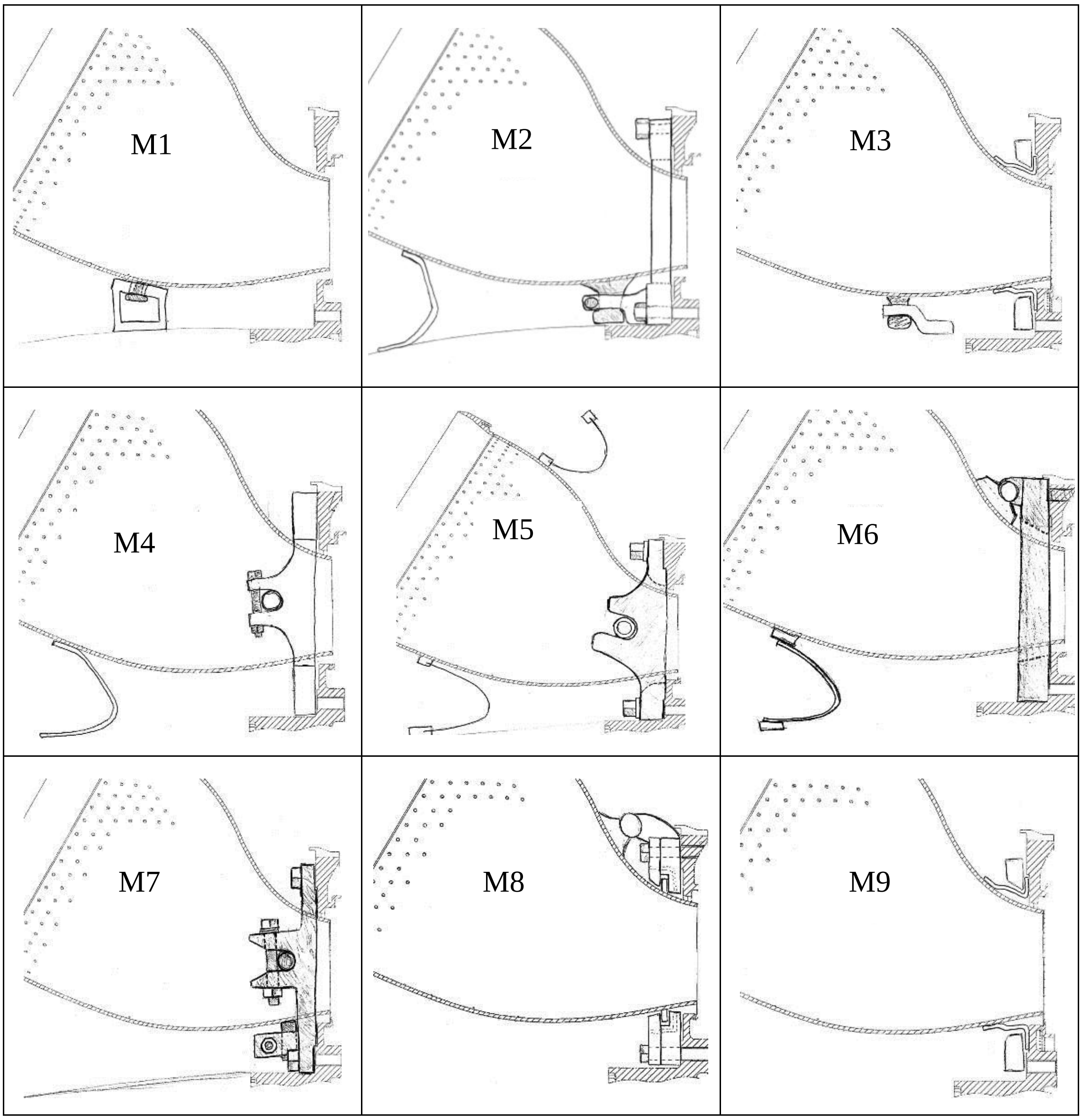

Figure 20. Mounting concepts.

Concept M1 inboard stiff bracket

The idea with this concept is a stiff bracket mounted in the inboard side of the transition duct. The bracket is stiff and handles all forces and torques acting at the transition duct. Due to the single point attachment of the transition duct it is allowed to expand in all directions from the bracket.

Concept M2 Inboard claw arrangement with flat spring bracket on the outboard

The claw is supposed to handle the radial and the axial force just like the inboard stiff bracket. It is placed at the inboard near the aft end, near the line where no torque acting at the transition duct. Vibrations and other oscillations are supposed to be eliminated with the spring bracket on the outboard side of the transition duct. The claw design should enable easy installation.

Concept M3 Inboard claw arrangement with annular flange in the aft end

This concept is rather like current design of the transition duct except the claw attached at the inboard side. The claw is supposed to relive the aft end flange and handle radial forces.

Concept M4 Inboard flat spring bracket with sockets on the sides

This is a concept that is supposed to be mounted easily. Two cylinders are welded to the sides of the transition duct and are placed at a point where no torque is acting. During the mounting of the duct the cylinders are pushed in two slots. The transition duct is then locked by two bolts. The cylinders handle forces in radial and axial direction. An extra spring bracket is placed at the inboard side to damp dynamic oscillations.

Concept M5 Inboard and outboard flat spring bracket with side sockets

This concept is the same as concept M4 except that an extra spring bracket is placed at the outboard side and no bolt is used. The spring brackets handle the axial forces instead of the locking bolts.

Concept M6 Inboard flat spring bracket with stiff bracket on the outboard

Axial and radial forces are handled by the stiff bracket at the outboard side and the spring bracket damps dynamic oscillations and torque.

Concept M7 Inboard socket with sockets on the sides

This concept is rather like concept M4 and M5 with the difference that no spring bracket is used. The dynamic torque around the side sockets is handled by a socket at the inboard side.

Concept M8 Outboard stiff bracket with annular flange in the aft end

The stiff bracket is supposed to handle forces in axial and radial direction and the annular flange handles torque acting on the transition duct. The annular flange acts as a sealing for the transition duct as well.

Concept M9 Annular flange at the aft end

This is current design. An annular flange is supposed to handle axial, radial forces and torque. The flange is floating in the slot to handle thermal expansions. The flange is acting as a sealing as in concept M8

5.4.3 Sealing Solutions

The sealing solutions that are showed here are taken directly from the means in the function- means tree. Due to the many different design variations of each solution, regarding sealing surfaces, sealing attachment and the angle in which the sealing is operating no morphology matrix is used to generate concepts. Instead sketches have been made directly from ideas on the different solutions. In Figure 21 sealing principles are showed to illustrate the function.

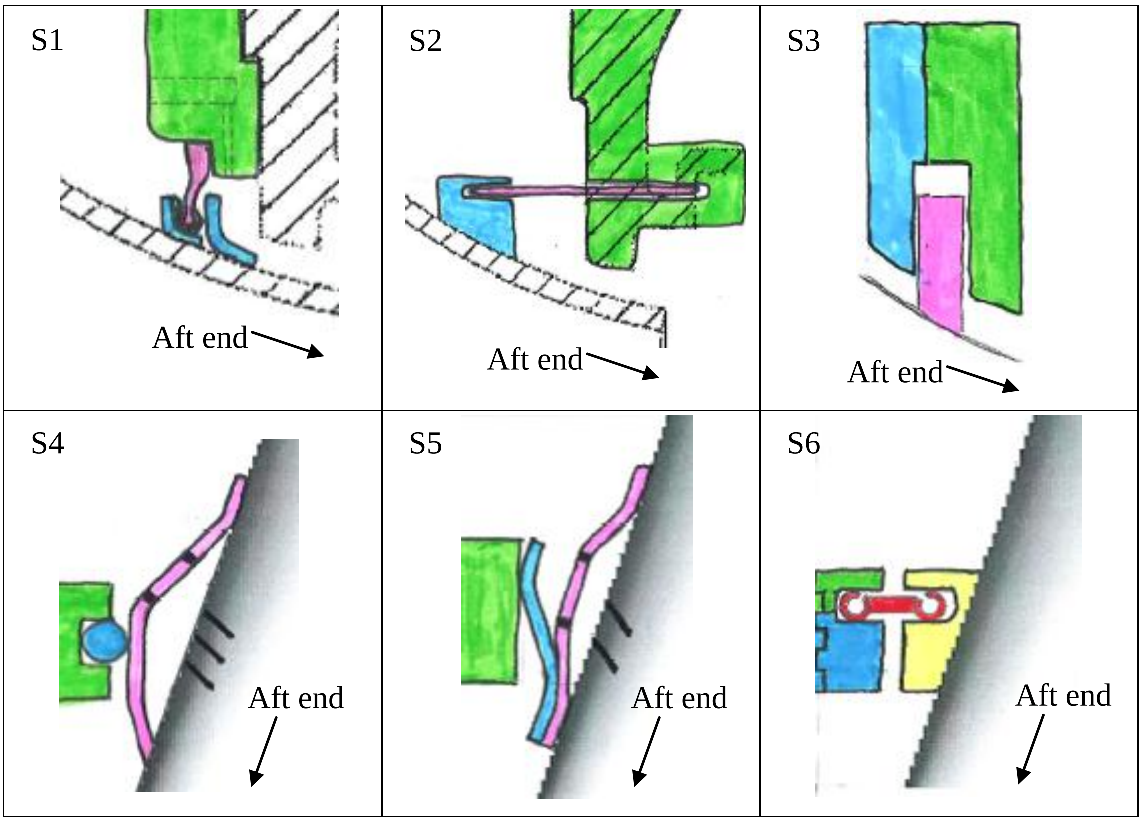

Figure 21. Sealing solutions, the first three sketches are cross sections seen from the side and the other ones are sections seen form the top of the transition duct.

S1 Brush seal

This type of sealing can be formed to fit the transition duct complex surface in the aft end. Sketch S1 in Figure 21 shows the brush fitted on the transition duct with the sealing surface placed in a frame mounted on the stator ring. The sealing surface can also be fitted directly in the stator ring. The brush in the sketch can be fitted upside-down and create the same type of sealing. This solution is based on the brush mounted in radial direction. This is not a demand, instead the brush can be placed in axial direction. With the design of the brushes some purge air can penetrate the bristles and function both as cooling and as barrier to preventing hot gas circulation.

S2 Cloth seal

Cloth seal is a flat metal structure made of woven metal. The idea is to keep the cloth in a slit where it can move in one end and are fixed in the other. The sealing is not the optimum solution for a low leakage coupling because the woven metal is porous. The leakage is not just a bad property as it brings cooling of the material. The benefit of this sealing is that it is flexible and can handle movement. Metal shims can be used together with the cloth to reduce the leakage. A schematic drawing, sketch S2 can be found in Figure 21. Cloth seals can not only be used as the sketch shows but can also be used as a brush seal, resting at a support instead of being inserted in a slit. The cloth is with advantage fitted at the transition duct and inserted in a slit in the stator ring. The slit needs a smooth entrance to enable easy installation.

S3 Flange

The sealing solution used in current design is a flange. Flanges are often fastened in one end and the other end is inserted in a slot where it can move in longitudinal direction. The only leakage that occurs in this seal is in the slot clearance between the flange and the slot wall. The clearance in the slot should be as small as possible to reduce the leakage. The flange in current design is designed to handle the forces acting on the transition duct. Another solution with a flange that is not supposed to handle forces can be seen in sketch 3, Figure 21. The flange slot can be fitted in a separate frame which is mounted at the transition duct before it is installed in the central housing. The flange can also be fitted as the current design between the stator ring and the clamping bars. Cooling of the mounting parts can be done with small holes drilled through the flange.

S4 Rope seal

Rope seals are quite like o-rings, but made of different materials. Rope seals are supposed to be rigid and handle vibrations well, the disadvantage can be the amount of leakage. Rope seals also known as cord seals are made of a core with some sort of silica or ceramic material. The core is covered by a braid made of woven high temperature resistant metal. The rope seal is fitted inside an o-ring type groove. The groove and the sealed part need a clearance to take care of thermal expansions. As the sealing not is expandable the groove needs to be fitted in the stator ring instead of at the outside of the transition duct to enable an easy fitting. A flat sealing surface must therefore be manufactured at the transition duct. A schematic drawing can be seen in sketch 4, Figure 21 where a cooling idea of the sealing surface structure is presented. This is obtained with impingement through the raised flange and effusion through the transition duct wall.

S5 Spring Clip

In order to create a sealing that can withstand the high temperatures the use of metal can be an obvious choice. As a result of forming metal shims like the blue S-formed detail in sketch 5, Figure 21 a sealing pressure will be created against the sealing surface. The force due to pressure difference will gain the sealing pressure. This solution is used best on applications with big wrapping radius. Small radius will make the spring shim stiff and may cause leakage.

In the sketch a principle of cooling the sealing area are showed as well. This is obtained with impingement through the raised flange and effusion through the transition duct wall.

S6 Floating flange

This idea is based on a flange that is placed in a surrounding groove which are placed both on the transition duct and in the mounting frame. This allows the duct to move and expand. In sketch 6, Figure 21 one idea is showed adding C-seals at both ends on the flange. This should add extra sealing performance at the same time as slight movement in axial direction is allowed, such as thermal expansion.

5.5 Concept Evaluation Mounting and Sealing

The evaluation of the mounting and sealing concepts is quite hard due to lack of information such as calculations and simulations. It is hard to know how well a certain concepts resist low cycle fatigue, the damping etcetera. The decisions will therefore rely at estimations and be made with datum matrixes.

5.5.1 Datum Matrix Mounting

Due to the complexity of gathering data on each criterion the datum method are used to evaluate the concepts based on estimations. The used criteria are based and translated from the criteria in the design specification. They are also weighted using pairwise comparison showed in Table 18

After the first datum matrix evaluation, Table 19 with the current design used as datum reference, concept M1 has the lowest ranking and is eliminated from the process. The problem with concept M1 is that the bracket certainly would start vibrating and damaged any kinds of sealing in the aft end. The strongest concept is M7 with a close presence of five concepts sharing the second place.

In the next datum evaluation, Table 20 is concept M7 the datum reference. Here is concept M3 eliminated from the process although it is not the worst one. That decision is made because of two reasons. The first one, Concept M9 is the current design and serves as a reference. The second one, concept M8 have potential to be further developed in order to be more robust solution. The strongest concept this time is concept M5 with just one weight unit more then four concepts shearing the second place.

The remaining concepts will be further developed and later joined together with sealing solutions before a combined evaluation will continue.

Table 18. Pairwise comparison of mounting criteria.

Criteria	LCF resistant	Good damping	Low complexity	Easy to assemble	Adds sealing solution	Wear resistant	Sum, x_i	Scale 1-5
LCF resistant	-	2	2	2	2	1	9	5
Good damping	0	-	2	2	2	1	7	4
Low complexity	0	0	-	1	0	0	1	1
Easy to assemble	0	0	1	-	2	2	5	3
Adds sealing solution	0	0	2	0	-	0	2	2
Wear resistant	1	1	2	0	2	-	6	4
						Total Sum	**30**	

Table 19. First datum matrix for mounting concept evaluation.

Criteria	W	Concepts								
		M1	M2	M3	M4	M5	M6	M7	M8	M9
LCF resistant	5	0	+	+	+	+	+	+	+	DATUM
Good damping	4	-	+	+	0	0	+	+	+	
Low complexity	1	+	+	-	+	+	0	+	0	
Easy to assemble	3	+	+	0	+	+	0	+	0	
Adds sealing solution	2	-	-	0	-	-	-	-	+	
Wear resistant	4	-	0	0	+	+	+	+	0	
Total		-1	3	1	3	3	2	4	3	0
Weighted total		-6	11	8	11	11	11	15	11	0
Rank		**5**	**2**	**3**	**2**	**2**	**2**	**1**	**2**	**4**

Table 20. Second datum matrix for mounting concept evaluation.

Criteria	W	Concepts							
		M2	M3	M4	M5	M6	M7	M8	M9
LCF resistant	5	0	-	0	0	0	DATUM	-	-
Good damping	4	0	0	0	+	0		-	-
Low complexity	1	0	-	0	0	-		-	-
Easy to assemble	3	0	-	0	-	-		0	-
Adds sealing solution	2	0	+	0	0	0		+	+
Wear resistant	4	0	-	0	0	+		-	-
Total		0	-3	0	0	-1	0	-3	-4
Weighted total		0	-11	0	1	0	0	-12	-15
Rank		**2**	**3**	**2**	**1**	**2**	**2**	**4**	**5**

5.5.2 Sealing Evaluation

Due to the lack of calculated leakage data for each sealing the evaluation will be preformed with the datum method. In order to get a more fair evaluation between the concepts a pairwise comparison between the sealing criteria are made and presented in Table 21. In the datum matrix, Table 22 the numbers are connected to each sealing principle sketch in Figure 21 in chapter 5.4.3. The strongest concept in this first evaluation is concept S4, the rope seal. Concept S6 is at second place with the floating flange solution. The weakest concept is concept S1, which correspond to the brush solution. The brushes are sensitive to vibrations and examples have showed sealing failure because of worn brushes. (SIT AB internal material)

Table 21. Pairwise comparison of criteria for sealing evaluation.

Criteria	Low leakage	Good damping	Low complexity	Easy to assemble	Wear resistant	Sum, x_i	Scale 1-5
Low leakage	-	2	2	2	0	6	4
Good damping	0	-	2	2	0	4	3
Low complexity	0	0	-	0	0	0	1
Easy to assemble	0	0	2	-	0	2	2
Wear resistant	2	2	2	2	-	8	5
					Total Sum	**20**	

Table 22. Datum matrix for sealing solution evaluation.

Criteria	W	S1	S2	S3	S4	S5	S6	
		Concepts						
Low leakage	4	0	0	DATUM	0	-	+	
Good damping	3	-	-		+	+	0	+ Better
Low complexity	1	-	-		+	-	0	- Worse
Easy to assemble	2	0	+		+	+	0	0 Equal
Wear resistant	5	-	0		0	0	0	
	Total	-3	-1	0	3	0	1	
	Weighted total	-9	-2	0	6	0	4	
	Rank	**5**	**4**	**3**	**1**	**3**	**2**	

5.5.3 Mounting and Sealing Combinations

After the first evaluation some of the mounting concepts have been developed further and combined with sealing concepts. It is the concepts with best potential that is taken to this stage. The spring bracket used in concept M2, M4, M5 and M6 are eliminated in further stages. It is an independent solution which can be used together with all remaining concepts in need of extra damping. The developed and combined concepts are presented here together with sketches of the mounting and sealing parts.

Concept MS1

This is a further developed combination of concept M4, M5 and M7. The circular bars have been replaced by half circle bars with a cross section like a large letter D. The D-shaped bars combined with D-shaped sockets will prevent rotation of the transition duct and the socket at the inboard side is therefore unnecessary. The sockets are integrated in the stator ring which reduces the number of assembly parts. The clearance between the bar and the socket will be just enough to ensure movements during startup, when the differences in thermal expansions are the largest. The lock part, the purple part in Figure 22 is designed to be easy to reach for installation and for tighten the bolt. The sealing for this concept is rope sealing integrated in the mounting frame. It is an easy solution that ensures an easy mounting procedure. The whole idea with this concept is an easy mounting procedure, it is just to push the transition duct into place and fit the locking parts and tighten the bolts. Due to the integration with the stator ring no separate frames are needed and there are no places between the transition ducts where leakage can occur.

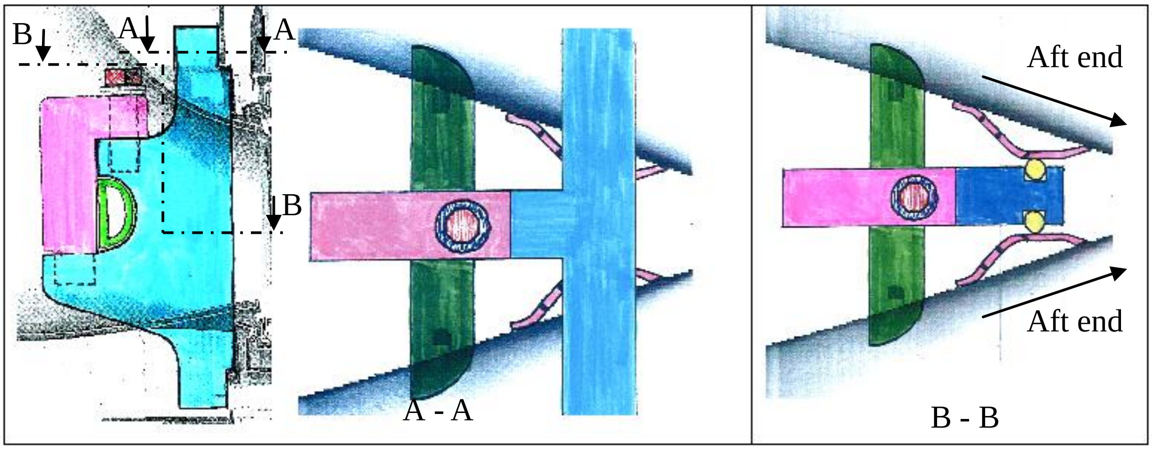

Figure 22. Concept MS1. D-shaped bars with rope seal.

Concept MS2

The sealing at this concept requires a pre installation before mounting in the gas turbine. The sealing is a floating flange which is installed in a slot fitted both in the transition duct and the mounting frame, see Figure 23. The concept is based on concept MS1 with the D sockets. But the sockets are integrated in the sealing frame, which is installed together with the sealing at the transition duct before it is mounted in the gas turbine. The frames from two adjacent transition ducts are interacted together with a labyrinth seal. As the transition duct frame has a V-shaped profile it slides a little bit from above to engage the labyrinth seal. Four bolts are holding the frame and transition duct in place in the gas turbine.

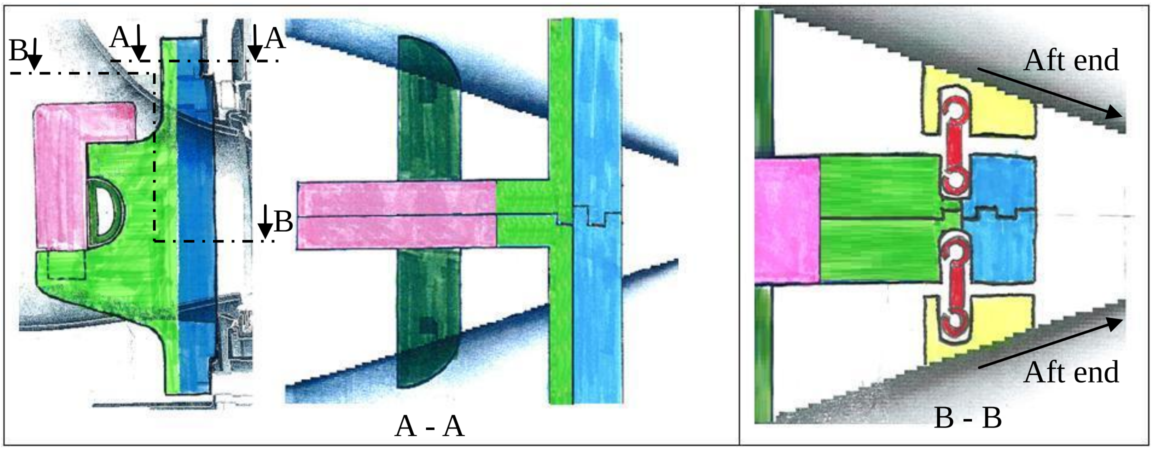

Figure 23. Concept MS2. D-shaped bars with floating flange.

Concept MS3

A further development of current design is presented in concept MS3. The transition duct is unchanged but the mounting parts, two clamping bars and two t-bone struts are combined to a frame, see Figure 24. The frame are mounted on the transition duct before it is mounted inside the turbine which reduces the number of lose part in the assembly moment. The frame has four parts, a top part (blue) a bottom part (green) and two side parts (purple). The side parts and the bottom part are held together with two small bolts. The bolts holds two shims with a flange that keeps the upper bar together with rest of the frame during installation. The frame is mounted as current design, bolted with four bolts in the stator ring, one in each corner of the frame. To ensure the sealing between the frames the stator ring has to be modified. Adding a connection between the outer and the inner ring provides a sealing surface.

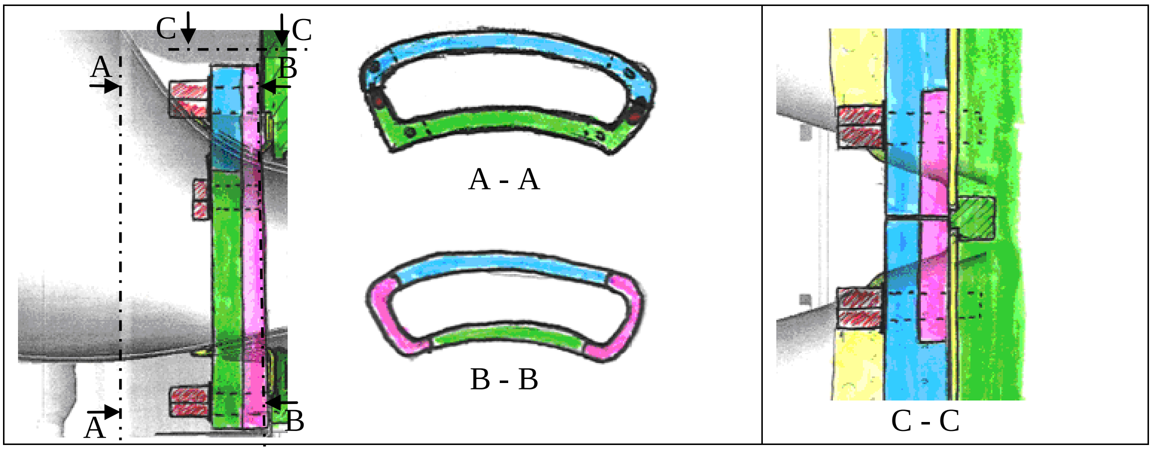

Figure 24. Concept MS 3. Improved solution of today.

Concept MS4

This concept is based on concept M8 together with a better sealing. At the outboard side a bracket is mounted which handle all tangential and radial forces but allows rotation in the connection point as the arrow in the Figure 25 shows. The rotation is mention to be handled by the flange that is welded to the transition duct and installed in a slot in an annular frame. A brush seal is mounted at the top of the flange and putted in another slot to keep the leakage down, see Figure 25. The frame consists of 3 parts, a back frame (green) and one front frame splitted in two (blue). The front frames are splitted to be able to assembly the frame with the flange at the transition duct, the frames are bolted together. The outboard bracket (yellow) is mounted to the frame to ensure an easy installation. The frame is mounted as current design, bolted with four bolts, one in each corner of the frame in the stator ring. To ensure the sealing between the frames the stator ring has to be modified by adding a connection between the outer and the inner ring.

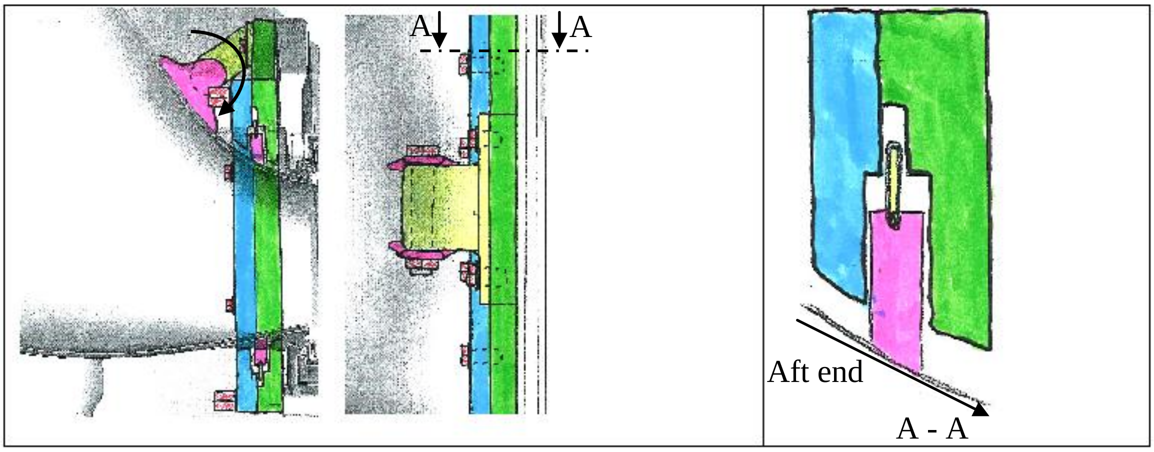

Figure 25. Concept MS4. Frame with integrated sealing.

Concept MS5

A claw is used to keep the transition duct in place in this concept. Seen from back side the claw is designed as a wedge with heels to lock the transition duct in radial and tangential direction. A bolt keeps the axial position of the claw. A rope seal is installed in the frame to make the installation easy. The frame is integrated in the stator ring to reduce the number of parts that have to be assembled. This also eliminates the possibility of leakage between the transition ducts compared to separate frames.

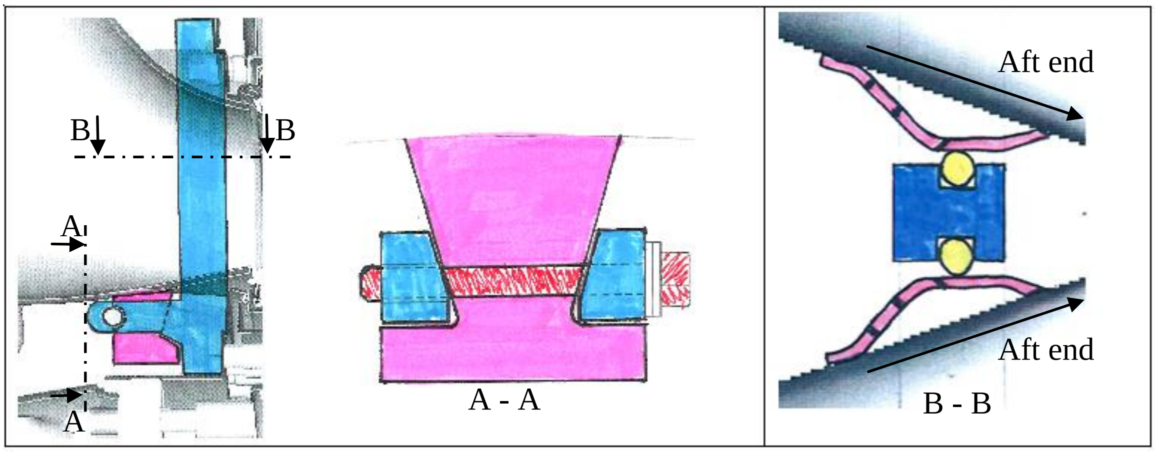

Figure 26. Concept MS5. Claw arrangement together with rope seal.

Concept MS6

This concept is similar to concept MS5 but with the sealing type used in concept MS2, the annular floating flange and the frame. The mounting principle with the claw has been taken from concept MS5. The claw is interacted with the frame and installed to the transition duct together with the floating flange before mounting in the gas turbine, see Figure 27. A labyrinth seal is used between two adjacent transition duct frames and as described before the transition duct is slided in from above. The frame is mounted in the turbine on to the stator ring with four bolts.

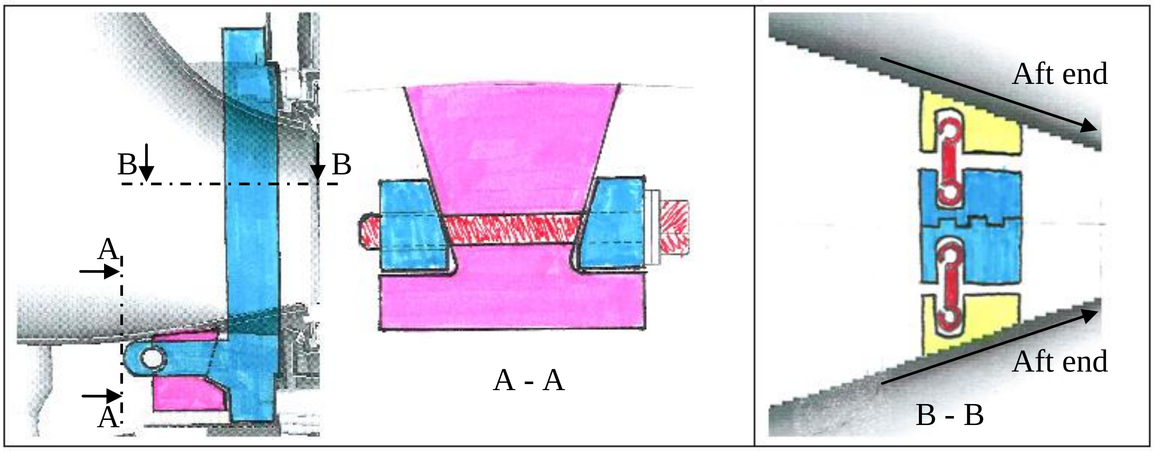

Figure 27. Concept MS6, Claw arrangement together with an annular flange for sealing.

5.5.4 Mounting and Sealing Evaluation

As written before mounting and sealing concept are hard to evaluate, the same applies to the combination of them. The evaluation is based on estimations and will be made with datum matrixes as before. The criteria are weighted just as before with pairwise comparison, see Table 23.

Table 24 shows the first evaluation where concept MS3 is reference. A noticeable difference between the concepts with a welded part around the transition duct, concept MS2, MS4, MS6 and the others is that the LCF resistance is lower. The LCF resistance is lower because a thick welded part on a hot structure builds up stresses in the material due to difference in thermal expansion. These concepts are also expected to be more expensive and more complex than the other concepts. The flange and sealing slot is hard to manufacture and requires more machining than the other concepts. The welding process is quite difficult due to low tolerances and can therefore be expensive. Both concept MS5 and MS6 have a lower damping than the other concepts due to the large clearance in the mounting parts. The rope seal used in concept MS1 and MS5 are estimated to leak as much as current design which is used in concept MS3. It is also expected that the brush seal in concept MS4 and the floating flange sealing in concept MS2 and MS6 will leak less than the other concepts. The turndown of concept MS4 is the wear resistance which is expected to be lower than the other concept based on brush experience in a vibrating environment. Because of that concept MS4 is eliminated. The other concepts are expected to have better wear resistance because the mounting and sealing parts are separated so that the sealing will be relieved from forces.

The best concept in the first evaluation, concept MS1 is set to be reference concept in the second evaluation, which can bee seen in Table 25. The noticeable difference from the first evaluation is that the wear resistance for concept MS5 is lower than concept MS1. That is because the mounting is placed at the inboard side instead of in the middle of the transition duct. This means that the sealing at the outboard side is more exposed for vibrations and compressive force due to thermal expansion of the transition duct. Concept MS1 is still the best concept and the result has converged, no more evaluation is needed.

Table 23. Pairwise comparison for mounting and sealing combination evaluation.

Criteria	LCF resistant	Good damping	Low complexity	Easy to assemble	Low leakage	Wear resistant	Sum, x_i	Scale 1-5
LCF resistant	-	2	2	2	2	1	9	5
Good damping	0	-	2	2	1	1	6	4
Low complexity	0	0	-	1	0	0	1	1
Easy to assemble	0	0	1	-	0	2	3	2
Low leakage	0	1	2	2	-	0	5	3
Wear resistant	1	1	2	0	2	-	6	4
						Total Sum	**30**	

Table 24. First datum matrix for mounting and sealing combinations.

		Concepts					
Criteria	**W**	MS1	MS2	MS3	MS4	MS5	MS6
LCF resistant	5	0	-	DATUM	-	0	-
Good damping	4	0	0		0	-	-
Low complexity	1	0	-		-	0	-
Easy to assemble	2	+	0		0	+	0
Low leakage	3	0	+		+	0	+
Wear resistant	4	+	+		-	+	+
	Total	2	0	0	-2	1	-1
	Weighted total	6	1	0	-7	2	-3
	Rank	**1**	**3**	**5**	**6**	**2**	**4**

Table 25. Second datum matrix for mounting and sealing combinations.

		Concepts				
Criteria	**W**	MS1	MS2	MS3	MS5	MS6
LCF resistant	5	DATUM	-	0	0	-
Good damping	4		0	0	-	-
Low complexity	1		-	-	0	-
Easy to assemble	2		-	-	0	-
Low leakage	3		+	0	0	+
Wear resistant	4		0	-	-	0
	Total	0	-2	-3	-2	-3
	Weighted total	0	-5	-7	-8	-9
	Rank	**1**	**2**	**3**	**4**	**5**

6 Final Concepts

This part presents the strongest concept combination from the evaluation. Alternative concepts and combination of concepts that can be of interest for SIT AB are also presented.

All of the cooling solution contains calculation results of the material temperature and air consumption. In this cooling calculation a new way of calculating the heat transfer coefficient at the hot side have been used to get more reliable results. The duct is divided in five parts, like in Figure 28 and the heat transfer coefficient is gained with a factor from SIT AB's earlier CFD calculations. These new calculations can be found in Appendix 5.

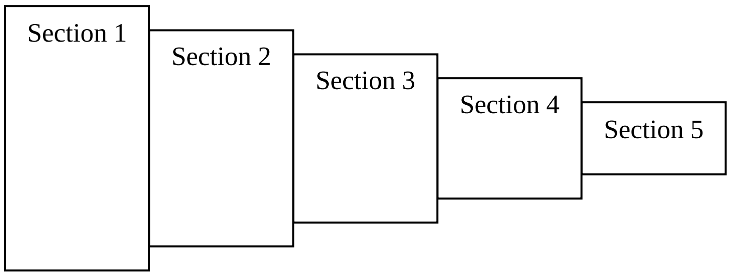

Figure 28. The transition duct divided in five sections with the aft end to the right.

6.1 Strongest Combination

This is a combination of D-shaped bars mounting with rope sealing and the serial cooling method with ribs. Impingement and effusion will also be used in the area around the sealing where serial cooling is difficult to achieve. A new sealing surface at the aft end is also designed. Examples how the combination can look like can be seen in, Figure 29 and Figure 30.

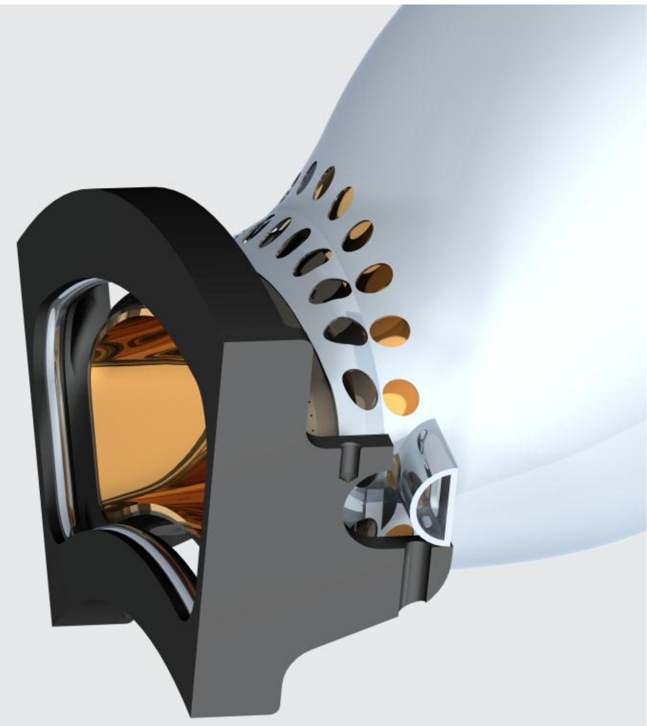

Figure 29. The strongest combination that is on the way to be mounted. The D-bars are sliding into the sockets.

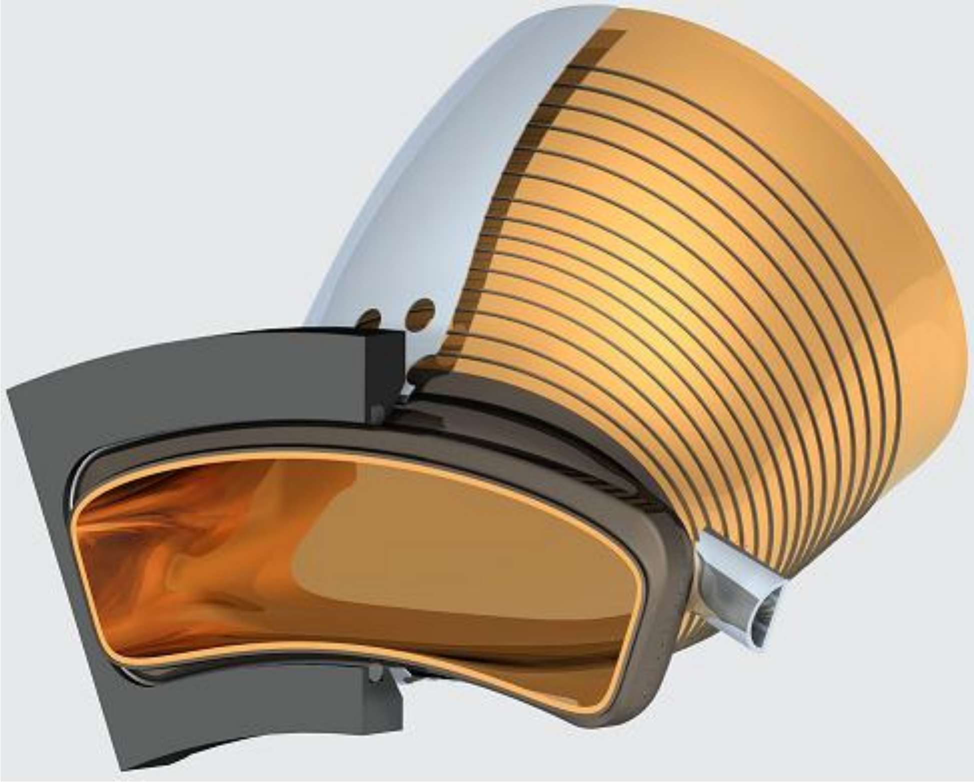

Figure 30. Partly cross sectioned transition duct and its mounting parts.

6.1.1 Mounting and Sealing Solution

This is a further development of concept MS1 from chapter 5.5. Two D-shaped bars are attached at the transition duct sides near the aft end. The bars are locked in D-shaped sockets in the turbine stator ring. By placing the bars at or near the line where no static torque is acting the bars on the transition duct just needs to handle forces and no torque. Small dynamic torques will occur anyway and to eliminate rotations the bars are D-shaped. The sockets are integrated in the stator ring and lock the bars with a lock pin on each side, Figure 31.

A plate with impingement holes is installed inside the D-bar to cool the attachment area of the bar. Effusion holes are drilled through the transition duct surface to let the impingement air out, which also gain the cooling. One big air inlet hole is machined at the flat surface on the D-bar to ensure that the air reaches the impingement plate. In Figure 32 the D-bar with the air inlet is showed in transparent green, the red part is the impingent plate and the effusion holes are showed on the duct surface. In Table 26 the result of the cooling calculation is presented of the area under the D-bar. The amount of spent cooling air with the specific setup of holes is also showed. One thing to notice is that the amount of spent cooling air is so low that it is no reason to add this to the total cooling calculation later.

Table 26. Results for the cooling inside the D-bars. Note that this is the results for two D-bars.

D-bar cooling both sides

Impingement	
Hole Spacing X [mm]	10
Hole Spacing Y [mm]	5
Number of Holes	18
Pressure loss [%]	0,80
Effusion	
Hole Spacing X [mm]	10
Hole Spacing Y [mm]	5
Number of Holes	12
Pressure loss [%]	3,70
Temperature Material [K]	1029
Mass flow [Kg/s]	0,008
Percent of Total Mass flow [%]	0,070

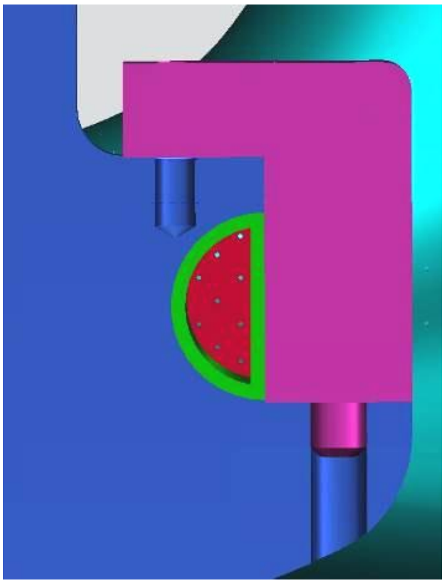

Figure 31. Lock pin in purple.

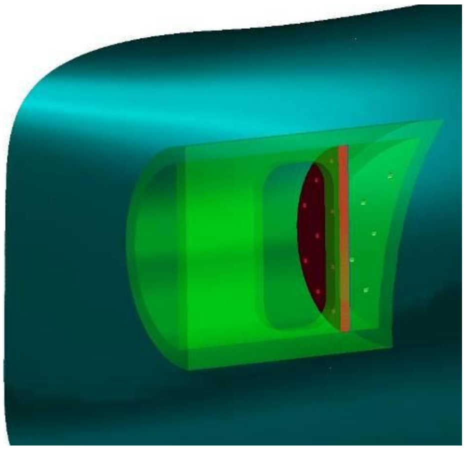

Figure 32. The green D-shaped bar shows the inside impingement cooling plate in red and also the effusion holes in the duct surface.

The two stator rings used in current design will be connected to each other with a strut in which the sockets holding the D-bars will be located. Together they form an annular framework consisting frames for all transition ducts as showed in Figure 33. In each frame a rope seal is installed in an o-ring type groove.

This combination is using a separate flange, Figure 37 welded to the duct to create a flat sealing surface for the rope seal. This flange will also be used to make cooling of the sealing area possible. Due to the chosen cooling method the D-bars have to be lead through the outer shell to reach the mounting sockets in the frame. There is no need to seal the gap between the outer shell and the D-bar. Air that leaks through the gap just adds to the cooling air.

Figure 33. The example of the modified stator ring for the strongest solution.

Advantages

- Serviceability

  This mounting solution is a simple and easy way to mount the transition duct. The transition duct is just pushed in placed and locked by the lock pins and two bolts. The fact that only one port hole needs to be opened to exchange a transition duct easier the serviceability. The sealing is easy to replace and the whole transition duct does not need to be replaced in case of worn out sealing.

Disadvantages

- Design

  Redesign of the stator ring has to be carried out.

- Central housing redesign

  To be able to drill out the bolt holding the lock pin in case of bolt fracture this solution requires a small redesign of the central housing. The attachment strut holding the upper stator ring in current design, Figure 34 blocks the inspection hole where the bolt is supposed to be drilled out from. As the stator rings are connected to each other in this new design the attachment strut for the outer stator ring may be unnecessary an alternative solution exist with a different lock pin splitted in two where the bolt is pointing outward against the port hole, see Figure 35. The space is rather limited in that direction why a small redesign of the central housing is a better solution.

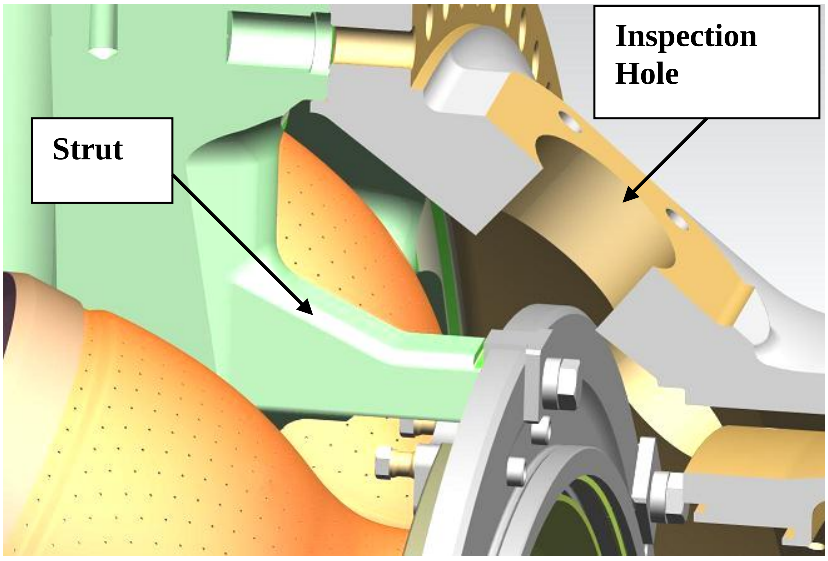

Figure 34. Inside the central housing, showing the strut that have to be redesign to enable access through inspection hole.

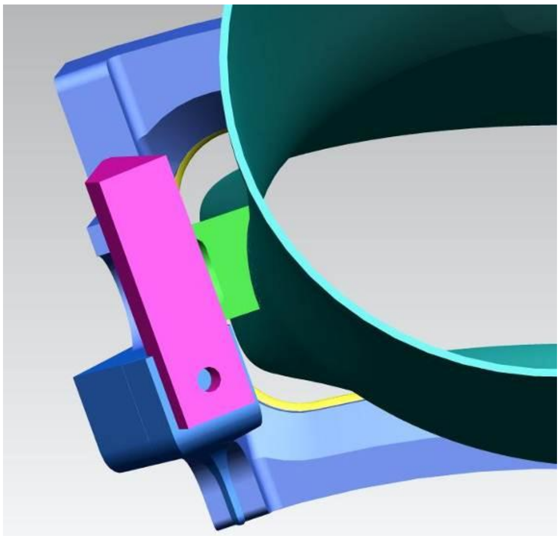

Figure 35. The purple colored part in the figure shows the other design of the look pin. Note that this pin only holds one transition duct instead of two ducts like the other design.

6.1.2 Cooling Solution

This cooling solution is a combination of concept C6, C2 and C12 from chapter 5.3. The main method that is used is serial cooling which cools the biggest part of the transition duct. When using that type of cooling method it is hard to get effective cooling at the aft end of the transition duct where the cooling air inlet and the sealing is located. In order to be able to cool that area impingement and effusion are used as assistant. Thermal barrier coating, TBC is applied to the whole inner surface to insulate the material.

About 80 percent of the transition duct is cooled by serial cooling. In order to gain the cooling effect serial cooling with ribs are used. The cooling air enters the dual shell in the aft end near the sealing. There are roughly two ways to construct the air inlet, one way is to use a flange that is shaped to create a smooth rounded inlet cone, showed in Figure 36. The other way is to connect the outer shell with the inner shell at the aft end and let the air enter between the shells through holes in the outer shell, showed in Figure 36. In the front end both the inner and the outer shells are connected to the combustion can. This makes, as mentioned earlier, that the air used for cooling are used later in the combustion process and no air are consumed in the cooling process. The setup with rib height and spacing, the shell offset and the results of the temperature calculations are showed in Table 27.

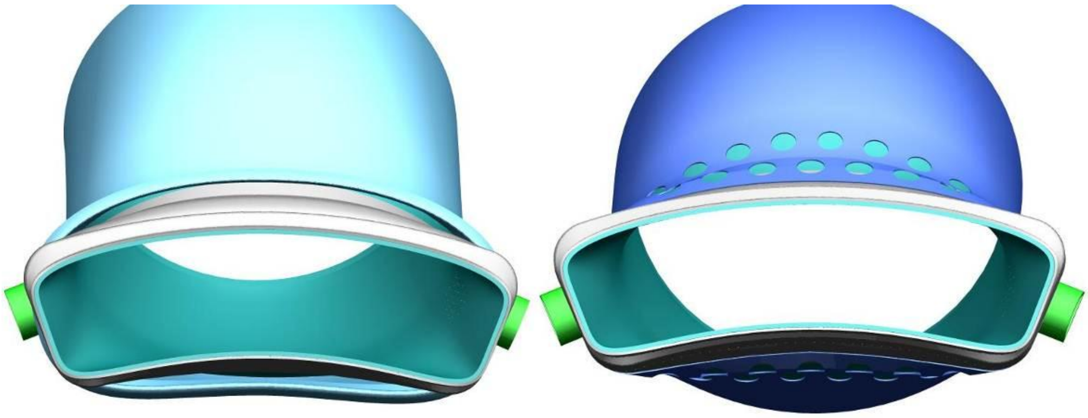

Figure 36. The duct to the left have a rounded inlet cone and the duct to the right have inlet holes for the cooling air.

Table 27. Cooling setup and result for section 1 to 4 where serial cooling is used.

Serial Rib Turbulated Cooling

Section:	1	2	3	4	5
Shell offset [mm]	9	10	10	10	-
Rib Height [mm]	1	1	1	1	-
Rib Spacing [mm]	10	10	10	10	-
Pressure loss [%]	0,15	0,10	0,12	0,15	-
Temperature Material [K]	**1046**	**1036**	**1034**	**1035**	**-**
Mass flow serial [Kg/s]		2,5			
Total Pressure loss [%]		0,51			

In the aft end where the sealing is located, impingement and effusion are used for cooling. There is about 20% of the transition duct that is cooled with those methods. The flange that is used to create a plane sealing surface around the duct aft end is also used to serve as an impingement plate as showed in Figure 37. Air that passing through the impingement holes forming jets which hits and cools the inner shell. The air that has entered through the impingement holes have to leave the cavity through effusion holes into the inside of the duct. In order to gain efficiency the impingement and effusion arrangement are designed to have large pressure drop over the impingement plate and less pressure drop over the effusion holes. With that arrangement air from the effusion holes will create a cooling film on the hot inside of the duct and lower the material temperature. In Table 28 the number of holes, cooling air consumption and material temperature are showed.

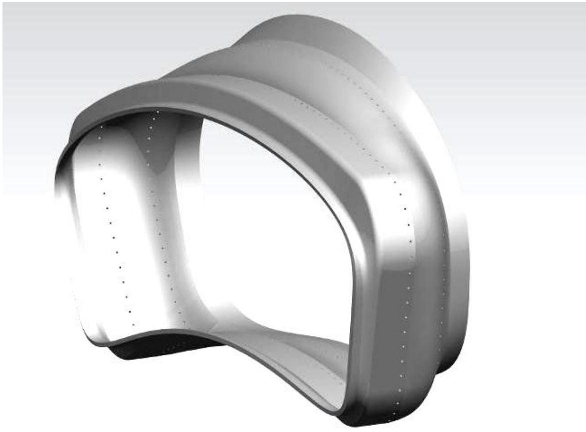

Figure 37. Sealing flange with impingement holes.

Table 28. Cooling setup and result in the aft end, section 5, where impingement and effusion are used.

Impingement and Effusion

Section:	1	2	3	4	5
Impingement					
Hole Spacing X [mm]	-	-	-	-	20
Hole Spacing Y [mm]	-	-	-	-	10
Number of Holes	-	-	-	-	128
Pressure loss [%]	-	-	-	-	3,94
Effusion					
Hole Spacing X [mm]	-	-	-	-	5
Hole Spacing Y [mm]	-	-	-	-	4
Number of Holes	-	-	-	-	481
Pressure loss [%]	-	-	-	-	0,56
Temperature Material [K]	-	-	-	-	**988**
Mass flow [Kg/s]		0,12			
Percent of Total Mass flow [%]		1,09			

One important thing that has to be taken to consideration is that the area behind the D-bar will be hard to reach for the cooling air. To avoid hot spots, effusion holes will be placed in a triangle behind the bars to cool that area. The setup for that arrangement is showed in Figure 38 and the data are showed in Table 29. The result of the temperature is depending on the convection from the holes and all other possible cooling effects are neglected. Note that the outer shell is not shown in Figure 38. The overall air consumption result for this cooling solution, with the impingement and effusion cooling in section 5 and the cooling behind the D-bars is presented in Table 30

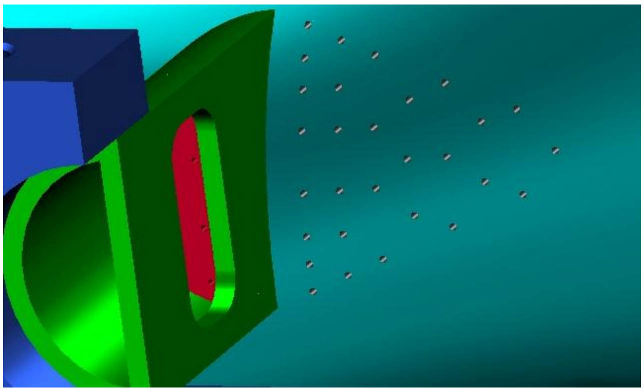

Figure 38. . Effusion hole pattern behind the D-bar.

Table 29. Result and setup for the cooling solution behind the D-bars. Note that the calculation regards both sides of the transition duct.

Convection holes behind D-bars, both sides	
Diameter [mm]	1
Number of Holes	58
Pressure loss [%]	4,5
Mass flow [Kg/s]	0,045
Percent of Total Mass flow [%]	0,43
Temperature [K]	1042

Table 30. This is the total result of the cooling air consumption for this cooling solution. Note that the serial cooling which is the main cooling method does not consume any air.

	[kg/s]	[%]
Impingement effusion	0,120	1,09%
Behind D-bar cooling	0,045	0,43%
Total:	**0,165**	**1,52%**

Advantages

- Air consumption

  This is the cooling method which consumes the smallest amount of air. The only place where air is consumed is at the sealing area where impingement and effusion are used and for cooling and inside and behind the D-bars.

- Design

  The use of ribs is a proven design used on other combustion chamber parts in gas turbines.

Disadvantages

- Design

  Space-consuming due to the larger shell offset in respect to the current design and also due to the extra connection flange which connects the transition duct outer shell with the outer shell on the combustion can.

6.1.3 Costs

The cost for the strongest combination is divided in two parts, one for the cooling solution and one for the mounting solution. The cooling solution will cost about 140% of the cost for current cooling solution and the mounting solution will cost about the same as the current mounting solution. See Appendix 6 for a detailed cost summary.

6.2 Alternative Cooling Solutions

In this chapter additional cooling concepts that can be of interest for Siemens are presented. Some of the concepts are further developed and some is recalculated. All of the concepts provide a table with results from the calculations.

6.2.1 Laminated Sheets

This concept is as described in the previous chapters, a design with one shell, constructed as a laminate with internal cooling channels. As laminated sheets can not be formed by pressing in the shape of current design this solution requires a complete redesign of the transition duct shape. This solution is therefore just considered as an alternative to the other combinations.

Impingement and effusion cooling are used at the aft end, section 5 as they are more suited for cooling of exposed parts such as the sealing flange. The rest, about 80 percent, section 1 to 4 of the transition duct is cooled by cooling channels. The channels lie side by side with alternating flow direction for a more even material temperature. At the fore end the channels are spread with a quite large distance about 2,5 mm. In the aft end the spread is quite small, about 1,5 mm due to the cross section shrinkage of the transition duct. The transition duct requires more cooling at the aft end, which the small distance between the channels provides. The result from the laminated sheets calculation in section 1 to 4 is showed in Table 31. For section 5 where impingement and effusion is used, the result is the same as before, Table 28. For the whole transition duct the air consumption result is showed in Table 32.

Table 31. The table shows the result for the laminated sheets calculations in the four first sections.

Laminated sheets

Section:	1	2	3	4	5
Number of channels	170	170	170	170	-
Space between [mm]	2,5	2,4	2	1,5	-
Channel width [mm]	2,5	2,5	2,5	2,5	-
Channel height [mm]	1,8	1,8	1,8	1,8	-
Temperature Material [K]	**1030**	**1030**	**1030**	**1032**	**-**

Mass flow [Kg/s]	0,30
Percent of Total Mass flow [%]	2,84%

Table 32. This is the total result of the cooling air consumption for the laminated sheets in section 1 to 4 and impingement and effusion in section 5.

	[kg/s]	[%]
Laminated sheets	0,30	2,84%
Impingement effusion	0,12	1,09%
Total:	**0,42**	**3,93%**

Advantages

- Air consumption

  Apart from the cooling solutions with serial cooling this solution consumes the smallest amount of cooling air.

Disadvantages

- Design

  It is not possible to machine press laminated sheets due to the small channels inside the material. Therefore this solution requires a complete redesign of the transition duct shape. The duct has to be more rectangular shaped with flat surfaces so that the duct can be welded together from sheets.

6.2.2 Impingement and Effusion with Film Effect

This is a further development of the cooling methods in concept C2 and C12 from chapter 5.3. This solution requires two shells just like current design but instead of dumping the cooling air inside the transition duct at the fore end, the air is purged through five double rows of effusion holes in the inner shell which creates a cooling film. The double rows are spaced 6 cm along the transition duct, which gives five sections. The impingement holes are located in the outer shell, between the effusion rows where the heat transfer from the effusion holes does not reach, see Figure 39.

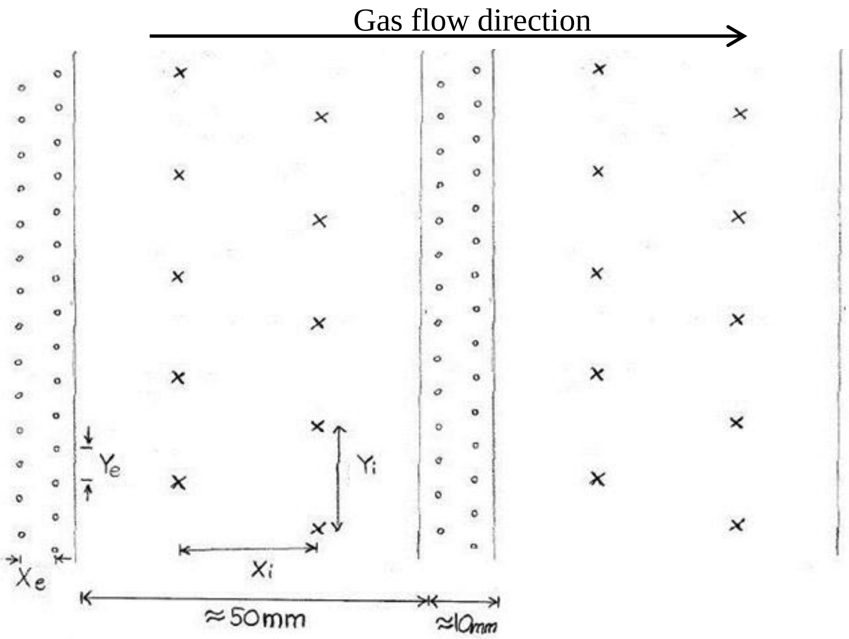

Figure 39. Two of five sections are showed with the hole pathern, the crosses are the impingement holes and the smal holes are the effusion holes.

The cooling combination is designed to create a large pressure drop over the impingement holes and a low pressure drop over the effusion holes to ensure good conditions for a cooling film. The impingement hole spacing is rather large, larger than the correlation admits and the holes are small, together with a large effusion hole area the pressure drop over the impingement is about 8 times higher than the pressure drop over the effusion holes. This results in high air velocity of the impingement jets and low air velocity through the effusion holes. That ensures a high mean heat transfer coefficient both at the impingement area and the effusion area and keeps a good insulating cooling film on the hot gas side. A thick layer of TBC can be used to reduce the temperature gradient which is caused by large hole spacing and high impingement air velocity. Result from the temperature calculations are presented in Table 33.

Table 33. In this table the total result of impingement and effusion is showed.

Impingement and Effusion

Section:	1	2	3	4	5
Impingement					
Hole Spacing X [mm]	20	20	20	20	20
Hole Spacing Y [mm]	20	20	17	15,5	10
Number of Holes	85	83	90	89	128
Pressure loss [%]	3,93	3,93	3,93	3,93	3,93
Effusion					
Hole Spacing X [mm]	5	5	5	5	5
Hole Spacing Y [mm]	5	4,5	4,5	4	4
Number of Holes	341	367	339	344	321
Pressure loss [%]	0,57	0,57	0,57	0,57	0,57
Temperature Material [K]	**1023**	**1024**	**1024**	**1031**	**1015**

Mass flow [Kg/s]	0,43
Percent of Total Mass flow [%]	4,04%

Advantages

- Design

  The shape of the transition duct is almost the same as current design, a few more holes in the inner skin and a few less in the outer skin.

- Flexibility

  It is easy to change the hole pattern to provide more cooling, no redesign of the pressing tools are required. Impingement had the best performance during the early concept evaluations, see chapter 5.3.

Disadvantages

- Manufacturing

  The effusion holes are angled and thus hard to manufacture, the fact that the transition duct is shaped as it is makes the hole drilling even harder.

- Air consumption

  Even that the amount of air spent on cooling is about 3.5 times less than current design it is rather high compared to other solutions.

6.2.3 Impingement and Effusion (without Film Effect)

This solution is similar to the cooling solution above. The large difference is that the impingement holes are evenly spread in each section on the outer skin surface and the effusion holes are evenly spread in each section on the inner skin. The hole spacing are smaller near the aft end and larger in the fore end because of the difference in heat transfer coefficient on the hot side. The effusion holes do not provide a cooling film due to the large effusion hole spacing and high blowing ratio. Instead it is only convection from the effusion holes and the impingement that matters. The result is shown in Table 34

Table 34. Result of the impingement and effusion calculation without film. The effusion holes are not gathered in rows, instead they are evenly spread in each section.

Impingement and Effusion without Film

Section:	1	2	3	4	5
Impingement					
Hole Spacing X [mm]	14	13	12	11	9
Hole Spacing Y [mm]	9	9	8	7	6
Number of Holes	406	423	477	536	713
Pressure loss [%]	0,47	0,47	0,47	0,47	0,47
Effusion					
Hole Spacing X [mm]	16	16	15	13	10
Hole Spacing Y [mm]	16	16	15	13	10
Number of Holes	200	194	204	244	385
Pressure loss [%]	4,03	4,03	4,03	4,03	4,03
Temperature Material [K]	1034	1035	1034	1035	1020

Mass flow [Kg/s]	0,84
Percent of Total Mass flow [%]	8,0%

Advantages

- Same as 6.2.2.

Disadvantages

- Air consumption

  This solution consumes almost twice as much cooling air as the solution in 6.2.2.

- Manufacturing

  Difficulties when apply thermal barrier coating due to the effusion hole pattern. Every hole have to be masked before applying the TBC, or a special laser have to be used to penetrate the layer if the holes are made after applying TBC.

6.3 Alternative Mounting and Sealing Solutions

In this chapter two more concepts which can be of interest for Siemens are presented. The first in order is a total redesign of the mounting and the second is an idea which improves the serviceability for the current transition duct without major redesign.

6.3.1 Floating flange with D-bars

In chapter 5.5 one of the strongest concepts was concept MS2 which used a sealing flange and D-bar mounting, see Figure 40. The difference with this mounting is that the frame is not annular like the one in Figure 33. Instead each transition duct has its own mounting frame which also consist the sealing flange. This change is due to the difficulty of installing the sealing in a frame which already is mounted in the central housing. This design with separate frames needs to be sealed against the adjacent frame. This can be achieved by either new design of the stator rings or labyrinth seal between the frames. The redesign of the rings just contains eight struts connecting the rings, one between each transition duct frame. The idea is that the frame will get a surface to seal against. If labyrinth seals will be used this seals should be machined in the sides of the actual frame. Because of the fact that the shape of the separate frames that can be likened with an arc of a circle, or a piece of a pie, the labyrinth seal can be engaged by lower one frame from a little distance above, down between the adjacent frames.

The sealing flange which is showed in Figure 41, the red part is made from what can be likened to two C-seals that are connected to each other with a flange. The C:s are located in grooves at the duct aft end and inside the duct frame, showed in Figure 41. The frame is also divided in different parts, blue part and green part, which enable the installation of the flange, see the principle in Figure 42. This design also gives the opportunity to pretension the C:s inside the groove creating a better sealing pressure against the sealing surfaces inside the groove. The Sealing flange is able to move inside the groove in order to allow thermal expansion in radial direction. The axial movement due to thermal expansion in the area of the flange will be small because of the short distains from the D-bar mounting. Most of the axial movement will be directed against the combustion can instead. The small movements that will occur in the flange area will be taking care of by the flange.

Advantages

- Low leakage

  This design should lower the leakage because of the use of C-seals instead of just a flange. The pre tensioned C:s should minimize the clearance where leakage can occur between the sealing and the groove.

- Serviceability

  This design with separate frames allows replacing of the transition duct from one open port hole.

Disadvantages

- Manufacturing

  The yellow flange located on the transition duct most be spited in half before the halves are welded in place on the transition duct. Otherwise the flange is impossible to fit. The red flange with the C:s also have to be welded together from two halves, when it is mounted in the yellow groove.

- Design

  Due to the separate frames leakage can occur between the frames and redesign of the stator ring may have to be carried out.

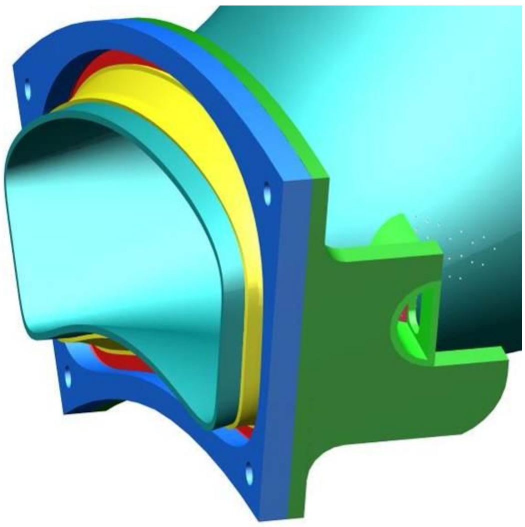

Figure 40. Floating flange with D-bar mounting.

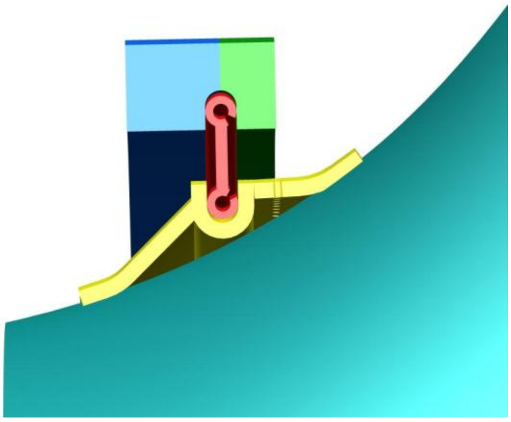

Figure 41. Cross section of the grooves in the frame and transition duct. The red flange is also showed in the picture.

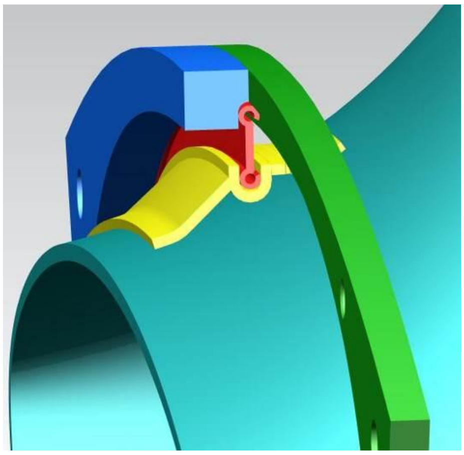

Figure 42. The figure shows the principle of splitting the blue and green mounting frame in part. Do not mind the cross section of the yellow part.

6.3.2 Current Improved Design

This is a refined version of concept MS3 from chapter 5.5. It was not one of the best concepts but it solves the serviceability problem in an easy way. The transition duct can be removed by open up only one port hole instead of three. This is possible because the transition duct mounting frame does not share bolts with the two adjacent frames. The frame is also installed at the transition duct before it is mounted in the gas turbine, which simplifies the montage, see Figure 43. To enable the installation on the transition duct, the frame is divided in four parts that are assembled around and held together by two small bolts. In Figure 44 the principle of the frame is showed with one of the side parts (half T-bone) hidden. The frame holds the flange in place just like the current design does. To be able to create a seal between the frames the same alternatives as in the solution with the floating flange in chapter 6.3.1 can be used. The alternatives are redesign of the stator rings or the labyrinth seal.

Advantage

- Design

  No change of the transition duct flange design is needed. The new frame which replaces the clamping bars works the same way, holding the flange.

- Serviceability

  There will not be any lose parts that have to be held in place when the mounting in the gas turbine take place.

Disadvantage

- Design

  Due to the separate frames leakage can occur between the frames and redesign of the stator ring may have to be carried out.

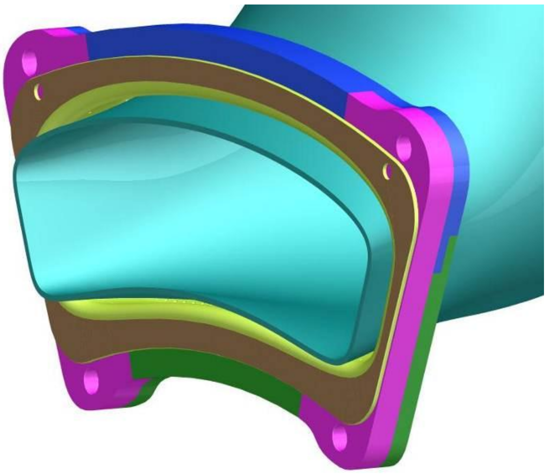

Figure 43. This is the new design of the current mounting which enable replacement relieve the mounting and replacement of the transition duct

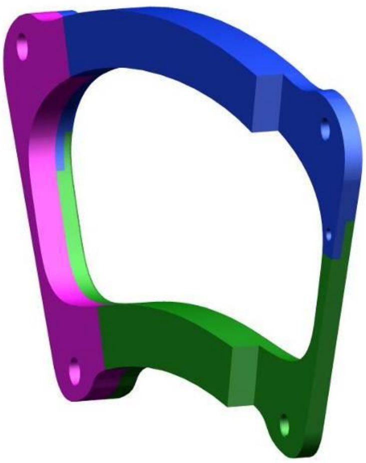

Figure 44. This figure shows the structure of the frame with the new shaped clamping bars and "T-bones".

7 Discussion

Due to the fact that gas turbine engineering is an established engineering art and many of the people designing these machines are proficient with the work. It can be of advantage to let, like in this case, more inexperienced engineers do the concept generation because of the wider perspective that comes with the lack of knowledge of difficulties.

7.1 Method Choices and its Limitations

In the beginning of this thesis work a project specification list was established based on what we comprehend SIT AB thought was important and what we did learn from the state of the art. This project specification maybe would have been better if we had used the gathered information in a quality function deployment, QFD. In the other hand it had taken more time from the remaining development process if the QFD only had been used for the project specification.

The method choice for concept generation may not have been the best choice for our case. The reasons for the difficulties have been that cooling, mounting and sealing have been hard to develop in the same process along with each other. Instead we had to split them apart and cooling was separated from the mounting and sealing which was developed and evaluated on the same basis. In the function mean tree for the cooling some of the sub functions did not had to be solved to satisfy the main function. To show that one of the means located under the sub function had the text saying “None”. On the mounting tree the same technique was used to show that some sub functions was not needed to be solved, the mean in that case had the text “Free”. To use that sort of non solving means in the function mean tree are not the idea of the method, but it helped us to visualize our thoughts.

The biggest difference in the method is shown when we came to the evaluation. In the cooling evaluation we had the calculated data on each concept, both from the cooling calculations and the cost calculation. That did it possible to use the weighted objectives method which gave us the strongest concept immediately. When using this method the only thing that can influence the result is the case of miscalculations, or if the criteria in the pairwise comparison have been weighted in an incorrect way. In the mounting and sealing evaluation no data had been calculated which did make the use of datum matrix more suitable. The criteria in this case were also weighted with pairwise comparison before the evaluation began. Because of the lack of data we had to do all of the judgment in the datum method by own estimation with some help from the experts at SIT AB. In order to get reliable results, the “datum” in the method was changed to represent the best concept after each evaluation and with that iteration process the best concept showed. With this method it can still be hard to be impartial and it is important to be fair.

7.2 Literature Limitations

Guidelines for hot constructions were hard to find in the literature. Most of the information is kept internally at the companies. SIT AB had some internal documents in the area, but to get a more open minded view at the problem, some external sources would have been helpful. It was also hard to find information about how other companies constructed theirs transition ducts. Instead mostly patents have been used as source for inspiration for new ideas.

Cooling methods with established correlations for guide vanes and turbine blades was easy to find in the literature, but it was harder to find methods for the combustion chamber parts. The different parts can often be cooled with the same methods, but correlations developed for turbine parts are often suited for much higher gas velocities. It was therefore hard to find correlations that suited our cases perfectly.

Commercial sealing solutions for transition ducts was also hard to find, most of the gas turbines that we saw was using solutions that was designed by the company itself. In the cases where commercial sealing solutions was suitable, it was hard to get information about sealing performance and durability.

7.3 Cooling

Some correlations for effusion cooling that have fit our case have required tests and measurement to determine some constants. It has therefore been hard for us to use these correlations as there has been no time for testing. The impingement correlations was made for a specific range in hole spacing. In the combination of impingement/effusion, see chapter 6.2 the hole spacing is larger than that. Similar hole spacing have been used in other gas turbines at SIT AB with satisfying result. The fact that we have used correlations that not completely fit our case and break some correlation limits may lead to a difference between our results and the reality.

Laminated sheets is a rather new technique and no specific correlations was found. A combination of heat transfer from channels and one dimensional conduction was used instead. Siemens Orlando has used similar equations with good result, so the result we received should give a good estimate of how good the method is.

No simulations have been made to evaluate our calculations. Even if the result not is completely corresponding to the reality, it should anyway give an understanding about the potential and difference of different cooling methods.

Current design gave a material temperature of 1032K in our calculations and the evaluated cooling methods were optimized to a material temperature of 1100K. This difference in temperature did lead to large reduction of air consumption for the new concepts, which can be misleading. Although this did not affect the results, the evaluation was a comparison between the new cooling methods to separate them.

7.4 Mounting

The mounting concept evaluation was based on assumptions and estimations. No calculations have been made except the force calculations. We did not calculate if the mounting parts would stand the forces but the work has been done with the forces in consideration. LCF and wear has also been evaluated with our assumptions. The assumptions were discussed with personnel at SIT AB to get more reliable results.

7.5 Sealing

This part is the most unsure in our concepts. No leakage calculations have been done for the sealing solutions. It was hard to determine the leakage flow without tests so these evaluations were also made with assumptions and estimations. Wear was also hard to determine and estimations was done here too. In the cases were a manufacturer have been involved, like with brush seals and rope seals, we had to believe their information even if it was biased for their best.

7.6 Cost

The cost has been very hard to estimate on each part, especially for the mounting and sealing solution. We have tried to estimate the new cost by asking the workshop and scale the current costs. When the workshop was estimating the price on regarding redesign of the old stator rings to consist the sealing groove and the D-shaped sockets, they just added the cost for the extra machining. What they did not do was to recalculate the current stator rings as one part instead of the current two. We believe the total cost should be reduced due to the fact that only one forging is needed to be machined.

It is also hard to estimate the stator ring material cost. We do not know if it is possible to use a forging that is close to the desired shape in this case, due to the more complex shape compared to the current. Anyhow we did increase the material cost just with the extra material for the sockets.

7.7 Patents

As we was using patent as an inspiration source it is important to investigate so that no patents have been violated. The best solution that we suggest have some similarities to the sealing used in patent US 7,584,620, see Appendix 1. The patent uses some sort of rope seal to seal and supports the transition duct in the aft end. The patent is owned by Siemens Orlando so there should not be a problem.

7.8 Future Work

CFD calculations and simulations have to be made at suggested concept to establish correct air consumption and material temperatures. The mounting parts need to be evaluated and simulated with both static forces and thermal forces.

Rope seals are an unproved method in transition duct sealing and must be evaluated with tests to ensure the function.

There are methods of applying ribs to the transition duct. A method has to be chosen to determine the real manufacturing costs.

Our suggested concept requires a new connection between the transition duct and combustion can. We have not reflected of a solution and a redesign has to be done.

8 Conclusions

After this thesis work we can without doubt say that there are great opportunities to lower the cooling air consumption on the transition duct. Especially by using serial cooling with ribs as the strongest combination, chapter 6.1. There are also other methods that have showed good results for lowering the air consumption. With just a slight design change regarding the hole pattern the current transition duct can be modified to lower the cooling air consumption, like the cooling solution in chapter 6.2.2.

The serviceability will be facilitated with the mounting and sealing concept used in our strongest combination. Only one combustor casing have to be removed to replace a transition duct. There will also be less loose parts that have to be held in place during the montage. If no major design changes wish be implemented, the current transition duct mounting details can be replaced with the one in chapter 6.3.2 to make the serviceability at current duct easier.

9 Bibliography

Abdon, A. (2001). *Numerical Simulations of Cooling Concepts Related to Gas Turbine Combustors*. Lund: Mrs Gunvi Andersson, Div. Heat Transfer.

Askeland, Donald R. & Phule, Pradeep P. (2005[2006]). *The science and engineering of materials.* 5. ed. Toronto: Thomson

Bejan, Adrian (2004). *Convection heat transfer*. 3. ed. Hoboken, N.J.: Wiley

Çengel, Yunus A. & Turner, Robert H. (2005). *Fundamentals of thermal-fluid sciences*. 2. ed. Boston: McGraw-Hill

Cerri, G., Giovannelli, A., & Fedrizzi, R. (2007). Advances in Effusive Cooling Techniques of Gas Turbines. *Applied Thermal Engineering Mar2007, Vol. 27 Issue 4*, 692-698.

Cohen, Henry, Rogers, G. F. C. & Saravanamuttoo, H. I. H. (1996). *Gas turbine theory.* 4. ed. Harlow: Longman

Cross, Nigel (1994). *Engineering design methods: strategies for product design*. 2. ed. Chichester: Wiley

Dahlberg, Tore (2001). *Teknisk hållfasthetslära*. 3., [red.] uppl. Lund: Studentlitteratur

Derelöv, M. (2002), *Produktutvärdering*, Linköping University, Sweden

General Electric Company (1988*) Impingement cooled transition duct* US004719748

Han, Je-Chin, Dutta, Sandip & Ekkad, Srinath (2000). *Gas turbine heat transfer and cooling technology*. New York: Taylor & Francis

Flowserve. (den 4 October 2008). Stress corrosion cracking. *Flowserve Materials Newsletter*.

Lakshminarayana, Budugur (1996). *Fluid dynamics and heat transfer of turbomachinery*. New York: Wiley

Liedholm, U. (1999), *Systematisk Konceptutveckling*, Linköping University, Sweden

Onwubiko, Chinyere Okechi (2000). *Introduction to engineering design optimization*. Upper Saddle River, N.J.: Prentice Hall

Power Systems Mfg (2002) *Three degrees of freedom aft mounting system for gas turbine transition duct* US006442946

Siemens Energy, Inc (2009) *Support system for transition ducts* US007584620

SGT - 750 - Siemens. (n.d.). Retrieved May 13, 2011, from Siemens Energy: http://www.energy.siemens.com/hq/en/power-generation/gas-turbines/sgt-750.htm

Storck, K., Karlsson, M., Andersson, I., Loyd, D. (2003*). Formelsamling i termo- och fluiddynamik, Institutionen för Konstruktion och Produktion*, Linköping University, Sweden

Ullman, David G. (2010). *The Mechanical design process*. 4. ed. Boston: McGraw-Hill

Young, Hugh D., Freedman, Roger A. & Sears, Francis Weston (2003). *Sears and Zemansky's university physics: with modern physics*. 11. ed. San Francisco, Calif.: Pearson Education

Zhang, C., Lin, Y., Xu, Q., Liu, G., & Song, B. (2009). Cooling Effectiveness of Effusion Walls with Deflection Hole Angles Measured by Infrared Imaging. *Applied Thermal Engineering, Vol. 29 Issue 5/6*, 966-972.

Ölvander J. (2010), *Design Optimization*, Linköping University, Sweden

10 Appendix

APPENDIX 1 – PATENT BRIEFING

APPENDIX 2 – FUNCTION- MEANS TREE

APPENDIX 3 – COOLING CONCEPTS

APPENDIX 4 – GO/NO GO SCREENING COOLING CONCEPTS

APPENDIX 5 – CALCULATIONS METHODS OF COOLING

APPENDIX 6 – COST CALCULATIONS

APPENDIX 7 – WEIGHTED OBJECTIVES METHOD, COOLING

APPENDIX 8 – FORCE CALCULATIONS

Appendix 1 – Patent Briefing

Cooling Patents

An alternative way for transition duct cooling is with a modular cooling panel shown in US patent 6,018,950. It is a technique based a corrugated sheet weld on a single walled transition duct, principle is showed in Figure 1. The corrugated shape defines cooling flow channels in which air can travel and to cool the transition duct.

Each channel has one open end and one closed end. In the closed end an exit hole connects the cooling air channel with the inside of the transition duct. This arrangement with open and closed ends alternates from one channel to the next adjacent channel, showed in Figure 1.

The principle of this design is that air from the compressor stage enters the open end of the channel, traveling along the transition duct and removing heat. At the end of the cannel the air flows through the exit hole to be mixed with the hot gas inside the duct. (Siemens Westinghouse Power Corporation, 2000)

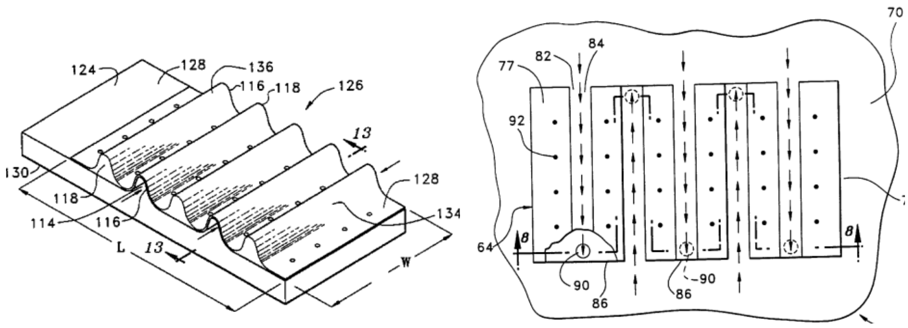

Figure 1. Cooling channels with corrugated sheet. The right sketch shows the flow path with alternating flow directions. (Siemens Westinghouse Power Corporation, 2000)

The inventor of US patent application, number 10/836,972 claims that impingement cooling which is an regular cooling technique are ineffective due to the pressure losses. The principle presented in this patent uses forced convection on the inboard panel and effusion cooling on the outboard surface.

The transition duct is made in single wall design with thin ribs on the inboard panel to increase the cooling area for the forced convection. Due to the decrease of direct flow on the outboard surface forced convection can’t be used. Instead the outboard sheet contains lots of holes which cooling air are flowing through, which creates effusion cooling. (Vincent C. Martling, 2005)

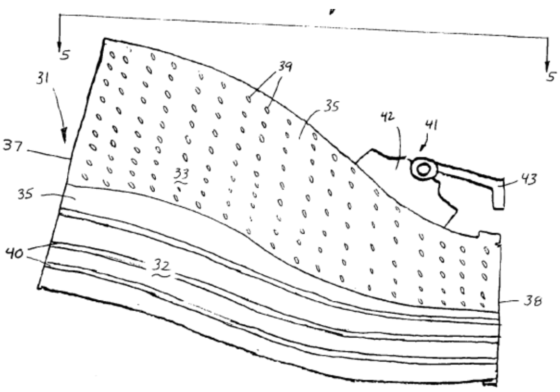

Figure 2.T-duct with inboard side cooled by forced convection and the outboard side is cooled by effusion. (Vincent C. Martling, 2005)

One way to cool the transition duct is to force compressor air to the outboard surface of the transition duct to increase the forced convection. This is shown in US Patent 4,903,477 where a saddle is formed over the outboard panel, see Figure 3. This solution only works when the forced convection on the inboard panel is sufficiently high. Compressor air is forced between the saddle and the transition duct. To ensure the air to flow between the surfaces, flanges may be used to lead air in to the slit, see Figure 3. The air flows out through large holes at the top of the saddle, and flows on to the combustion. (Westinghouse Electric Corp, 1990)

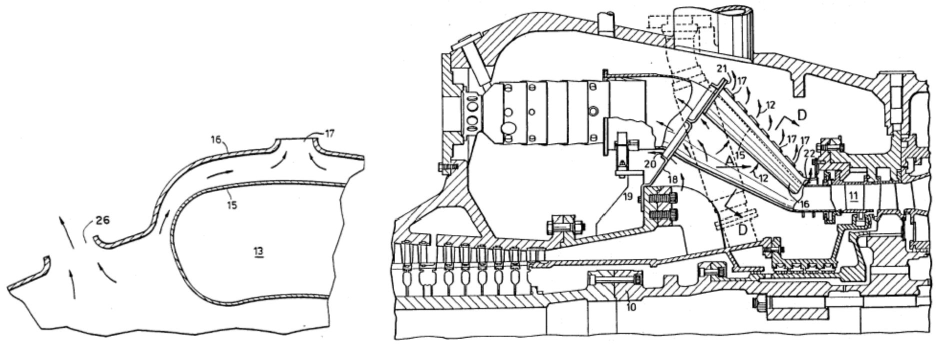

Figure 3. A saddle is used to cool the transition duct.. The left figure shows the cross section D-D in the right figure. The right figure is a layout over a combustion system with a transition duct. Westinghouse Electric Corp, 1990)

US patent application, number 11/014,294 is about a cooling method that combines effusion cooling holes and cooling channels. At areas with large cooling need, like in the upstream bend, the channels is placed tight, between plate 58, 60 and 54 in Figure 4. To keep an efficient cooling with low thermal gradient the cooling channels is alternately directed, orientated upstream and downstream. A drawback with cooling channels is weakening of the structure and to compensate for that stiffening ribs are used. The ribs raise the heat transfer and stress fields occur at the rib ends. To avoid too large stresses, in sensitive areas, like in the double bend region, 48 in Figure 4 and near the stiffening ribs, no active cooling that generates stress due to thermal gradients is used near that area. (Siemens Westinghouse Power Corporation, 2006)

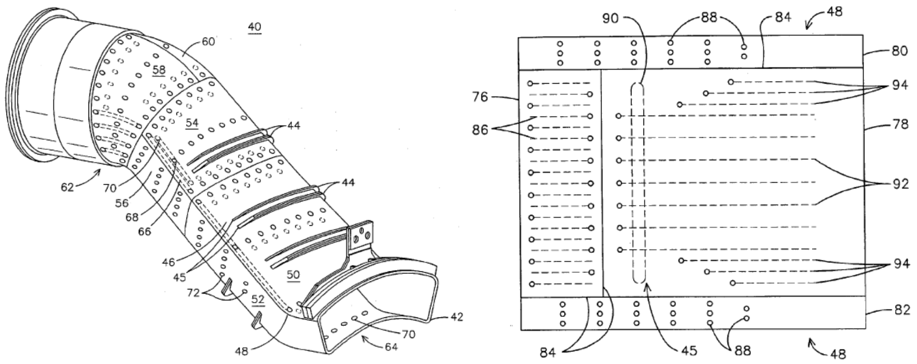

Figure 4. To the left a transition duct cooled by cooling channels and effusion cooling. To the right the channel structure of the transition duct. (Siemens Westinghouse Power Corporation, 2006)

One impingement cooled double walled design transition duct is presented in patent US 4,719,748. The outer sleeve on the transition duct is connected to the outer combustor sleeve. Allowing the impingement air to travel between the shells up to the combustor, instead of dumping the air inside the transition duct. That reduces the consumption of compressor air for cooling and the air can be used in the combustion process instead. One more advantage should be that more air is traveling past the combustor which increases the cooling effect. In Figure 5 the double wall structure shows, also the impingement holes in the outer shell of the transition duct can be seen. (General Electric Company, 1988*)*

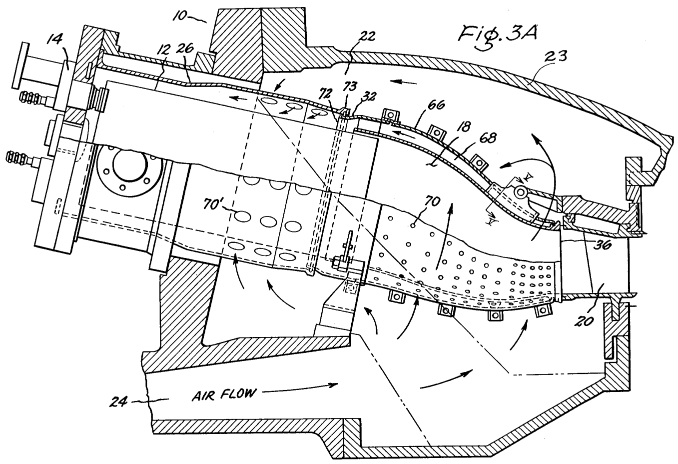

Figure 5. Impingement cooled transition duct. (General Electric Company, 1988)

Mounting Patents

The patent US 6,442,946 presents a three degrees of freedom aft mounting system for transition ducts. This type of mounting allows the transition duct to compensate for the thermal expansions in three directions to maintain the accurate position align to the turbine. That should lower the thermal and mechanical stresses on the mounting and the transition duct.

The structural system includes a central bracket with a spherical ball mount, showed in Figure 6. The spherical ball has a diametrical double-conical shaped hole, Figure 6, in which the attachment axle is mounted. That solution allows the axel to move relatively to the bracket in three directions, pitch, roll and yaw.

The bracket is mounted in turbine inlet hosing and a dome plate is welded on to the transition duct. The connection in between is the ball with the conical shape. This means that the transition duct gets the ability of movement from the axel. (Power Systems Mfg 2002)

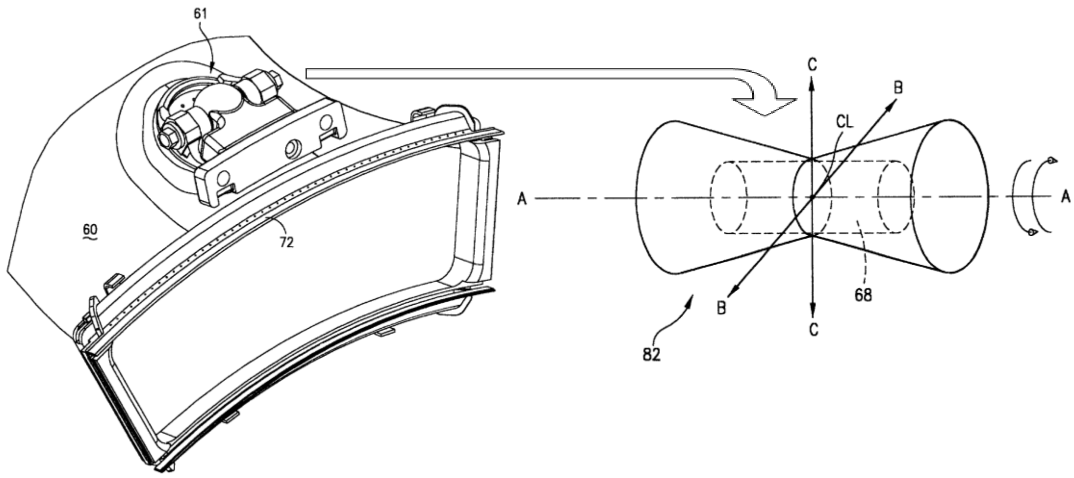

Figure 6. Bracket with three degrees of freedom. (Power Systems Mfg 2002)

An idea of a support system for transition ducts are presented in the patent US 7,584,620. It also contains a concept for sealing the exit end of the transition duct from the turbine section.

The invention is based on two circle segments, shaped to one inner and one outer span joined together with a central column, seen in Figure 7. With a plurality of those shapes joined together, a circular support system for the transition ducts are obtained, see Figure 7.

Support to the transition duct is obtained by the surface created between the circle spans and central column. An edge prevents the duct to slide in to the turbine section, see the Figure 7 no 78. Also showed in the picture are the potential to fit a seal 62 in a groove at the surface. The inserted portion of the transition duct will seal against the lateral opening. Thanks to the thermal expansion of the transition duct the sealing capacity will increase. Also vibrations are claimed to be reduced thanks to the sealing.

The idea to get the support system fixed to turbine housing is by the braces on the upper part of the support, showed in Figure 7 no 64.

With this system the inventor claims that mounting will be easy hence installation of the support system can be performed without any of the transition ducts being in place. (Siemens Energy Inc, 2009)

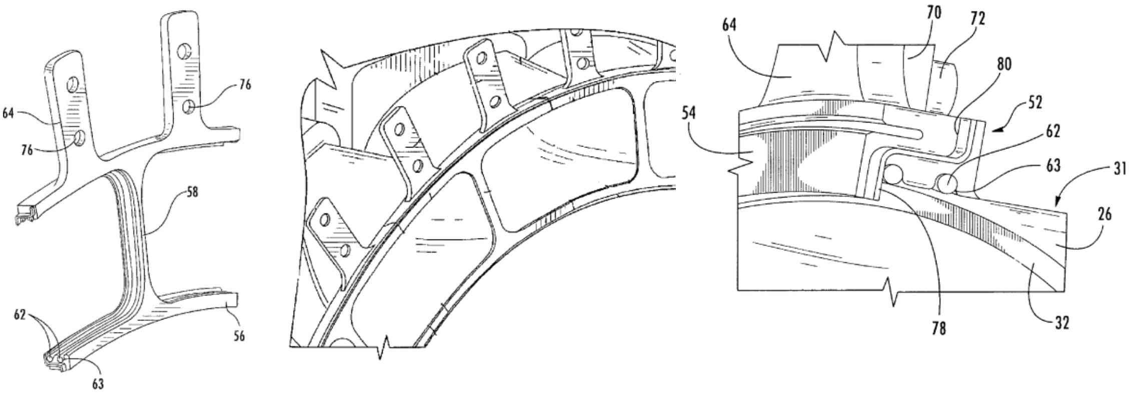

Figure 7. Support system for a transition duct with a integrated sealing. (Siemens Energy Inc, 2009)

A thermally free mounting frame is described in patent US 6,619915 B1, the invention uses a frame that is welded to the aft end of the transition duct. The frame is mounted to the bulkhead with three bolts on the outboard and inboard side of the transition duct. The middle bolt goes through a circular retention hole and the outermost bolts goes through retention holes of a different type. These holes are more rectangular and bushings are located within the holes. The bushings are smaller but longer than the holes which enables the frame to move relative the bolt and the bulkhead, see Figure 8. This patent also emphasizes the opportunity to use a sealing between the ducts. Ribs are located on the sides of the frame and when the duct is mounted, the ribs interlocks, see Figure 8. During operation the ribs works as a sealing when the distance between them decreases, due to thermal expansion. (Power Systems Mfg, 2003)

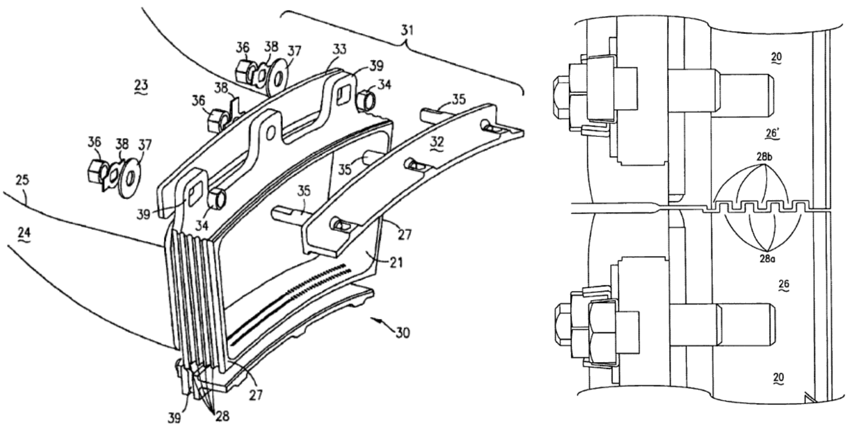

Figure 8. Thermally free mounting frame for a transition duct. (Power Systems Mfg, 2003)

In US patent 5,761898 a few support solutions are presented. Common for all them is some sort of stiffening frame for the transition duct outlet, which has tendency to deform, due to creep deformation. The idea is to clamp the frame to the duct at only one place and then only have some support point for the rest of the frame. Figure 9 shows a frame that enclose the whole duct, it is a little bit large than the duct so thermal expansion is allowed. The frame is clamped in the middle of the outboard part, upper part in the figure. A different solution that is mention in the patent is also showed in Figure 9. On the inboard side a bar is acting as a frame. The bar is clamped at the middle and supported by saddles in the ends. The duct is also attached with three locating pins on the outboard part. Just like the US patent 6,619915 B1 mentioned above, the middle pin is locked and they outermost is free to move within some boundaries. (General Electric Company, 1988*)*

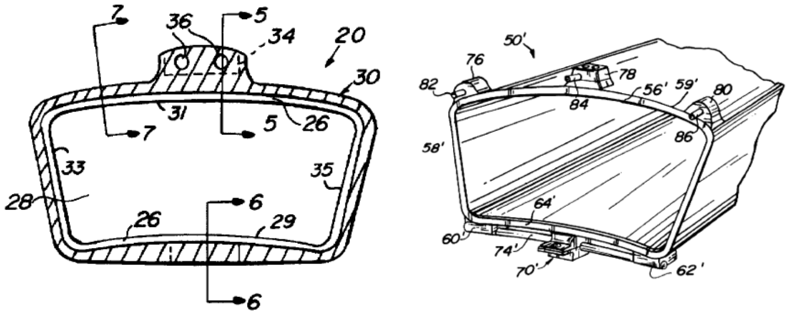

Figure 9. Example of two mounting frames used for a transition duct. (General Electric Company, 1988)

In the rather old US patent 4,016,718 some similarities with the transition duct in SGT-750 can be found. The patent describes a mounting of the transition duct in an outer and inner ring, concentric to the turbine axle, see 50 and 52 in Figure 10. The outer ring is fixed to the central housing and the inner ring is mounted with a flexible sleeve, se 84 in Figure 10, so that thermal expansion is allowed. A strut, see 54 in Figure 10, is located between the rings that strength the inner ring. The transition duct is mounted to the rings with a flange on a sleeve that is welded to the rear end of the transition duct, se 56 in Figure 10. The flange is bolted to the outer ring and clamped to the inner ring with a list, see 60 in Figure 10. (United Technologies Corporation, 1977)

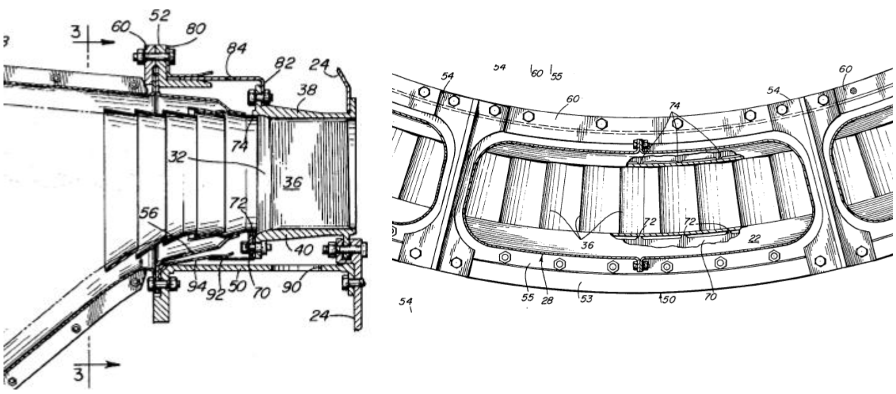

Figure 10. Transition duct mounting system with some similarities of current design. (United Technologies Corporation, 1977)

One way to deal with high temperature gradients in the mounting parts is described in US patent 7,278,254 B2. This patent deals with bracket transition duct mountings and the idea is to create a heat shield on the bracket. The bracket is attached to the hot transition duct and the cold housing. A large temperature variation occurs when the bracket is cooled by compressor air, therefore a heat shield is attached, that insulate the bracket from compressor air, see Figure 11. (Siemens Power Generation, 2007)

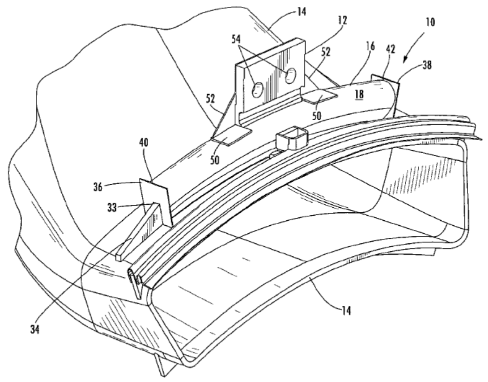

Figure 11. Heat shield for transition duct mounting. (Siemens Power Generation, 2007)

A support system for a transition duct is described in us patent application 11/805,057. The aft frame, see 22 in Figure 12 that is welded to the transition duct is attached to the housing by a bolt at the top. To prevent the transition duct to rotate upward a support system is used. The support system consists of two equally mechanisms, a flange is welded in the aft frame and another flange is welded on the duct outboard surface, see Figure 12. The flanges are coupled together with a flexible bolt joint, tightened with conical spring washer in between. Because the bolt holes in the flanges are larger than the bolt it is possible for the flanges to move relative each other due to thermal expansion. A number of hard metal washers are used in the bolt joint to prevent wear, see Figure 12. (Siemens Power Generation Inc, 2010)

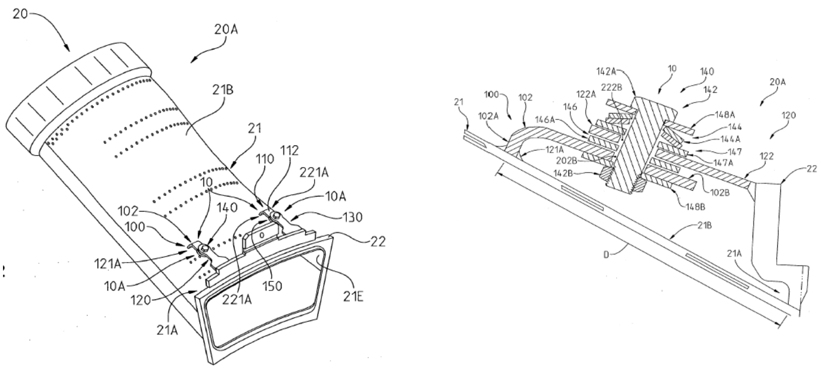

Figure 12. Support system for a transition duct. (Siemens Power Generation Inc, 2010)

Sealing Patents

To avoid stress in the material and simultaneously maintain good sealing efficiency, a setup with flanges can be used. The patent US 4,640,092 present a sealing device that is mounted to the combustion chamber and to the turbine inlet ring. The junction is made by weak flanges that are allowed to flex due to expansion of the combustion chamber. In Figure 13, the combustion chamber shows at 14 and the turbine inlet ring at 2. (United Technologies Corporation, 1987)

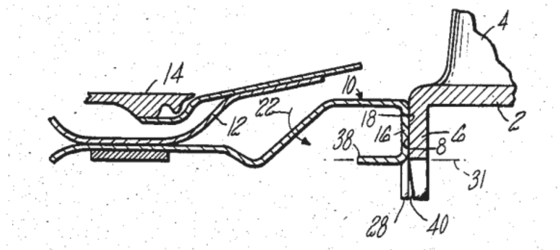

Figure 13. Weak flanges used as a sealing. (United Technologies Corporation, 1987)

A brush seal is used to seal between the transition duct and the turbine inlet in US patent 5,400,586. The seal is suppose to self accommodate by using flanges and the flexible properties of a brush. The brush end fitted in a slit and held at place with a spring clip, which also prevent air to leak around the brush, see Figure 14. The slit where the brush is fixed is located in the end of the transition duct or in the stator ring by the turbine inlet. The brush top is pressed against a flange located at the other part, stator ring or transition duct. The brush is bent outward the high pressure air. The flange is also inserted in a slit and double bended to act as a self sealing in the slit, see Figure 14. The flange where the brush is engaged has to be flat, because if the tip hits any edge or similar it will buckle and loose sealing efficiency. (General Electric Co. 1995)

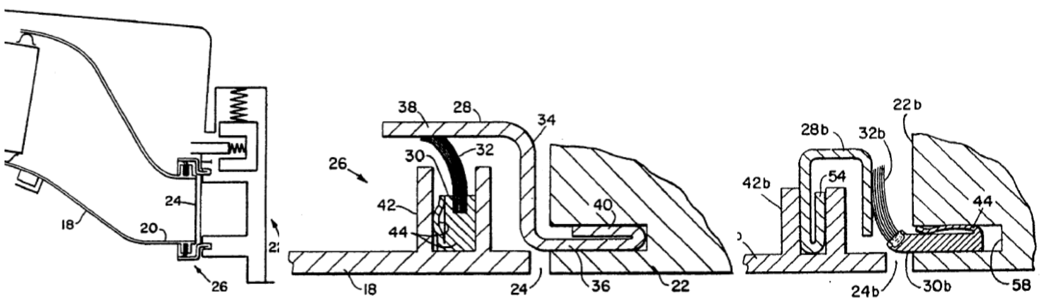

Figure 14. Brush sealing used in two different ways. (General Electric Co. 1995)

Similar to the sealing solution described above is found in US patent application number 09/798,842. This solution seals with a metallic cloth, 36 in Figure 15 instead of a brush. A metallic shim, 42 in Figure 15 is attached on the high pressure side of the cloth to press the cloth against the sealing wall and to prevent air to leak through the cloth. The cloth is flexible even with the shim attached and movement between the sealing parts is allowed within a specific range. (General Electric Company, 2002)

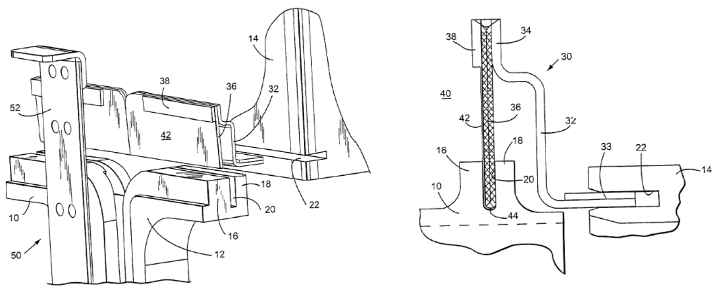

Figure 15. Cloth seal used in a transition duct application. (General Electric Company, 2002)

Bibliography

General Electric Company (2002) *Low leakage flexible cloth seals for turbine combustors* US20020121744

General Electric Company (1988*) Impingement cooled transition duct* US004719748

General Electric Company (1998) *Transition piece external frame support* US005761898

General Electric Co. (1995) *Self-accommodating brush seal for gas turbine combustor* US005400586

Power Systems Mfg (2002) *Three degrees of freedom aft mounting system for gas turbine transition duct* US006442946

Power Systems Mfg (2003) *Thermally free aft frame for a transition duct* US006619915

Siemens Energy, Inc (2009) *Support system for transition ducts* US007584620

Siemens Power Generation (2007) *Cooling system for a transition bracket of a transition in a turbine engine* US007278254

Siemens Westinghouse Power Corporation (2006) *Cooled gas turbine transition duct* US20060130484

Siemens Westinghouse Power Corporation (2000), *Combustion turbine modular cooling panel* US006018950

Siemens Power Generation, Inc (2010) *Gas turbine transition duct coupling apparatus* US20100011576

United Technologies Corporation (1977) *Gas turbine engine having an improved transition duct support* US004016718

United Technologies Corporation (1987) *Combustion chamber rear outer seal* US004640092

Vincent C. Martling (2005) *Transition duct apparatus having reduced pressure loss* US20050241321

Westinghouse Electric Corp (1990) *Gas turbine combustor transition duct forced convection cooling* US004903477

Appendix 2 – Function- means Tree

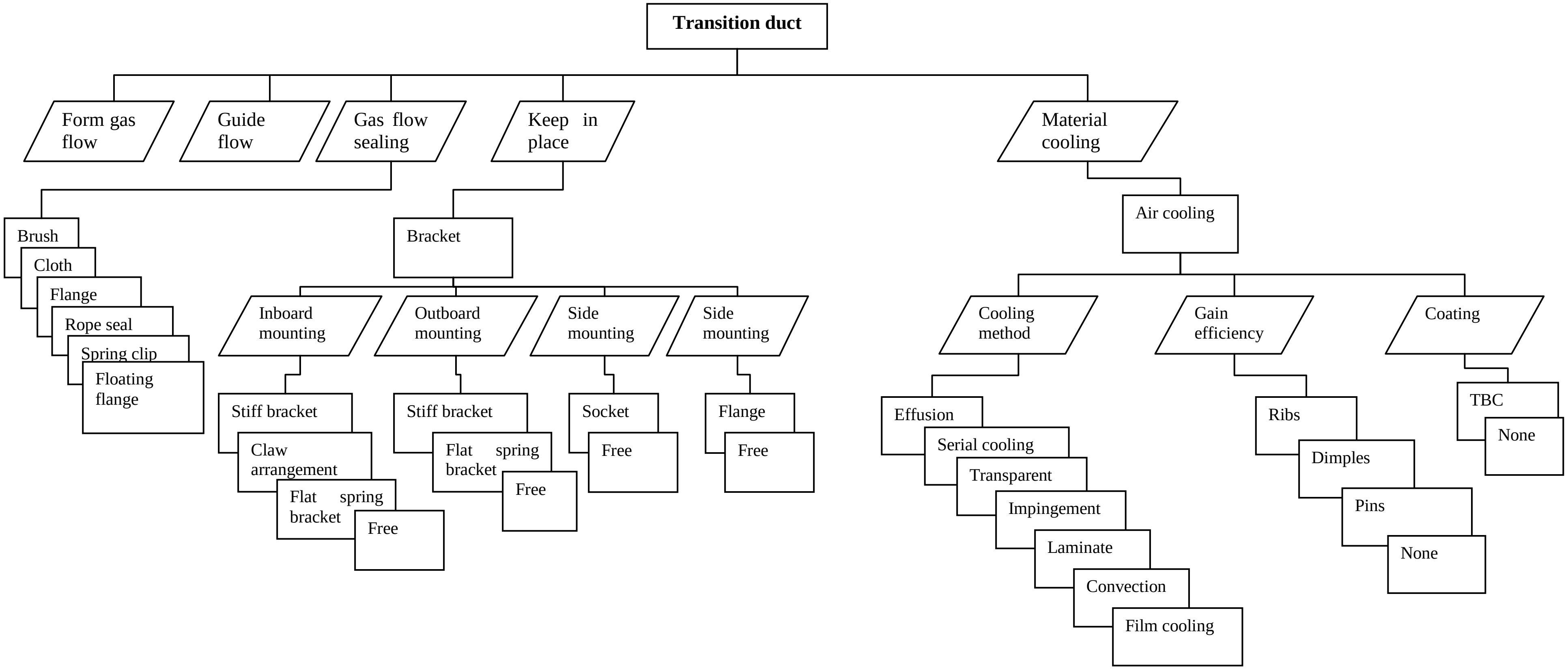

Figure 1. Function/Means tree for the complete transition duct.

Appendix 3 – Cooling Concepts

Table 1. Cooling concepts generated from the morphology matrix.

■	C1	Effussion
■	C2	Effussion with TBC
◎	C3	Serial with dimples and TBC
◎	C4	Serial with dimples
◎	C5	Serial with ribs
◎	C6	Serial with ribs and TBC
◎	C7	Serial with pins and TBC
◎	C8	Serial with pins
◎	C9	Serial
◎	C10	Serial with TBC
◆	C11	Impingement
◆	C12	Impingement with TBC
◆	C13	Impingement with ribs
◆	C14	Impingement with ribs and TBC
◆	C15	Impingement with dimples
◆	C16	Impingement with dimples and TBC
◆	C17	Impingement with pins
◆	C18	Impingement with pins and TBC
☾	C19	Laminate
☾	C20	Laminate with TBC
★	C21	Convection
★	C22	Convection with TBC
★	C23	Convection with ribs
★	C24	Convection with ribs and TBC
★	C25	Convection with dimples
★	C26	Convection with dimples and TBC
▲	C27	Film
▲	C28	Film with TBC

Appendix 4 – Go/no Go Screening Cooling Concepts

Go-/ no Go screening							
	Elimination Criteria (+) Yes (-) No (?) More information necessary				**Decision** (+) Go (-) No go (?) More information necessary		
	A: Solves the problem						
		B: Meets all requirements					
			C: Realizable				
				D: Within cost limits			
					F: Inside our limitations		
Concept	**A**	**B**	**C**	**D**	**F**	**Comment**	**Decision**
Concept 1	+	+	+	+	+	Not.1	Go
Concept 2	+	+	+	+	+	Not.2	Go
Concept 3	?	-				Not.3	No go
Concept 4	?	-				Not.3	No go
Concept 5	+	+	+	+	+		Go
Concept 6	+	+	+	+	+		Go
Concept 7	?	-				Not.4	No go
Concept 8	?	-				Not.4	No go
Concept 9	+	+	+	+	+		Go
Concept 10	+	+	+	+	+		Go
Concept 11	?	+	+	+	+	Not.1	Go
Concept 12	?	+	+	+	+	Not.1	Go
Concept 13	?	+	+	+	+	Not.5	Go
Concept 14	?	+	+	+	+	Not.5	Go
Concept 15	?	-				Not.6	No go
Concept 16	?	-				Not.6	No go
Concept 17	?	-				Not.7	No go
Concept 18	?	-				Not.7	No go
Concept 19	+	+	+	?	+	Not.8	Go
Concept 20	+	+	+	?	+	Not.8	Go
Concept 21	?	?	+	+	-	Not.9	No go
Concept 22	?	?	+	+	-	Not.9	No go
Concept 23	?	?	+	+	-	Not.9	No go
Concept 24	?	?	+	+	-	Not.9	No go
Concept 25	?	?	+	?	-	Not.9	No go
Concept 26	?	?	+	?	-	Not.9	No go
Concept 27	+	?	+	?	?	Not.10	Go
Concept 28	+	?	+	?	?	Not.10	Go

Not.1 This solution are a known method which is used in hot structure. The downside is that it consumes a great volume of air but maybe it can be combined with other concepts and/or used on small local areas.
Not.2 When applying TBC the manufacturing gets more complicated regarding the holes trough the TBC. More expensive.
Not.3 Negative impact to the strength of the material. Difficulties in the manufacturing process which is synonym to high expenses. Equal performance as ribs.
Not.4 Difficulties in the manufacturing process which is synonym to high expenses. Equal performance as ribs.
Not.5 Consumes much air. The cooling effectiveness will gain between 10 and 20%. Maybe this can be used on some small parts.
Not.6 Consumes much air. Negative impact to the strength of the material. Difficulties in the manufacturing process which is synonym to high expenses.
Not.7 Consumes much air. Will probably not be an alternative for small surfaces. No good correlations for computing the cooling effectiveness
Not.8 Calculations have to be made regarding the expenses. Interesting technique to investigate
Not.9 The solution with convection are hard to calculate in a one dimensional case due to the complex flow distribution inside the central casing. This have to be done with CFD to get reliable results, which means that it is outside the limitations.
Not:10 Known way for combustion chamber cooling using slots to create a homogenously film between the hot gas and the wall. This Consumes a grate volume of air and modifications have to be done to the inner shell of the transition duct. May be used on smal surfaces to cool hot spots.

Appendix 5 – Calculations Methods of Cooling

The calculations of each cooling method are based on the theory chapter. Here is the calculation procedure presented together with individual equations for each cooling method. Heat transfer coefficient is calculated according to Chapter 2.1 in the report. This appendix describes how the Nusselt number for each cooling method is calculated and how the heat transfer coefficient at the hot side is calculated.

Heat Transfer Coefficient Calculations at Hot Side

The heat transfer calculations are made with some simplifications. During the first concept evaluations the transition duct is imagined as a one section cylinder with the mean diameter of the transition duct as diameter. The final concepts heat transfer calculations are made with the transition duct imagined as a cylinder with five sections with different diameter.

One Section

On the hot inside of the transition duct the heat transfer coefficient needs to be calculated in order to be able calculating the temperature of the material. To be able to do that, the transition duct is first assumed to be a pipe with a constant radius, r and a length, L, see Figure 1 which creates the same mantel area as the real transition duct. In this pipe the mass flow, and the density of the combustion gas are constant and gives in that hand the velocity and thereby the Reynolds number. With this numbers known the Nusselt number is calculated with Equation 1 in order to determine the heat transfer coefficient, α_{conv} created by the convection. The formula for α_{conv} are found in the heat transfer theory chapter, 2.1.2.

The radiation also gives raise to the heat transfer coefficient and is calculated by the temperature difference between the hot gas and the material surface, which is set to a reference temperature, the same as the material goal temperature. The material also affects the amount of heat transfer from radiation, which means that there is a slight difference depending if TBC is used or not. To get the heat transfer coefficient, α_{rad} from the radiation, the radiation formula, Equation 2 and the linearized formula Equation 3 are combined giving the formula Equation 4. The total heat transfer coefficient α_{tot} is given by Equation 5 and the results are presented in Table 1

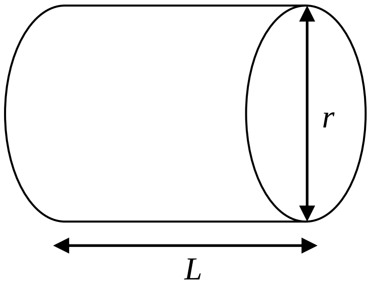

Figure 1. Sketch of a one section transition duct.

$$Nu_d = \frac{0{,}038\,\mathrm{Re}_d^{3/4}\,\mathrm{Pr}}{1+1{,}5\,\mathrm{Re}_d^{-1/8}\,\mathrm{Pr}^{-1/6}(\mathrm{Pr}-1)} \tag{1}$$

$$\dot{Q} = \sigma\varepsilon_{12}A\left(T_1^4 - T_2^4\right) \tag{2}$$

$$\dot{Q} = \alpha_s A\left(T_1 - T_2\right) \tag{3}$$

$$\alpha_{rad} = \alpha_s = \sigma\varepsilon_{12}\frac{T_1^4 - T_2^4}{T_1 - T_2} \tag{4}$$

$$\alpha_{tot} = \alpha_{conv} + \alpha_{rad} \tag{5}$$

Table 1. Heat transfer coefficients for the hot side.

Heat transfer coefficient [W/m2/K]	
α_{conv}	440,00
$\alpha_{rad\_Hastelloy}$	232,00
α_{rad_TBC}	218,00
$\alpha_{tot\_Hastelloy}$	672,00
α_{tot_TBC}	658,00

Five Sections

In this calculation the transition duct have been divided in five sections to get a more detailed heat transfer coefficient in different parts of the duct, see Figure 2. This also means that each part will have a separate cross section area and thereby different gas velocity etcetera. One more thing that is added to these calculations is a constant from prior CFD calculations performed at Siemens. This constant is multiplied to the heat transfer coefficient created by the convection, α_{conv}. Otherwise it is the same calculations as above. The results with the total heat transfer coefficient for each section, with TBC used, are presented in Table 2.

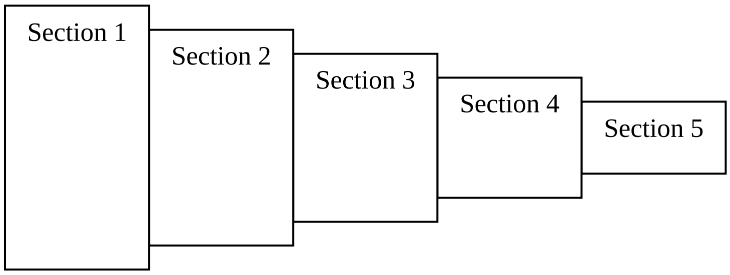

Figure 2. Transition duct divided in fine sections.

Table 2. Heat transfer coefficient from the hot side divided in five sections.

Heat transfer coefficient [W/m2/K]

Section:	1	2	3	4	5
α_{conv}	318	335	384	460	520
α_{rad_TBC}	218	218	218	218	218
α_{tot_TBC}	695	720,5	794	908	998

Calculation of impingement cooling

Nusselt number formula for an impingement plate, Figure 3 is presented in Equation 6. In Table 4 all the empirical constants can be founded both for in line and staggered impingement jet arrays. (Han, Dutta, Ekkad, 2000)

With greater number of hole-rows the cross flow between the jet plate and target plate will increase down stream. That cross flow will deflect the jet stream from the target plate. In order to get Nusselt number correct due to the deflection of the jet stream, the cross flow will be taken to consideration. The rate of the cross flow is determined with the impingement hole row number, n_r, the hole area A and the flow area between the both plates, showed in Equation 7. At no cross flow the Nusselt number is calculated from Equation 8 alone. (Han et. al. 2000)

The x_n, y_n and z are presenting the characteristic length of the surface in the impingement case, see Figure 3. (Han et. al. 2000)

The range in which this correlation gives reliable results in is presented in Table 3. This range is based on the data from which the correlation has been made from. It has also shown in practice that this correlation give good results on larger hole spacing than the x_n/d and y_n/d in the table. (Han et. al. 2000)

Table 3. Correlation range for impingement cooling.

Correlation range
$5 \leq x_n \leq 15$
$4 \leq y_n \leq 8$

$$Nu = 1 - C\left(\frac{x_n}{d}\right)^{n_x}\left(\frac{y_n}{d}\right)^{n_y}\left(\frac{z}{d}\right)^{n_z}\left(\frac{G_c}{G_j}\right)^{n} * Nu_1 \tag{6}$$

$$\frac{G_c}{G_j} = A(n_r - 0{,}5)/(z \cdot y_n) \tag{7}$$

Table 4. Constants for Nusselt number calculations for inline and staggered arrays of impingement rows.

Jet array	C	nx	ny	nz	n
Inline	0,596	-0,103	-0,38	0,803	0,561
Staggered	1,07	-0,198	-0,406	0,788	0,66

$$Nu_1 = 0.363\left(\frac{x_n}{d}\right)^{-0.554}\left(\frac{y_n}{d}\right)^{-0.422}\left(\frac{z}{d}\right)^{0.068}\mathrm{Re}^{0.727}\,\mathrm{Pr}^{1/3} \tag{8}$$

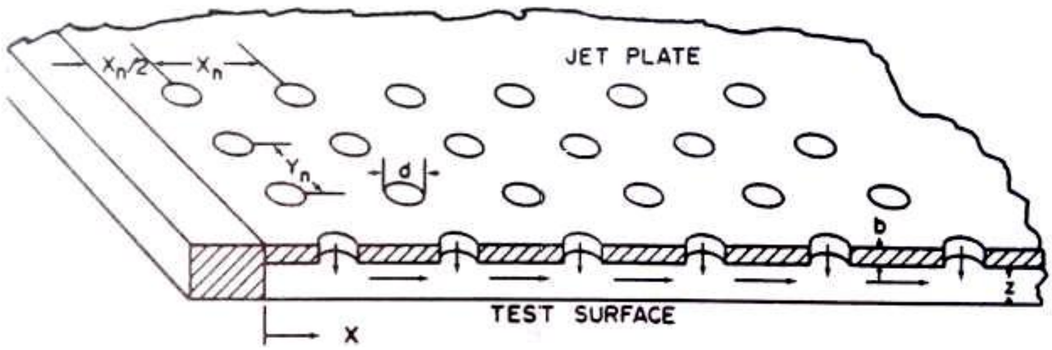

Figure 3. Schematic sketch of an impingement plate. (Han et. al. 2000)

Laminated sheets

The heat transfer in this concept is build upon theory of heat transfer in ducts. The Nusselt number can be calculated according to Equation 9. The Reynolds number is calculated with the hydraulic diameter as the characteristic length, see chapter 2.1. Because the cooling channels are rather long, the coolant will be significant warmer when traveling through the channel. Therefore the calculations will be made with the fluid properties at the mean temperature, see chapter 2.1.5. The mass flow is calculated as above, see chapter 2.2. In this channels there are typically five type of losses, inlet hole, 90º upstream elbow, friction, 90º downstream elbow and an exit. The loss factors are presented in Table 5, and the friction is calculated as chapter 2.2. (Bejan, 2004)

$$Nu = 0{,}0214\left(\mathrm{Re}_d^{\;0{,}8} - 100\right)\mathrm{Pr}^{0{,}4} \quad \left(0{,}5 \le \mathrm{Pr} \le 1{,}5 \quad 10^4 \le \mathrm{Re}_d \le 5 \times 10^6\right) \tag{9}$$

Table 5. Loss factors for a cooling channel.

Inlet hole	ζ=0,5
90º upstream elbow	ζ=1,15
90º downstream elbow	ζ=1,21
Outlet hole	ζ=0,8

The temperature of the channel walls will not be constant around the channel wall due to the fact that the plate where the channel is located has one hot and one cold side. The duct wall will therefore be calculated at the middle of the plate thickness. The middle of the plate is also where the cooling effect will work. The thermal resistance to the middle of the plate thickness can be divided in two parts. One part is between the channels, Equation 10 and one part is under a channel, Equation 11. These two resistances are considered to be in series and are combined according to Equation 12. The rest of the calculations are made according to the theory chapter.

$$R_1 = \frac{x}{kA} = \frac{b/2}{kA_1} \tag{10}$$

$$R_2 = \frac{x}{kA} = \frac{(b-h)/2}{kA_2} \tag{11}$$

$$\frac{1}{R_{cond}} = \frac{1}{R_1} + \frac{1}{R_2} \tag{12}$$

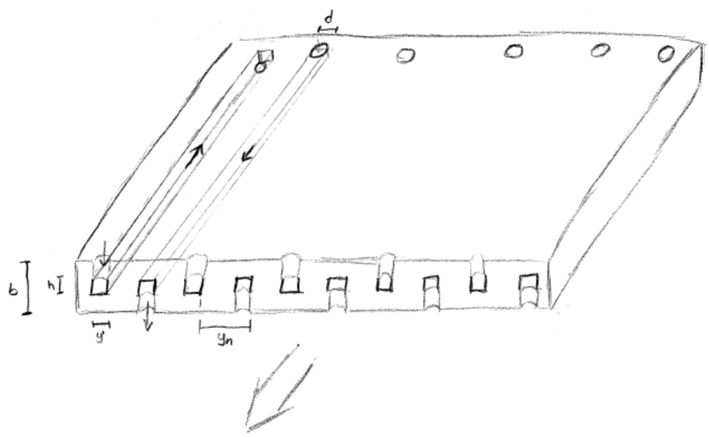

Figure 4. Schematic sketch of laminated sheets.

Calculation of Serial Cooling

This calculation is made by approximating the double shell transition duct as one channel were the Nusselt, Equation 13 can be used with the Reynolds number. To be able to calculating the pressure loss using the friction factor the Reynolds number needs to be calculated. Those equations can be found in the theory chapter in the report. At the same time as the Reynolds number is calculated from the velocity which is dependent on the friction factor for the channel. This needs to be performed with an iteration process. (Bejan, 2004)

$$Nu = 0{,}0214\left(\mathrm{Re}_d^{\,0,8} - 100\right)\mathrm{Pr}^{0,4} \quad \left(0{,}5 \le \mathrm{Pr} \le 1{,}5 \quad 10^4 \le \mathrm{Re}_d \le 5 \times 10^6\right) \tag{13}$$

Calculation of Serial Rib-Turbulated Cooling

In order to increase the heat transfer coefficient in a serial cooled transition duct, ribs can be fitted on the material surface adjacently to the hot side. With that configuration the het transfer coefficient are expected to increase by a factor 1,5 to 3,5 and the pressure drop increase, and cold go up to 3-15 times of a passage without ribs.

This calculation is preformed with the ribs applied transversely to the flow direction. To satisfy the used correlation, virtual broad aspect channels are assumed on the test surface. This had to be done because of the lack of walls in the annular shaped channel created between the transition ducts inner and outer skin. The virtual channels are ribbed on one side and that are taken in consideration in this calculations. The channel is showed in Figure 5 with the height *H*, width *W*, rib height *e*, and rib pitch *P*.

The channels friction factor with one ribbed wall, Equation 14 is determined from the friction factor for channels with four ribbed walls, Equation15, and the fanning friction factor, Equation 16. With this friction factor for channels with one single ribbed wall the roughness Reynolds number, Equation 17 is calculated.

For the transversely applied ribs in broad aspect channels the Stanton number *St*, Equation 18 are determined using the roughness friction factor *R*, Equation 19 and the roughness heat transfer coefficient *G*, Equation 20. With this Stanton number know the Nusselt number is calculated, Equation 21.

This correlation has the range that is presented in Table 6. In the calculations for typical combustion systems the Reynolds number, *Re* use to be larger then the Reynolds number range for the correlation. It has shown that the results have been satisfying anyway in prior calculations on SIT AB. (RT GRC 206/05, 2006)

Table 6. Correlation range for serial cooling.

Correlation range		
0,021≤	e/D_h	≤0,078
10≤	P/e	≤20
1≤	W/H	≤4
8000≤	Re	≤80000

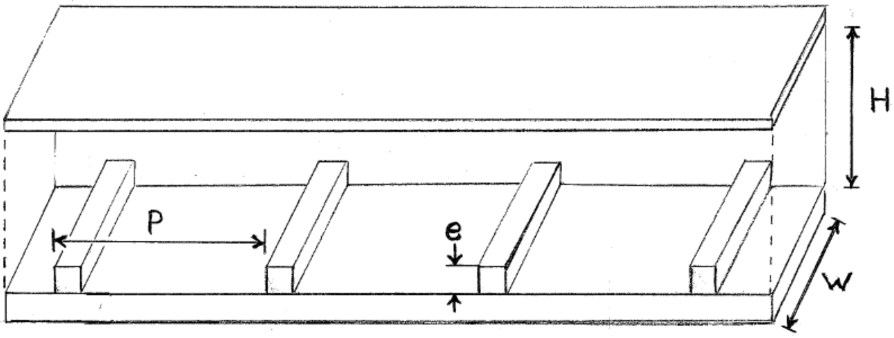

Figure 5. Schematic sketch of rib turbulated cooling.

$$f_{1r} = \frac{W \cdot f_{4r} + (2 \cdot H + W) \cdot f_s}{2(W + H)} \tag{14}$$

$$f_{4r} = \frac{2}{\left\{ R - 2{,}5 \ln\left[\dfrac{4 \cdot e \cdot W}{D_h (H + W)} \right] - 2{,}5 \right\}^2} \tag{15}$$

$$f_s = 0{,}046 \cdot \mathrm{Re}_{D_h}^{-0{,}2} \tag{16}$$

$$e^+ = \frac{e}{D_h} \mathrm{Re}_{D_h} \sqrt{\frac{f_{4r}}{2}} \tag{17}$$

$$St_r = \frac{f_r / 2}{(G - R) \cdot \left(f_r / 2 \right)^{1/2} + 1} \tag{18}$$

$$R = 3{,}1 \left(\frac{P}{10e} \right)^{0{,}35} \tag{19}$$

$$G = 2{,}24 \left(\frac{W}{H} \right)^{0{,}1} \left(e^+ \right)^{0{,}35} \tag{20}$$

$$Nu = St_r \cdot \mathrm{Pr} \cdot \mathrm{Re}_{D_h} \tag{21}$$

Calculation of Effusion Cooling

This is the concept that is hardest to predict the cooling effectiveness with calculations. There are two driving forces in this cooling principle. The first one is convection inside the cooling holes, the other one is an insulating cooling film on the hot side. The nusselt number inside the holes is calculated according to Equation 22. The first part of the equation considers the entrance effect in the cooling hole. The other part comes from usual duct flow. The other cooling force in this concept is film cooling. A thin film of cool air covers the hot wall and insulates it from the hot gas. This part is the hard one to calculate because the film behavior and mixing with the hot gas is hard to predict. Instead of the hot gas it is the film that heats the wall with temperature, T_f. In the literature film cooling is often connected to a performance index, efficiency, $\overline{\eta}_f$, see Equation 24 that is used to calculate the film temperature together with Equation 23. Equation 24 are described by Equation 25 to 50 and a sketch that shows variables that is used in the Equations.(Bradley, 2009)

$$\alpha = \left[1 + \left(\frac{d}{l}\right)^{0,7}\right] \cdot 0,023 (\mathrm{Re}_d)^{0,8} (\mathrm{Pr}_f)^{0,33} \tag{22}$$

$$\overline{\eta}_f = \frac{T_h - T_f}{T_h - T_c} \tag{23}$$

$$\overline{\eta}_f = \eta_c \frac{DR^{0,9/\frac{P}{D}}}{\sin\alpha^{0,006\frac{P}{D}}} \tag{24}$$

$$\eta_c = \frac{\eta_{c0}\eta^* \left(\frac{\mu}{\mu_0}\right)^a}{\left[1 + \left(\frac{\mu}{\mu_0}\right)^{(a+b)c}\right]^{1/c}} \tag{25}$$

$$a = 0,2 \tag{26}$$

$$b = \exp\left[1,92 - 7,5\left(\frac{P^{(-1,5)}}{D}\right)\right] \tag{27}$$

$$c = 0,7 + 336e^{\left(-1,85\frac{P}{D}\right)} \tag{28}$$

$$\mu = U \cdot DR^{0,8}\left(1-\left[0,03+0,11\left(5-\frac{P}{D}\right)\right]\cos\alpha\right) \tag{29}$$

$$\mu_0 = 0,125 + 0,063\left(\frac{P}{D}\right)^{1,8} \tag{30}$$

$$\eta_{c0} = \frac{0,465}{1+0,048\left(\frac{P}{D}\right)^2} \tag{31}$$

$$\eta^* = 0,1\left(\frac{\eta'^*}{0,1}\right)^{1/\eta_s}\left[1+\left(\frac{\xi'}{\xi_1}\right)^{b_1 c_1}\right]^{1/c_1} \tag{32}$$

$$\xi_1 = \frac{65}{\left(\frac{M}{2,5}\right)^{a_1}} \tag{33}$$

$$a_1 = 0,04 + 0,23\left(\frac{P}{D}\right)^2 + \left(1,5-\frac{2}{\sqrt{\frac{P}{D}}}\right)\sin\left(0,86\alpha\left[1+\frac{0,754}{1+0,87\left(\frac{P}{D}\right)^2}\right]\right) \tag{34}$$

$$b_0 = 0,8 + 0,014\left(\frac{P}{D}\right)^2 + \left(1,5-\frac{2}{\sqrt{\frac{P}{D}}}\right)\sin\left(0,86\alpha\left[1+\frac{0,754}{1+0,87\left(\frac{P}{D}\right)^2}\right]\right) \tag{35}$$

$$b_1 = \frac{b_0}{1+M^{-3}} \tag{36}$$

$$c_1 = 7,5 + \frac{P}{D} \tag{37}$$

$$\eta'^* = \frac{\eta_{0T}\left(\frac{\xi'}{\xi_0}\right)^{a^*}}{\left[1+\left(\frac{\xi'}{\xi_0}\right)^{\left(a^*+b_T^*\right)c^*}\right]^{1/c^*}} \tag{38}$$

$$\xi' = \xi^{\xi_s} \tag{39}$$

$$\xi = \frac{\frac{x}{D}\frac{P}{D}\xi_c}{\frac{\pi}{4}U^{\left(\frac{P}{D}/3\right)^{-0,75}}} \tag{40}$$

$$\xi_c = 0,6 + \frac{0,4(2-\cos\alpha)}{1+\left(\frac{P/D-1}{3,3}\right)^6} \tag{41}$$

$$\eta_s = 1 + \frac{\hat{\eta}}{1+\left(\frac{U \cdot DR^g}{k}\right)^{-5}} \tag{42}$$

$$\xi_s = 1 + \frac{\hat{\xi}}{1+\left(\frac{U \cdot DR^g}{k}\right)^{-5}} \tag{43}$$

$$g = 0,75\left[1-e^{-0,8\left(\frac{P}{D}-1\right)}\right] \tag{44}$$

$$k = 2\left[1-e^{0,57\left(1-\frac{P}{D}\right)}\right] + 0,91\cos^{0,65}\alpha \tag{45}$$

$$\hat{\xi} = 1,17\left[1-\frac{\left(\frac{P}{D}-1\right)}{1+0,2\left(\frac{P}{D}-1\right)^2}\right](\cos 2,3\alpha + 2,45) \tag{46}$$

$$\hat{\eta} = 0,022\left(\frac{P}{D}+1\right)(0,9-\sin 2\alpha) - \left[0,08+\frac{0,46}{1+\left(\frac{P}{D}-3,2\right)^2}\right] \tag{47}$$

$$\eta_{0T} = 2,5\left(\frac{5,8}{2,5}\right)^{\frac{b_T^*}{0,7}} \tag{48}$$

$$b_T^* = 0,7\left(1+\left[\frac{1,22}{1+7\left(\frac{P}{D}-1\right)^{-7}} + 0,87 + \cos 2,5\alpha\right]e^{\left[2,6Tu-\frac{0,0012}{Tu^2}-1,76\right]}\right) \tag{49}$$

$$\begin{aligned} \xi_0 &= 9 \\ \eta_0 &= 5{,}8 \\ \alpha^* &= 4 \\ c^* &= 0{,}24 \end{aligned} \tag{50}$$

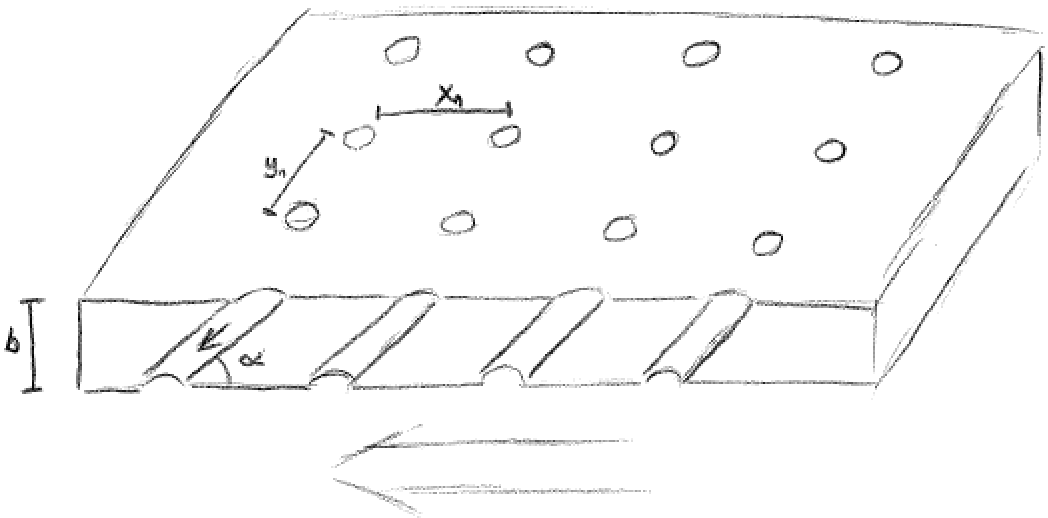

Figure 6. Schematic sketch of an effusion cooled plate.

Calculation results

Here the optimized results for the cooling calculations are showed. The first table, Table 7 shows the current transition ducts result with the impingement calculation method. This specific calculation is not optimized because of the known data from the current duct. The temperature and air consumption result from this calculation is similar to the real temperature and air consumption on the current transition duct which is around 1030K and 14% air on the impingement.

The result from the other calculations which is optimized is used in the evaluation process for the cooling methods. One thing to notice is that all of the optimization is made with the goal temperature of 1100K.

Impingement

Table 7. Impingement calculation result for the current transition duct with. Note the temperature of 1038K

Impingement with current design (1038K)	
Hole diameter, d [mm]	1,5
Hole spacing, Xn [mm]	15
Hole spacing, Yn [mm]	13
Jet to target, z [mm]	7
Number of holes	1102
Massflow [Kg/s]	**1,42**
Percent of Total Mass flow [%]	**13,5**

Impingement without TBC	
Hole diameter, d [mm]	1
Hole spacing, Xn [mm]	14,5
Hole spacing, Yn [mm]	8,8
Jet to target, z [mm]	8
Number of holes	1501
Massflow [Kg/s]	**0,645**
Percent of Total Mass flow [%]	**6,1**

Impingement with TBC	
Hole diameter, d [mm]	1
Hole spacing, Xn [mm]	15
Hole spacing, Yn [mm]	9
Jet to target, z [mm]	7
Number of holes	1482
Massflow [Kg/s]	**0,462**
Percent of Total Mass flow [%]	**4,4**

Laminated Sheets

Laminated Sheets without TBC

Channel height, h [mm]	1,5
Channel width, y [mm]	2
Channel spacing, Yn [mm]	5
Plate thickness, b [mm]	3
Number of rows	2
Number of channels	250
Massflow [Kg/s]	**0,34**
Percent of Total Mass flow [%]	**3,2**

Laminated Sheets with TBC

Channel height, h [mm]	1,5
Channel width, y [mm]	3
Channel spacing, Yn [mm]	5,8
Plate thickness, b [mm]	3
Number of rows	1
Number of channels	120
Massflow [Kg/s]	**0,19**
Percent of Total Mass flow [%]	**1,8**

Serial Cooling without Ribs

Serial cooling without TBC

Pressure loss [%]	**0,5**
Channel height, h [mm]	6,9
Mass flow [Kg/s]	**3,45**
Percent of Total Mass flow [%]	**32,7**

Serial cooling with TBC

Pressure loss [%]	**0,5**
Channel height, h [mm]	3,7
Mass flow [Kg/s]	**1,18**
Percent of Total Mass flow [%]	**11,2**

Serial cooling without TBC

Pressure loss [%]	**0,25**
Channel height, h [mm]	15,8
Mass flow [Kg/s]	**9,35**
Percent of Total Mass flow [%]	**88,7**

Serial cooling with TBC

Pressure loss [%]	**0,25**
Channel height, h [mm]	7,1
Mass flow [Kg/s]	**2,58**
Percent of Total Mass flow [%]	**24,5**

Serial Cooling with Ribs

Serial cooling with ribs, without TBC

Pressure loss [%]	**0,5**
Channel height, h [mm]	5
Rib height, e [mm]	0,5
Rib spacing, P [mm]	5,8
Mass flow [Kg/s]	**0,78**
Percent of Total Mass flow [%]	**7,4**

Serial cooling with ribs, with TBC

Pressure loss [%]	**0,5**
Channel height, h [mm]	4
Rib height, e [mm]	0,5
Rib spacing, P [mm]	5
Mass flow [Kg/s]	**0,48**
Percent of Total Mass flow [%]	**4,5**

Serial cooling with ribs, without TBC

Pressure loss [%]	**0,25**
Channel height, h [mm]	9,3
Rib height, e [mm]	0,6
Rib spacing, P [mm]	6
Mass flow [Kg/s]	**1,68**
Percent of Total Mass flow [%]	**15,9**

Serial cooling with ribs, with TBC

Pressure loss [%]	**0,25**
Channel height, h [mm]	5,9
Rib height, e [mm]	0,73
Rib spacing, P [mm]	7,3
Mass flow [Kg/s]	**0,6**
Percent of Total Mass flow [%]	**5,6**

Effusion

Effusion with TBC

Hole diameter, d [mm]	0,7
Hole spacing, Xn [mm]	3,5
Hole spacing, Yn [mm]	1,75
Row spacing [mm]	54,5
Number of rows	5
Number of holes in Y per row	2
Number of holes in X per row	402
Total number of holes	4020
Massflow [Kg/s]	**0,49**
Percent of Total Mass flow [%]	**4,6**

Bibliography

Bejan, Adrian (2004). *Convection heat transfer*. 3. ed. Hoboken, N.J.: Wiley

Bradley, Andreas (2009), *Prediction of vane film cooling in gas turbines* Linköping University, Sweden

Han, Je-Chin, Dutta, Sandip & Ekkad, Srinath (2000). *Gas turbine heat transfer and cooling technology*. New York: Taylor & Francis

RT GRC 206/05 (2006) *Empirical correlations for the cold side of combustor cooling*
SIT AB internal report

Appendix 6 – Cost Calculations

Costs for Cooling Concepts

The costs for cooling concepts are evaluated against the total cost for current design. The mounting part, suspension cone are not included in the total cost and the costs can bee seen in Table 1, where all numbers are related to the total cost. All costs presented here are referring to the total cost of current design.

Table 1. The costs for current design which of the other cooling concepts costs calculation are based on.

		Current Design			
Detail	Quantity	Current In house	Current Hired	Mtrl / Purchase	**Total /SET**
T-duct	1	15,6%	0,0%	0,0%	**15,6%**
Flange inlet	1	0,2%	23,7%	0,0%	**23,9%**
Ring	1	11,7%	1,2%	2,9%	**15,8%**
Outer skin, outboard	1	4,0%	7,7%	0,3%	**12,0%**
Outer skin, inboard	1	4,0%	7,7%	0,3%	**12,0%**
Innerskin, 3D laser	1	5,2%	2,3%	0,0%	**7,5%**
Innerskin, pressing	1	3,3%	1,2%	2,1%	**6,7%**
Innerskin, pressing	1	3,3%	1,2%	2,1%	**6,7%**
				Total:	**100,0%**

Effusion Cooling

The design of the transition duct will almost be the same as current design. As the outer shell will be removed all that's costs is eliminated. The assembly work will also be reduced, this cost by 40%. More, smaller and angled holes takes longer time to drill, the cost will therefore increase with the current cost per hole times the amount of holes. As the large damping holes are eliminated the 3D laser cost is reduced by 5%. The inlet ring can be simpler as the outer shell is removed. A cost reduction of 30% is estimated for the material and about 55% of the work. Costs for applying TBC are 29% of the total cost of current design. The holes in the shell that needs to be masked during TBC apply makes that cost higher than for other concepts. The costs can bee seen in Table 2.

Table 2. Costs for an effusion cooled transition duct with TBC. A green cell stands for a lower cost, a red for a higher and an orange for a new cost.

		Effusion + TBC						
Detail	Quantity	Current In house		Current Hired		Mtrl / Purchase		**Total /SET**
T-duct	1	-40,0%	9,3%		0,0%		0,0%	**9,3%**
Flange inlet	1		0,2%	-55,0%	10,7%		0,0%	**10,9%**
Ring	1		11,7%		1,2%	-30,0%	2,0%	**14,9%**
Outer skin, outboard	0		4,0%		7,7%		0,3%	**0,0%**
Outer skin, inboard	0		4,0%		7,7%		0,3%	**0,0%**
Innerskin, 3D laser	1	-5,0%	5,0%	768,7%	19,7%		0,0%	**24,7%**
Innerskin, pressing	1		3,3%		1,2%		2,1%	**6,7%**
Innerskin, pressing	1		3,3%		1,2%		2,1%	**6,7%**
TBC	1		0,0%		29,0%		0,0%	**29,0%**
							Total:	**102,1%**

Serial Cooling

These concepts are made of two shells as in current design. Booth the outer shell and inner shell have holes in current design which will be removed in this concept. For the outer skin the cost for the 3D laser will be completely removed, this means a reduction of 43,4% of the posts named “Outer skin”. The inner skin 3D laser are reduced by 5% because that procedure contains some end cuttings as well. The inlet flange will have a simpler geometry and a cost reduction of 30% is estimated for the material and about 55% of the work. Both the inner and outer skins need to be sealed against the combustion can and two inlet flanges is therefore needed instead of one. Costs for applying TBC is 17,5% of the total cost of current design. The costs can bee seen in Table 3, Table 4, Table 5 and Table 6 for concept C5, C6 ,C9 and C10.

Table 3. Costs for a serial cooled transition duct with ribs. A green cell stands for a lower cost, a red for a higher and an orange for a new cost.

		Serial + Ribs						
Detail	Quantity	Current In house		Current Hired		Mtrl / Purchase		**Total /SET**
T-duct	1		15,6%		0,0%		0,0%	**15,6%**
Flange inlet	2		0,2%	-55,0%	10,7%		0,0%	**21,8%**
Ring	2		11,7%		1,2%	-30,0%	2,0%	**29,8%**
Outer skin, outboard	1		4,0%	-43,4%	4,3%		0,3%	**8,6%**
Outer skin, inboard	1		4,0%	-43,4%	4,3%		0,3%	**8,6%**
Innerskin, 3D laser	1	-5,0%	5,0%		2,3%		0,0%	**7,2%**
Innerskin, pressing	1		3,3%		1,2%		2,1%	**6,7%**
Innerskin, pressing	1		3,3%		1,2%		2,1%	**6,7%**
Ribs	0		0,0%		4,5%		0,0%	**4,5%**
TBC	1							
							Total:	**109,5%**

Table 4. Costs for a serial cooled transition duct with ribs and TBC. A green cell stands for a lower cost, a red for a higher and an orange for a new cost.

		Serial + Ribs + TBC						
Detail	Quantity	Current In house		Current Hired		Mtrl / Purchase		**Total /SET**
T-duct	1		15,6%					**15,6%**
Flange inlet	2		0,2%	-55,0%	10,7%			**21,8%**
Ring	2		11,7%		1,2%	-30,0%	2,0%	**29,8%**
Outer skin, outboard	1		4,0%	-43,4%	4,3%		0,3%	**8,6%**
Outer skin, inboard	1		4,0%	-43,4%	4,3%		0,3%	**8,6%**
Innerskin, 3D laser	1	-5,0%	5,0%		2,3%			**7,2%**
Innerskin, pressing	1		3,3%		1,2%		2,1%	**6,7%**
Innerskin, pressing	1		3,3%		1,2%		2,1%	**6,7%**
Ribs	1				4,5%			**4,5%**
TBC	1				17,5%			**17,5%**
							Total:	**127,0%**

Table 5. Costs for a serial cooled transition duct. A green cell stands for a lower cost, a red for a higher and an orange for a new cost.

		Serial						
Detail	Quantity	Current In house		Current Hired		Mtrl / Purchase		**Total /SET**
T-duct	1		15,6%					**15,6%**
Flange inlet	2		0,2%	-55,0%	10,7%			**21,8%**
Ring	2		11,7%		1,2%	-30,0%	2,0%	**29,8%**
Outer skin, outboard	1		4,0%	-43,4%	4,3%		0,3%	**8,6%**
Outer skin, inboard	1		4,0%	-43,4%	4,3%		0,3%	**8,6%**
Innerskin, 3D laser	1	-5,0%	5,0%		2,3%			**7,2%**
Innerskin, pressing	1		3,3%		1,2%		2,1%	**6,7%**
Innerskin, pressing	1		3,3%		1,2%		2,1%	**6,7%**
TBC	0							
Ribs	0							
							Total:	**105,0%**

Table 6. Serial cooled transition duct without ribs and with TBC. A green cell stands for a lower cost, a red for a higher and an orange for a new cost.

		Serial + TBC						
Detail	Quantity	Current In house		Current Hired		Mtrl / Purchase		**Total /SET**
T-duct	1		15,6%		0,0%		0,0%	**15,6%**
Flange inlet	2		0,2%	-55,0%	10,7%		0,0%	**21,8%**
Ring	2		11,7%	0,0%	1,2%	-30,0%	2,0%	**29,8%**
Outer skin, outboard	1		4,0%	-43,4%	4,3%		0,3%	**8,6%**
Outer skin, inboard	1		4,0%	-43,4%	4,3%		0,3%	**8,6%**
Innerskin, 3D laser	1	-5,0%	5,0%		2,3%		0,0%	**7,2%**
Innerskin, pressing	1		3,3%		1,2%		2,1%	**6,7%**
Innerskin, pressing	1		3,3%		1,2%		2,1%	**6,7%**
Ribs	0		0,0%		0,0%		0,0%	**0,0%**
TBC	1				17,6%			**17,6%**
							Total:	**122,6%**

Impingement Cooling

These concepts are a copy of current design except some more holes in the outer shell and a few less in the inner shell. The cost for the holes in the outer shell is calculated with the current cost divided by number of holes and multiplies with the new number of holes. TBC cost is 17,5% of the total cost of current design. The costs can bee seen in Table 7 and Table 8.

Table 7. Costs for an impingement cooled transition duct. A green cell stands for a lower cost, a red for a higher and an orange for a new cost

		Impingement						
Detail	Quantity	Current In house		Current Hired		Mtrl / Purchase		**Total /SET**
T-duct	1		15,6%		0,0%		0,0%	**15,6%**
Flange inlet	1		0,2%		23,7%		0,0%	**23,9%**
Ring	1		11,7%		1,2%		2,9%	**15,8%**
Outer skin, outboard	1		4,0%	5,3%	8,1%		0,3%	**12,4%**
Outer skin, inboard	1		4,0%	5,3%	8,1%		0,3%	**12,4%**
Innerskin, 3D laser	1		5,2%		2,3%		0,0%	**7,5%**
Innerskin, pressing	1		3,3%		1,2%		2,1%	**6,7%**
Innerskin, pressing	1		3,3%		1,2%		2,1%	**6,7%**
TBC	0		0,0%		0,0%		0,0%	**0,0%**
							Total:	**100,8%**

Table 8. Costs for an impingement cooled transition duct with TBC. A green cell stands for a lower cost, a red for a higher and an orange for a new cost

		Impingement + TBC						
Detail	Quantity	Current In house		Current Hired		Mtrl / Purchase		**Total /SET**
T-duct	1		15,6%		0,0%		0,0%	**15,6%**
Flange inlet	1		0,2%		23,7%		0,0%	**23,9%**
Ring	1		11,7%		1,2%		2,9%	**15,8%**
Outer skin, outboard	1		4,0%	5,3%	8,1%		0,3%	**12,4%**
Outer skin, inboard	1		4,0%	5,2%	8,1%		0,3%	**12,4%**
Innerskin, 3D laser	1		5,2%		2,3%		0,0%	**7,5%**
Innerskin, pressing	1		3,3%		1,2%		2,1%	**6,7%**
Innerskin, pressing	1		3,3%		1,2%		2,1%	**6,7%**
TBC	1		0,0%		17,6%		0,0%	**17,6%**
							Total:	**118,4%**

Laminated Sheets

This cost estimate is the most insecure because the shape of the transition duct will be different in these concepts. The inlet flange will have a more simple design when the outer skin is removed as described above. The assembly will be 40% less expensive, the ring material will be 30% cheaper and the inlet flange work cost will be reduced by 55%. Discussions with a laminated sheets manufacturer have resulted in a cost estimation of the laminated sheets. They claim that the inner skin costs will be twice as expensive as current design. The cost be seen in Table 9 and Table 10.

Table 9. Cost for laminated sheets. A green cell stands for a lower cost, a red for a higher and an orange for a new cost.

		Laminated Sheets						
Detail	Quantity	Current In house		Current Hired		Mtrl / Purchase		**Total /SET**
T-duct	1	-40,0%	9,3%		0,0%		0,0%	**9,3%**
Flange inlet	1		0,2%	-55,0%	10,7%		0,0%	**10,9%**
Ring	1		11,7%		1,2%	-30,0%	2,0%	**14,9%**
Outer skin, outboard	0		4,0%		7,7%		0,3%	**0,0%**
Outer skin, inboard	0		4,0%		7,7%		0,3%	**0,0%**
Innerskin, 3D laser	1	100,0%	10,4%	100,0%	4,5%		0,0%	**15,0%**
Innerskin, pressing	1	100,0%	6,6%	100,0%	2,4%	100,0%	4,3%	**13,3%**
Innerskin, pressing	1	100,0%	6,6%	100,0%	2,4%	100,0%	4,3%	**13,3%**
TBC	1				0,0%			**0,0%**
							Total:	**76,7%**

Table 10. Cost for laminated sheets with TBC. A green cell stands for a lower cost, a red for a higher and an orange for a new cost.

		Laminated Sheets + TBC						
Detail	Quantity	Current In house		Current Hired		Mtrl / Purchase		**Total /SET**
T-duct	1	-40,0%	9,3%		0,0%		0,0%	**9,3%**
Flange inlet	1		0,2%	-55,0%	10,7%		0,0%	**10,9%**
Ring	1		11,7%		1,2%	-30,0%	2,0%	**14,9%**
Outer skin, outboard	0		4,0%		7,7%		0,3%	**0,0%**
Outer skin, inboard	0		4,0%		7,7%		0,3%	**0,0%**
Innerskin, 3D laser	1	100,0%	10,4%	100,0%	4,5%		0,0%	**15,0%**
Innerskin, pressing	1	100,0%	6,6%	100,0%	2,4%	100,0%	4,3%	**13,3%**
Innerskin, pressing	1	100,0%	6,6%	100,0%	2,4%	100,0%	4,3%	**13,3%**
TBC	1				17,5%			**17,5%**
							Total:	**94,2%**

Costs for the Strongest Combination

The costs for the strongest combination are presented here. They are divided in two parts. The first one regards the cooling solution and the other one regards the mounting solution.

Cooling Solution

The costs for the cooling solution are compared to the total cost for the cooling solution used in current design. These costs are the same as for serial cooling with ribs and TBC except the effusion holes cost and the sealing flange which is added. The effusion holes cost is located in the hired cost of the inner skin 3D laser, it is calculated in the same way as in the effusion example. The sealing flange is added to the cooling cost as it also has the task to cool the aft end of the transition duct. It is estimated to have the same cost as the sealing flange used in current design.

Table 7. The costs for the cooling solution in the strongest combination. A green cell stands for a lower cost, a red for a higher and an orange for a new cost.

		Strongest Combination						
Detail	Quantity	Current In house		Current Hired		Mtrl / Purchase		**Total /SET**
T-duct	1		15,6%		0,0%		0,0%	**15,6%**
Flange inlet	2		0,2%	-55,0%	10,7%		0,0%	**21,8%**
Ring	2		11,7%		1,2%	-30,0%	2,0%	**29,8%**
Outer skin, outboard	1		4,0%	-43,4%	4,3%		0,3%	**8,6%**
Outer skin, inboard	1		4,0%	-43,4%	4,3%		0,3%	**8,6%**
Innerskin, 3D laser	1	-5,0%	5,0%	71,7%	3,9%		0,0%	**8,9%**
Innerskin, pressing	1		3,3%		1,2%		2,1%	**6,7%**
Innerskin, pressing	1		3,3%		1,2%		2,1%	**6,7%**
TBC	1		0,0%		4,5%		0,0%	**4,5%**
Ribs	1				17,5%			**17,5%**
Sealing flange	1		11,6%					**11,6%**
							Total:	**140,2%**

Mounting Solution

Theses costs are compared to the cost of the mounting parts in current design, see Table 8. The stator rings costs are reduced by removing the cost for wear coating. The material is increased with 0,3 times the current material cost for the two stator rings used in current design. This because of the extra material were the sockets are located. The stator rings need more machining and the cost estimate is given from the workshop of 10,2% of the total cost of current design. The cost for the lock pin and the D-bar are also estimated by the workshop as 2,5% respective 6,5% of the total cost and this is for a set of details, one gas turbine. See Table 8 for the detailed costs.

Table 8. Cots for the mounting solution in the strongest combination. A green cell stands for a lower cost, a red for a higher and an orange for a new cost.

Detail	Quantity	**Current Design**	**Strongest Combination**	
Suspensioncone, outbord	8	**6,4%**		**0,0%**
Suspensioncone, inboard	8	**6,4%**		**0,0%**
T-bone	8	**3,3%**		**0,0%**
Inner clamping bar	8	**2,9%**		**0,0%**
Outer clamping bar	8	**3,9%**		**0,0%**
Stator ring outer	1	**40,4%**	-8,3%	**37,1%**
Stator ring inner	1	**36,5%**	-9,2%	**33,2%**
D-bar	16		6,5%	**6,5%**
Lock pin	8		2,5%	**2,5%**
Stator ring, extra machining	1		10,2%	**10,2%**
Stator ring extra material	1		2,0%	**2,0%**
Sealing	8		10,9%	**10,9%**
	Total:	**100,0%**		**102,4%**

Appendix 7 – Weighted Objectives Method, Cooling

				Ideal solution			Current design			C2		
Criteria	W	Parameters	Unit	Magnitude m_{i1}	Score V_{i1}	Weighted score WV_{i1}	Magnitude m_{i2}	Score V_{i2}	Weighted score WV_{i2}	Magnitude m_{i3}	Score V_{i3}	Weighted score WV_{i3}
Low air consumption	10	Air consumption	[kg/s]	0	5	50	1,42	1	10	0,49	3	30
Low temperature gradient	5	HTC peaks	[-]	Perfect	5	25	Adequate	2	10	Weak	1	5
Slim design	2	Shell thickness	[mm]	3	5	10	11,7	3	6	3	5	10
Performance	6	Potential	[%]	100	5	30			0	---	0	0
Cost	1	Of current	[%]	90	5	5	100	4	4	102	4	4
Sum W_i	23				OWV_1	120		OWV_2	30		OWV_3	49
				OWV_{1norm}		1	OWV_{2norm}		0,25	OWV_{3norm}		0,408333

				C5			C6			C5*			C6*		
Criteria	W	Parameters	Unit	Magnitude m_{i4}	Score V_{i4}	Weighted score WV_{i4}	Magnitude m_{i5}	Score V_{i5}	Weighted score WV_{i5}	Magnitude m_{i10}	Score V_{i10}	Weighted score WV_{i10}	Magnitude m_{i11}	Score V_{i11}	Weighted score WV_{i11}
Low air consumption	10	Air consumption	[kg/s]	0	5	50	0	5	50	0	5	50	0	5	50
Low temperature gradient	5	HTC peaks	[-]	Good	4	20	Exellent	5	25	Good	4	20	Exellent	5	25
Slim design	2	Shell thickness	[mm]	13,5	2	4	10,5	3	6	10,2	3	6	8,3	3	6
Performance	6	Potential	[%]	264	5	30	366	5	30	279	5	30	231	5	30
Cost	1	money	[kkr]	110	4	4	127	2	2	110	4	4	127	2	2
Sum W_i	23				OWV_4	108		OWV_5	113		OWV_{10}	110		OWV_{11}	113
				OWV_{4norm}		0,9	OWV_{4norm}		0,941667	OWV_{4norm}		0,916667	OWV_{4norm}		0,941667

				C9			C10			C9*			C10*		
Criteria	W	Parameters	Unit	Magnitude m_{i6}	Score V_{i6}	Weighted score WV_{i6}	Magnitude m_{i7}	Score V_{i7}	Weighted score WV_{i7}	Magnitude m_{i7}	Score V_{i7}	Weighted score WV_{i7}	Magnitude m_{i8}	Score V_{i8}	Weighted score WV_{i8}
Low air consumption	10	Air consumption	[kg/s]	0	5	50	0	5	50	0,645	5	50	0,462	5	50
Low temperature gradient	5	HTC peaks	[-]	Good	4	20	Exellent	5	25	Good	4	20	Exelent	5	25
Slim design	2	Shell thickness	[mm]	20,9	0	0	11,9	3	6	11,7	3	6	8,3	3	6
Performance	6	Potential	[%]	---	0	0	340	5	30	---	0	0	273	5	30
Cost	1	money	[kkr]	105	4	4	123	2	2	105	4	4	123	2	2
Sum W_i	23				OWV_6	74		OWV_7	113		OWV_7	80		OWV_8	113
					OWV_{4norm}	0,616667		OWV_{4norm}	0,941667		OWV_{4norm}	0,666667		OWV_{4norm}	0,941667

				C11			C12			C19			C20		
Criteria	W	Parameters	Unit	Magnitude m_{i7}	Score V_{i7}	Weighted score WV_{i7}	Magnitude m_{i8}	Score V_{i8}	Weighted score WV_{i8}	Magnitude m_{i9}	Score V_{i9}	Weighted score WV_{i9}	Magnitude m_{i10}	Score V_{i10}	Weighted score WV_{i10}
Low air consumption	10	Air consumption	[kg/s]	0,645	3	30	0,462	3	30	0,34	4	40	0,19	4	40
Low temperature gradient	5	HTC peaks	[-]	Adequate	2	10	Satisfactory	3	15	Adequate	2	10	Satisfactory	3	15
Slim design	2	Shell thickness	[mm]	12,7	2	4	11,7	3	6	3	5	10	3	5	10
Performance	6	Potential	[%]	146	4	24	138	5	30	174	2	12	169	3	18
Cost	1	money	[kkr]	101	4	4	118	3	3	101	4	4	118	3	3
Sum W_i	23				OWV_7	72		OWV_8	84		OWV_9	76		OWV_{10}	86
					OWV_{4norm}	0,6		OWV_{4norm}	0,7		OWV_{4norm}	0,633333		OWV_{4norm}	0,716667

Appendix 8 – Force Calculations

There are two types of forces acting on the transition duct that has to be handled by the mounting. The pressure difference between the inside and outside of the transition duct causes the large force. The other force arises from the impulse of the flowing gas inside the transition duct. Because the transition duct is symmetric, only two dimensions have to be investigated, radial and axial dimensions relative the gas turbine axle. Figure 1 shows the factor that affects the static forces.

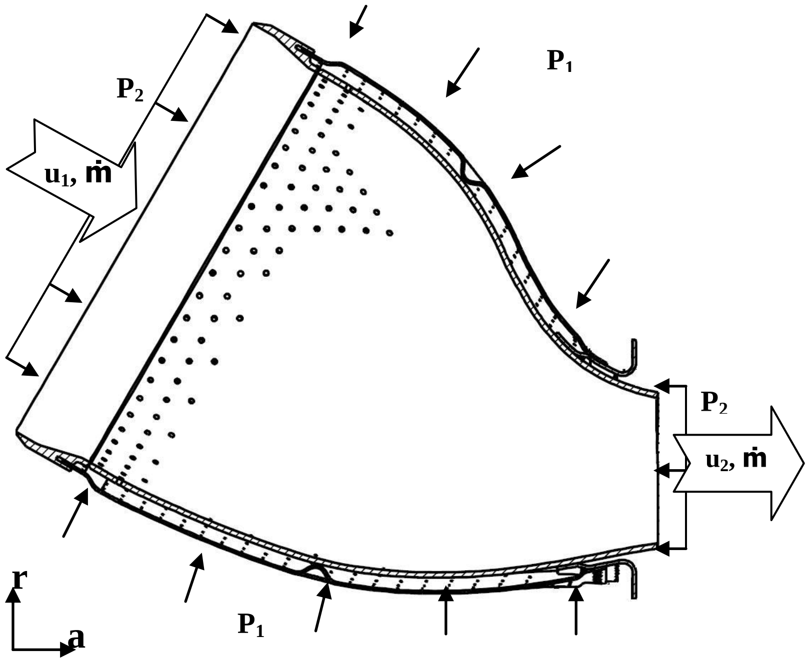

Figure 1. Factor that affect the forces.

Impulse forces

The impulse force is caused by velocity changes in the hot gas stream and is calculated according to Equation 32 in chapter 2.2.3. The forces are calculated in each direction therefore are the inlet and outlet velocities in each direction necessary. The velocities are calculated according to Equation 1, 2, 3 and 4, where index 1 refers to inlet, 2 to outlet, a for axial and r for radial. The force acts in the middle of the transition duct and is calculated in Equation 5 and 6.

$$u_{1a} = u_1 \cos(30^\circ) = \frac{\dot{m}RT}{A_{inlet}\, p_2} \cos(30^\circ) \tag{1}$$

$$u_{1r} = u_1 \sin(30^{\circ}) = \frac{\dot{m}RT}{A_{inlet}\, p_2} \sin(30^{\circ}) \tag{2}$$

$$u_{2a} = u_2 = \frac{\dot{m}RT}{A_{outlet}\, p_2} \tag{3}$$

$$u_{2r} = 0 \tag{4}$$

$$F_{fa} = \dot{m}(u_{2a} - u_{1a}) = \dot{m}^2 \frac{RT}{p_2}\left(\frac{1}{A_{outlet}} - \frac{\cos(30^{\circ})}{A_{inlet}}\right) = 175N \tag{5}$$

$$F_{fr} = \dot{m}(u_{2r} - u_{1r}) = \dot{m}^2 \frac{RT}{p_2}\left(0 - \frac{\sin(30^{\circ})}{A_{inlet}}\right) = \dot{m}^2 \frac{RT \sin(30^{\circ})}{p_2 A_{inlet}} = -178N \tag{6}$$

Pressure forces

The transition duct is exposed for large pressures therefore will the relative small pressure drop of 4,5 % make a large impact. As the transition duct is shaped as a potbelly the pressure will act at different large areas which will cause reaction forces. The forces are calculated at current design in radial and axial direction. The line A-A in Figure 2 crosses the inner shell two times, at the upper point the pressure difference will cause a force, same thing at the lower point. These two forces in radial direction will have the same magnitude, due to same area and pressure difference but they will be opposite directed. The forces will eliminate each other according to Equation 7. The other line, B-B will only cross the inner shell one time. At that point the pressure difference will cause a force in radial direction and no other force will eliminate that one, see Equation 8. That why the total radial force due to the pressure only depends on the projected inlet and outlet areas, according to Equation 9. Same thing about the forces in axial direction according Equation 10.

$$F_{r\,A-A} = \Delta A \cdot (p_1 - p_2) + \Delta A \cdot (p_2 - p_1) = 0 \tag{7}$$

$$F_{r\_B-B} = \Delta A \cdot (p_2 - p_1) \neq 0 \tag{8}$$

$$F_{pr} = \sum F_{r\,j-j} = A_{inlet} \sin(30^{\circ})(p_1 - p_2) = 3493N \tag{9}$$

$$F_{pa} = \sum F_{a\,i-i} = A_{inlet} \cos(30^{\circ})(p_2 - p_1) + A_{outlet}(P_1 - P_2) = -895N \tag{10}$$

Total forces and torque equilibrium

The sum of the impulse and pressure force will be the total reaction forces that will act on the mounting parts. They are calculated with Equation 11 and 12.

To be able to determine where no torque acts on a considered mounting point the transition duct, it is important to know where the forces act. The impulse forces will act in the middle of the transition duct and the pressure forces will act in the middle of the inlet and outlet areas see Figure 2. The torque are calculated with Equation 13, where Δa is the axial distance between the force and mounting point and Δr the radial distance. If you set the torque in Equation 13 to zero and solve the equation system you will get a line where no torque acts on the mounting, line C-C in Figure 2.

$$F_r = F_{pr} + F_{fr} = 3494 - 178 = 3316N \tag{11}$$

$$F_a = F_{pa} + F_{fa} = -895 + 175 = -720N \tag{12}$$

$$T = F_{pr\,inlett}\Delta a_{inlet} + F_{a\,poutlet}\Delta r_{outlet} - F_{pa\,inlett}\Delta r_{inlet} - F_{fr}\Delta a_{middle} + F_{fa}\Delta r_{middle} \tag{13}$$

$$T = F_{pr\,inlett}\Delta a_{inlet} + F_{a\,poutlet}\Delta r_{outlet} - F_{pa\,inlett}\Delta r_{inlet} - F_{fr}\Delta a_{middle} + F_{fa}\Delta r_{middle} = 0 \tag{14}$$

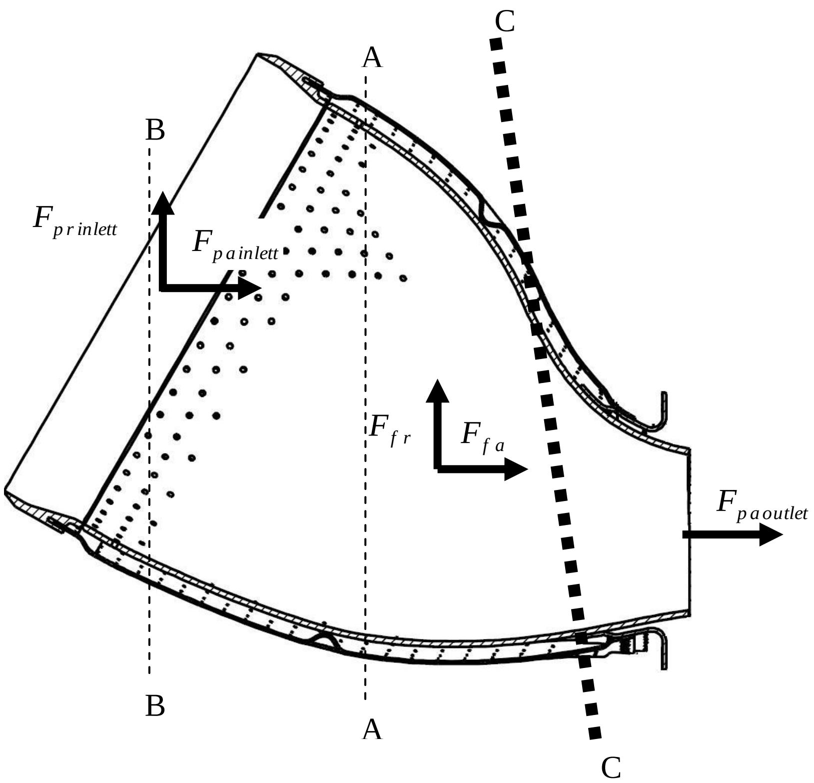

Figure 2. Forces that acts on the transition duct. The torque is zero along the line C-C.

Linköpings universitet
TEKNISKA HÖGSKOLAN